SOME GEOMETRICAL AND TOPOLOGICAL PROBLEMS IN POLYMER PHYSICS

A.L. KHOLODENKO[a], **T.A. VILGIS**[b]

[a] *375 H.L. Hunter Laboratories, Clemson University, Clemson, SC 29634-1905, USA*

[b] *Max-Planck Institut für Polymerforschung, Postfach 3148, D-55021, Mainz, Germany*

ELSEVIER

AMSTERDAM – LAUSANNE – NEW YORK – OXFORD – SHANNON – TOKYO

ELSEVIER

Physics Reports 298 (1998) 251–370

PHYSICS REPORTS

Some geometrical and topological problems in polymer physics

A.L. Kholodenko[a], T.A. Vilgis[b]

[a] *375 H.L. Hunter Laboratories, Clemson University, Clemson, SC 29634-1905, USA*
[b] *Max-Planck Institut für Polymerforschung, Postfach 3148, D-55021, Mainz, Germany*

Received June 1997; editor: I. Procaccia

Contents

PII S0370-1573(97)00081-1

Abstract

In this work we discuss some problems of polymer physics which require use of the geometrical and topological methods for their solution. Selection of problems is made to provide some balanced view between the real physical situations and the mathematical methods which are required for their understanding. We consider both static and dynamic properties of polymer solutions which depend on the presence of entanglements. These include: problems related to polymer collapse, statics and dynamics of individual circular polymers and concentrated polymer solutions, problems related to elasticity of rubbers and gels, motion of polymers through pores, etc. This work serves both as an introduction to the field and as a guide for further study.

PACS: 61.41 +e; 02.40.Pc; 05.90. +m

Keywords: Polymer entanglements; Knots and links; Path integrals; Differential geometry of curves; Statistical mechanics

1. Introduction

Knot theory was born in Scotland around the year of 1867. Two Scotsmen living in Edinburg: J.C. Maxwell and P.G. Tait and one Irishman living in Glasgow: W. Thomson (Lord Kelvin) were the founders of what has become a knot theory.

According to Thomson's theory of chemical elements all atoms are made of small knots formed by vortex lines of ether, Knott (1911), which have to be "kinetically stable". Hundred years later Sakharov (1972), following ideas of Wheeler, Lee and Yang, had suggested that the elementary particles are made of knots. Whether this is true or not remains to be seen but what is known to be true is that, starting from the work of Symanzik (1969), all quantum field theories admit polymer representation. This means that, for some reason, polymer and particle physics are very closely related. Moreover, recently Ashtekar (1996) had argued that polymer representation plays an important role in gravity.

Since the nonperturbative gravity involves knots (Gambini and Pullin, 1996), the circle of ideas which are more than hundred years old appears to be closed (or, may be, even "knotted"!). More seriously, the interplay between the knot theory and physical phenomena is not at all a recent feature. In a series of papers (reproduced in "Knots and Applications" Edited by Kauffman, 1995) Kelvin (W. Thomson) had formulated hydrodynamics of knotted vortex rings with such degree of completeness, that hundred years later his results have not lost their significance (Ricca and Berger, 1996). At the same time, the role of topology in quantum mechanics had been recognized much later by Aharonov and Bohm (1959) and Finkelstein and Rubinstein (1968).

Since polymer physics and quantum mechanics/quantum field theory are closely related to each other (Symanzik, 1969; de Gennes, 1979), evidently, that the same (or very similar) topological problems should occur in polymer physics as well. For example, the Aharonov–Bohm effect (Kleinert, 1995), has its analogue in the statistics of planar Brownian walks in the presence of a hole. (For a quick introduction to this topic, please, see the Appendix.)

It is *not* our purpose in this review to provide the reader with a chronological list of developments both in the knot theory and in polymer physics. Anyone who would like to make such a list is going to run inevitably into the dilemma: how to keep a balance between the genuinely mathematical developments in knot theory and truly physical, chemical or biological applications of knot theory. At this moment, to our knowledge, there is a series of monographs on "Knots and Everything" edited by L. Kauffman, which, has no less than seven volumes to date starting with "Knots and Physics" by Kauffman himself (1993). At the same time, there is yet another series entitled "Proceedings of Symposia in Applied Mathematics" by the American Mathematical Society. These proceedings, e.g. Vols. 45 and 51, contain also very valuable information about the applications of knot theory to various natural phenomena. To these proceedings one may add series such as "Regional Conference Series in Mathematics". In particular, a very nice summary of the results by Jones is published in Vol. 80 of this series. In addition, the series "Advances in the Mathematical Physics" and the "Journal of Knot Theory and its Ramifications" occasionally also contain applied information. Unfortunately, even this list of references is not sufficient if one wants to work actively in this rapidly developing field of research. To keep up to date on the developments related to knots and links, perhaps, it is not too unusual to use the already existing electronic databases. These are at Duke University http://eprints.math.duke.edu/archive.html; at the Los Alamos National Laboratory http://xxx.lanl.gov; at the Geometry Centers of the

University of Minnesota, http://www.umn.edu and the University of Massachusetts, http://www.gang.umass.edu.

With all this information the question arises: Is it possible to say something new (or different) on the subject of knots (links)? We believe that the answer is "yes". It is possible to say something new, provided, that one can keep a delicate balance between the mathematical rigor and the physical reality. We hope, that this work serves exactly this purpose. That is, we tried as much as we could to provide a sufficient mathematical background which is truly needed for the development but, at the same time, we tried to use a language which is familiar to the researchers in polymer and, more general, in condensed matter physics so that, hopefully, the reader will not find himself (herself) lost in mathematics. Lately, we had become aware of similar efforts, e.g. see Murasugi (1996) and Nechaev (1996). These works are more mathematical and have a little or no overlap with the content of this review. Selection of the material for this review is based mainly on our own original works and, whence, necessarily reflects our vision of this field. Nevertheless, we wholeheartedly encourage the reader to develop his (or her) own opinion about the field and, for this purpose, to look at other sources of information.

This work is organized as follows. In Section 2 we provide some illustrative examples of the relevance of entanglements to various phenomena in polymer physics. We use the examples and the language which is commonly accepted in this field. We hope that by choosing such style people of various fields, tastes and skills should be able to decide for themselves how far they want to go into this boundless field. We apologize to those who would like to see this review to be more mathematical and to those who think that it is too mathematical. Whence, immediately, beginning from Section 3, we tend to be more mathematically precise without loosing physics from our sight. In particular, the content of our Section 3, incidentally, is closely related to the latest published results of Stasiak et al. (1996) and Katrich et al. (1996) on the average writhe and the average crossing number for biological knots and by Zurer (1996) on the probability of knotting in proteins. The average crossing number is of interest in connection with the mobility of knotted DNA in gels under electrophoresis or upon centrifugation. We discuss these issues in Sections 2 and 7. In Section 4 we provide a background needed for the actual calculation of these observables. In particular, we emphasize the role of differential geometric as well as algebraic and field-theoretic concepts needed for computations which involve *real* physical knots. We also provide a unifying link between different approaches. It is important to keep in mind that the very concept of a knot *is dimension-dependent*. This precisely means that all *nontrivial* knots in 3-dimensions are *trivial* unknots in 4 dimensions (Bing and Klee, 1964). This implies that ε-expansions used in physics literature are, strictly speaking, not permissible for problems which involve knots. We do not consider higher dimensional knotting in this review. For example, if a usual knot is just an embedding of a circle S^1 into $\mathbf{R}^3$ (or, more generally, $S^3 = \mathbf{R}^3 \cup \{\infty\}$) one can think more generally about embedding(s) of S^p into S^q, $p < q$ (Rolfsen, 1976).

By the way, the opposite embeddings are also possible and are known as Hopf mappings (or Hopf fibrations), e.g. see Ono (1994). Example of such mapping is only briefly discussed in Section 6. Some physical applications of the Hopf fibrations could be found, e.g. in Monastyrsky (1993). We also do not discuss the case when S^1 is not embedded but immersed into S^3. In this case we should allow the self-interaction of the knot/link-segments between themselves. Such situation would require us to consider the Vassiliev invariants, Murasugi (1996). As it was shown very recently by Bar-Natan (1996) the Vassiliev invariants are related to more traditionally used

invariants (e.g. HOMFLY or Jones polynomials defined in Section 4) through use of quantum group methods (Chari and Pressley, 1995). Since we touch upon these methods only very gently in Section 5, we do not elaborate on this very physically important subject. But we have decided to mention about it in this review since we anticipate potentially significant physical applications of Vassiliev invariants in the future, e.g. see Deguchi and Tsurusaki (1994) for steps in this direction.

Extension of the notion of linking and self-linking to higher dimensional manifolds is also *not* only of academic interest. For example, extension of the concept of self-linking, Section 4.2, to higher dimensional manifolds leads to its connection with the Euler's characteristics for these manifolds (Guillemin and Pollack, 1974). Moreover, a simple extension of this connection leads to the Lefschetz fixed point theory which is an extension of the famous Brower fixed point theorem dealing with the question of how many roots, the equation $f(x) = x$, could have. The questions of this sort are being frequently asked in the context of quantum field theories (Zinn-Justin, 1993), in connection with problems which involve stochastic quantization. Moreover, since the Lefschetz fixed point theory (which is aimed at the calculation of the Lefschetz index) is closely connected with the Morse theory, this leads quantum mechanically to the consideration of various kinds of supersymmetric problems (Witten, 1981). We mention these facts to the reader who is interested in physical applications of the apparently exotic concepts development by mathematicians.

If Section 3 only introduces some basic knot observables while Section 4 provides some basic tools to describe these observables, Section 5 already provides the first application of these results. It deals with the long standing problem formulated by Delbrück (1962) about the probability of knot formation P_N as a function of polymer length N. This problem was solved, in part, by Sumners and Whittington (1988) and Pippenger (1989) who produce for the quantity $\zeta_N = 1 - P_N$ an estimate given by Eq. (3.2) with c being some undetermined constant, $c < 1$. In Section 5 we determine this constant while in Section 7 we calculate the topological persistence length N_T which also enters the result for ζ_N, e.g. see Eq. (3.5). Solution of the Delbrück problem has profound implications on all aspects of polymer physics since, according to Delbrück (1962) (and now proven), for $N \to \infty$ and in absence of the excluded volume effects almost all polymers are knotted or quasi-knotted. In the last case, following Delbrück, one can (at least in our imagination) "close" the ends of otherwise *linear* polymers with some straight line so that the resulting *circular* polymer will be almost surely knotted. If $\langle \mathbf{R}^2 \rangle$ is the mean square end-to-end distance, then at θ conditions $\langle \mathbf{R}^2 \rangle \sim N$ so that the ratio $\sqrt{\langle \mathbf{R}^2 \rangle}/N \to N^{-1/2} \to 0$, i.e. for $N \to \infty$ all polymers at θ conditions could be considered as effectively closed and, whence, effectively knotted. In order to obtain additional results about knotted polymers, the information presented in Section 4 turns out to be insufficient. Whence, in Section 6 we provide an additional geometrical background which is needed for solutions of the physical problems presented in Sections 7 and 8. The material of Section 6 is by no means exhaustive since we have selected only those geometrical problems which are directly used later. The reader should be warned, however, at this point, that the material of this section is so comprehensive that only a small portion of it, e.g. that presented in Section 6.2, could serve as an introduction to the whole field of surface-related phenomena, e.g. see Eisenriegler (1993). Moreover, the delicate interplay between the topological and geometrical effects discussed in Section 6.1 could also be readily generalized (Kholodenko, 1990, 1995), and is related to the statistical mechanics of semiflexible polymers. Usefulness of the Dirac propagators (Kholodenko, 1990, 1995), for the description of conformational properties of semiflexible polymers has been proven recently experimentally by Hickl et al. (1997) in a series of measurements of the static

scattering function $S(\boldsymbol{k})$ for polymers of arbitrary flexibility based on the theoretical calculations of $S(\boldsymbol{k})$ which involve the Dirac propagator (Kholodenko, 1993). Unlike the traditionally used Kratky–Porod propagators (Kleinert, 1995), which do not allow to obtain $S(\boldsymbol{k})$ in closed analytic form, use of the Dirac propagators for this purpose creates no computational difficulties. In addition, use of the Dirac-like propagators is essential for the theory of semiflexible polymers to account for the hairpin effects (see, de Gennes, 1982; Kholodenko and Vilgis, 1995; and Section 6.1). Confinement of polymers into tubes, discussed in Section 6.3, is not an intrinsic feature of polymer physics and has some similarities with motion of electrons in quasi-one-dimensional conductors. We provide some information in this regard in Sections 6.3 and 8.6. Already this observation makes some aspects of polymer physics, e.g. reptation, closely connected with the theory of quantum chaos. A simple extension of the problem which was first discussed by Levi (1965) about the planar Brownian walk which encloses a prescribed area A, presented in Section 6.4 and further used in Section 8, leads to very deep results connected with Selberg's trace formula. Incidentally, the recently published book by Grosche (1996), could serve as an excellent supplement to some of the results presented in Section 8. Unlike Grosche's book, however, the results of Section 8 are targeted towards polymer applications.The results of Section 6 are also being extensively used in Section 7 where we provide details of calculations of observables introduced and discussed in Sections 2 and 3. In this section it is possible to push calculations to the extent that *all* our results can be compared against available numerical data. The material of this section could be especially useful for biological applications as discussed, e.g. in Vologodskii et al. (1979) or Stasiak et al. (1996). At the same time, the results of Section 7.6 may also play an important role in the development of the theory of entangled polymer networks (Everaers and Kremer, 1996; Kholodenko and Vilgis, 1997; Vilgis and Otto, 1997). The reader who is interested mainly in biological applications may not read any further since Section 8 deals with a typical polymer problem about the rheological properties of dense polymer networks. The effects of topology and geometry on these properties was always suspected, e.g. see Doi and Edwards (1986), but, to our knowledge, were not properly implemented so that the many-body topological and geometrical effects remained hidden in the tube which surrounds the "reptating" polymer chain, de Gennes (1979). The existence of such a tube was postulated and the transition from the reptation regime, where the tube is expected to be well defined, to the Rouse regime, where it ceases to exist, was poorly understood. Since the experimental data which accompany such type of transition are readily available, e.g. see Fetters et al. (1994), we compare these data against our theoretical predictions in Tables 1 and 2. Earlier accounts of our theoretical results could be found in Kholodenko and Vilgis (1994), and Kholodenko (1996a,b,c). It is important, that the reader understands that the results of this section are valid in both static and dynamic conditions since they mainly involve topological arguments. For the reader's convenience we provide some essentials of these arguments in Appendix A.1. Appendix A.1 should be read very much independently of the main text and has a value on its own. We provide in it some arguments which are unobscured by technical or polymer-related details so that the topological issues should become more obvious. Since we do not expect that most of our potential readers are familiar with some specialized mathematical literature, the emphasis is made on concepts rather than on rigorous definitions, etc. Nevertheless, we provide a sufficient number of references in order to make our presentation sufficiently serious. In particular, we argue that the natural logic of development of topological ideas goes from considering the planar Brownian motion in the presence of just one

hole through generalization of this problem to include many holes and, then, through discussion of the Brownian motion in three-dimensional space in the presence of a knot. The last topic is briefly discussed in Appendix A.2. All these problems are interrelated and, in the last case, the potential for biological applications should be apparent. Since most living DNAs are knotted the Brownian motion in the vicinity of such knotted DNAs can, in principle, recognize the different knotted structures. This fact should be taken into consideration in all theories of molecular recognition. Unfortunately, to cover just these subjects in sufficient depth would require reviews even longer than ours. Hence, if our readers make an effort in these directions, we would feel that our goals are achieved.

2. Relevance of entanglements (some experimental facts and related theoretical works)

2.1. Some properties of ring polymers in dilute solutions and in melts

The role of circular polymers in biology is well documented, e.g. see Wasserman and Cozzarelli (1986), while synthetically the ring-shaped polystyrenes were obtained relatively recently, e.g. see ten Brinke and Hadziioannou (1987) and references therein. Their synthesis had led to a number of interesting experimental studies which we shall briefly discuss in this section and in more detail in the rest of this paper.

There are several conditions for the ring polymers which need to be added to the list of conditions of synthesis for the linear polymers. These include:

(a) conditions under which the rings can be formed (e.g. in good solvent the chances of ring formation should be much smaller due to the excluded volume effects);

(b) conditions under which the rings could be knotted;

(c) conditions under which the rings can be interlocked.

All these conditions were qualitatively analyzed in the past. For example, the dynamics of ring closure was analyzed by Wilemski and Fixman (1974), by Szabo et al. (1980) and, more recently, by Pastor et al. (1996). The role of solvent quality on ring formation was analyzed by de Gennes (1990b) and, independently, by von Rensburg and Wittington (1990). Conditions under which the rings could be knotted were analyzed by Sumners and Whittington (1988), by Pippenger (1989) and by Kholodenko (1991, 1994).These results will be discussed in more detail below in Sections 3–5. In addition, there are related problems, e.g. how knot formation is affected by the polymer stiffness (this defines the topological persistence length, Section 3), how many different knots can be made of linear polymers of length N (e.g. see Sections 3 and 7), how one can recognize these different knots (the rest of this paper), and to what extent topologically different knots behave physically different (Section 7 and Appendix A.2.). The important issue of link formation which was initially discussed in the pioneering work by Frisch and Wasserman (1961), raises several additional questions. For example, assume that we have a solution of both linear and ring polymers of equal concentrations and we are interested in forming a simple link (a catenane), e.g. see Fig. 10. Following Frisch and Wasserman (1961), we may be interested to know the conditional probability $\bar{\beta}$ that the threading of a particular ring by a given linear chain (with subsequent cyclization) will result in a stable catenane. The probability p_{12} that a given ring and now cyclized but initially open forms a catenane is $\bar{\beta}$-times the probability of overlap of their segmental distributions, i.e. the ratio of their

spherical covolume $\frac{4}{3}\pi(R_1 + R_2)^3$ to the total volume V, that is

$$p_{12} = \bar{\beta}\tfrac{4}{3}\pi(R_1 + R_2)^3/V\,, \tag{2.1}$$

where R_1 and R_2 are the corresponding radii of gyration. Frisch and Wasserman (1961) had made a plausible assumption that $\bar{\beta} \simeq \frac{1}{2}$ which provides an yield Y of catenanes per cyclized chain as

$$Y = \rho\tfrac{2}{3}\pi(R_1 + R_2)^3\,. \tag{2.2}$$

This produces for the total concentration of catenanes C_K the result

$$C_K = \rho^2 B\,, \tag{2.3}$$

where the density $\rho = n/V$ with n being the total number of rings (or linear chains), and B is defined by Y/ρ and has a meaning of the (topological!) second virial coefficient. The most spectacular outcome of these simple calculations lies in the fact that the subsequent Monte Carlo results of Vologodskii et al. (1975), indeed, had produced B which is in remarkable agreement with simple qualitative analysis by Frisch and Wasserman (1961). In Section 7 we reproduce analytically the result for B using path integral methods. In the same section we also reproduce the Monte Carlo results for the probability of linking (entanglement) between two ring polymers. This result has some implications for calculation of the elastic moduli of the crosslinked entangled polymer networks to be discussed below and in Section 7. Biological applications of the results related to catenanes can be found in recent papers by Levene et al. (1995) and Vologodskii and Cozzarelli (1993) while the real experiments on knotting of DNA molecules are discussed by Rybenkov et al. (1993), and Shaw and Wang (1993).

The above results include only static properties of rings. New additional effects arise when dynamical effects are considered. Since these effects are being understood much less than static effects, we shall only briefly discuss some recent theoretical and experimental results for completeness of our presentation. They are naturally going to be only qualitative and should serve only as a starting point of further more systematic investigations.

To begin we would like to recall the statement made in the classical paper by Brochard and de Gennes (1977). "At this stage it appeared natural to extend the analysis toward the case of theta solvents, where the static conformations of the chains become nearly ideal. We decided to do this and found, to our great surprise, that theta solvents are considerably more difficult than good solvents! ....In a good solvent, the chain is very much swollen and makes no knots on itself. In a poor solvent, it is more compact and makes many *self-knots* .... *The single-chain analysis in the entangled* (*i.e.* θ*-point*) *regime is the most delicate exercise in dynamical scaling and requires very long explanations* .... Thus, after a long reflection, we decided to restrict the present discussion to the many-chain problem (semidilute solutions) at the θ-point; this remains comparatively simple, because the fluctuation modes are plain waves". Since 1977 not much had changed as we shall demonstrate shortly. For the recent experimental results in this field, please, see Brulet et al. (1996). Subsequently, de Gennes (1984) had noticed that concentrated polymer solutions (melts) also present a puzzle if their dynamics is of interest. This happens, for instance, if one can rapidly quench the melt by abruptly changing the melt temperature below the temperature of crystallization. If then one measures the relaxation time τ_R which is required to bring the melt back to its initial state, one then observes that this time is much longer than the terminal time $\tau_t \propto M^{3.3}$ (where M is the molecular weight of the chain). This could be understood (qualitatively) if one recognizes that in the

melt the individual chains are Gaussian-like with $R_g \propto \sqrt{M}$. Since the length N of the polymer is proportional to M, the ratio $\sqrt{N}/N$ goes asymptotically to zero for $N \to \infty$, i.e. the melt could be viewed as a solution of randomly interlocked (quasi)rings (see below). Since most of these rings will be (quasi)knotted (see Sections 3–6) the rapid temperature quenching (from above) will leave this melt in a glassy-like state, since the ring of length N could be in $K(c(N))$ different *topological* states (Section 7) due to the fact that the number $c(N)$ of crossings in the knot projection (see Sections 3–7) which characterizes the knot complexity grows rapidly with N. When the temperature is rapidly raised (from below) the tight knots could be readily formed, de Gennes (1984), thus causing an enormous relaxation time τ_R which is associated with their untightening. Moreover, since not only knots but the links could be formed as well during quenching, this process could provide an additional strong contribution to the observed effect. We calculate the probability of link formation in Section 7, and in this section we shall describe how this quantity is related to the elastic moduli of the crosslinked entangled networks.

An attempt to understand the dynamics of the collapse of the individual polymer chain was also made by de Gennes (1985). His results were subsequently refined by Grosberg et al. (1988), Rabin et al. (1995) and others. Some numerical results related to these works could be found in the paper by Ma et al. (1995) which also provides references on the related numerical work. The main outcome of this work is the consensus that for *the linear* polymers the dynamics of collapse is two-stage process. This has been recently confirmed experimentally, e.g. see Chu et al. (1995), Ueda and Yoshikawa (1996). However, there is a considerable disagreement, e.g. see Chu and Ying (1996) and Chu et al. (1995), about the role of knotting in the dynamics of the collapse process. For instance, in the de Gennes (1985) paper there is no mentioning of knots; in the Grosberg et al. (1988) paper there is an argument in favor of tight knot formation at the *second* stage of the two-stage collapse process, while in Chu et al. (1995), based on the experimentally observed comparability of the relaxation times for *both* stages, the suggestion is made that the knotting effects could be important at *the first* stage as well. Chu and Ying (1996) argue, however, that the interpretation of experimental data suggests that knotting plays no role (or dominant role) in the kinetics of individual chain collapse. Finally, according to Grosberg et al. (1988) the collapse of an *unknotted* ring polymer should be a one-stage process. Since there are no experimental data available on collapse of rings (knotted or unknotted), no further discussion on this topic is possible at the time this review is written.

2.2. Polymer dynamics and topology

Although we have discussed some dynamical aspects of ring polymers and melts in Section 2.1, we would like to present here some additional (less controversial) results related to dynamics of individual circular polymer chains and to dynamics of melts.

Let us begin with the paper by Brinke and Hadziioannou (1987). These authors had performed extensive Monte Carlo calculations for ring polymers. They had taken into account the topology effects so that their calculations provided data for both knotted and unknotted rings. Calculation of the radius of gyration R_g as well as scattering form factor $S(\boldsymbol{q})$ for both knotted and unknotted rings, and comparison with *real* experimental data indicates that the difference between the knotted and the unknotted observables is marginal. That is, although the dimensions of knotted

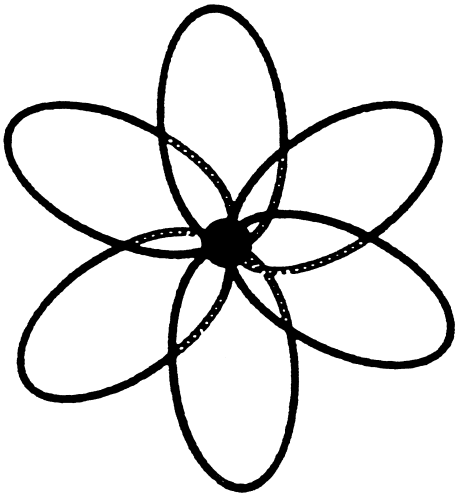

Fig. 1. Example of a daisy-like ring system.

rings are slightly smaller for rings (as compared with the linear polymers of the length N), the critical exponents (in good solvent regime) are *the same* and are independent of the knot type (i.e. the same as for unknots). The same conclusion had been reached in the subsequent work by von Rensburg and Wittington (1991). We are not discussing here more recent Monte Carlo results by Orlandini et al. (1996) which provide exponents depending upon the knot type. These latest results should await some experimental verification, since they are not related to observables such as R_g or $S(\boldsymbol{q})$. Both $S(\boldsymbol{q})$ and R_g can be used in hydrodynamical calculations (e.g. calculation of the diffusion coefficient D of the macromolecule). Comparison with *real* experimental data indicates that dynamical data (e.g. for D) are in accord with static data, i.e., the value(s) of critical exponent(s) (e.g. for the hydrodynamic radius) are the same for both linear and circular polymers, with the overall dimensions of the circular polymers being uniformly smaller as compared with the linear polymers of the same molecular weight.

The above results can be explained qualitatively based on recent arguments by Quake (1994) (please, see also Section 7). Quake makes the assumption that, independent of knot complexity, the fundamental scaling law for polymers, $R_g \propto N^{\nu}$, is retained. Then, a knot $K$of length N with $c[K]$ essential crossings (e.g. see Section 3.2) is considered as $c[K]$ loops each of length $N/c[K]$, e.g. see Fig. 1 and Burkchard et al. (1996). Each loop has a radius of gyration $R_g \propto (N/c[K])^{\nu}$ so that the total volume V of K is $V \propto c\,V_{\text{loop}} \propto c(N/c[K])^{3\nu}$. Whence, the radius of gyration $R_g(K)$ for K should scale as

$$R_g(K) \propto V^{1/3} \propto N^{\nu}[c[K]]^{1/3-\nu}. \tag{2.4}$$

If ν is taken to be of Flory-type, i.e. $\nu = \frac{3}{5}$, then the above estimate provides for $R_g(K)$ the following result:

$$R_g(K) \propto N^{3/5}[c[K]]^{-4/15}. \tag{2.5}$$

In Sections 3 and 7 we are going to demonstrate that $c[K]$ is an actually N-dependent quantity, so that the estimate given by Eq. (2.5) is, strictly speaking, inconsistent with the initial assumption about the behavior of R_g. Nevertheless, Quake's arguments could be somehow repaired if, instead of $c[K]$ we would use the average writhe $\langle|W_r[K]|\rangle$ which is directly related to $c[K]$, e.g. see Sections 3 and 7. Since, as we have demonstrated (Kholodenko and Vilgis, 1996), $\langle|W_r[K]|\rangle \propto \sqrt{N}$, we obtain, instead of Eq. (2.5), the following estimate for R_g:

$$R_g(K) \propto N^{3/5} N^{-0.13} . \tag{2.6}$$

The obtained qualitative results explain why knotted rings are always smaller than the linear polymers of the same length. Alternative results based on the concept of porosity $P(N)$ are presented in Section 7. Based on these static results, Quake was able to provide an estimate for the relaxation time τ_R based on the assumption that the Rouse model can adequately describe the dynamics of knotted rings. The argument is rather standard (Kremer and Binder, 1988), and goes as follows. The fundamental relaxation time τ_R is a long distance relaxation time which is determined when the center of mass of the polymer has moved a distance of the order R_g. When it is interpreted in terms of *local* monomer–solvent interaction, each flip of the monomer changes position of the center of mass by a factor of $1/N$. Since the flips are uncorrelated, they add up as in the case of random walk, i.e. $(\Delta R)^2 \propto (1/N)^2$. During the Rouse time τ_R there are $\tau_R N$ such displacements, so that *the total* displacement is

$$(1/N)^2 \tau_R N \simeq R_g^2 . \tag{2.7}$$

From here we obtain

$$\tau_R \propto N^{2\nu+1} [c[K]]^{2/3-2\nu} . \tag{2.8}$$

We have used $c[K]$ in Eq. (2.8) just to be in accord with Quake (1994). Evidently, for consistency reasons, $c[K]$ should be replaced by $\langle|W_r[K]|\rangle$ or by $P(N)$. This is especially true in view of the fact that Monte Carlo data provided by Quake cannot be directly used to plot τ_R as a function of N. In the absence of excluded volume interactions we have $2\nu = 1$ and Eq. (2.8), indeed, produces the Rouse time (if $c[K]$ is independent of N).

The above results are relevant only to very dilute solutions of knotted rings in good or θ-solvents. Below the θ-point the dynamics of the collapsed individual linear chains was recently studied by Monte Carlo methods by Milchev and Binder (1994). Even for the linear chains the obtained results are inconclusive (e.g. dynamical critical exponents are temperature-dependent, etc.). We hope that this fact will stimulate more research in this area in the future.

In the opposite limit of polymer melts the situation is relatively better, since the reptation theory of de Gennes (1971) and Doi and Edwards (1978) provides rather satisfactory qualitative explanation of the viscoelastic properties of melts of linear polymers. As for melts of ring polymers, an attempt had been made (see e.g. Kholodenko, 1991; Obukhov et al., 1994), to extend the existing linear polymer theory. Since the experimental data by McKena et al. (1989) strongly indicate that the results for rings parallel that for the linear polymers (just like in the dilute regime), we tend to believe that the linear theory can be used for melts of rings as well (Kholodenko, 1991). This can be understood if we recall, e.g. see Section 2.1, *that even linear polymers at θ-conditions are asymptotically closed*, since $\sqrt{\langle \mathbf{R}^2 \rangle}/N \to 0$ for $N \to \infty$. This argument could be traced back to Delbrück

(1962) and Kholodenko (1994). The fact that polymer melt of linear polymers can be also viewed as melt of randomly linked quasi-rings has some profound effect on the individual chain(s) in such melt, to be discussed in Sections 7 and 8. Here we would like to provide only some qualitative arguments.

Following Doi and Edwards (1978), and de Gennes (1990a), we shall assume that "every chain, at a given instant, is confined within a 'tube' as it cannot intersect the neighboring chains. The chain thus moves inside the tube like a snake" (i.e. reptates). The diffusive motion of such trapped chain is Rouse-like so that the diffusion coefficient $D_{\mathrm{R}}(N)$ scales like

$$D_{\mathrm{R}}^{-1}(N) = N\tau_0/b^2\,, \tag{2.9}$$

where τ_0 is solvent relaxation time, while b is the characteristic parameter of the Rouse model of the order of the size of the individual bead, e.g. see Eq. (2.7). The length of the tube L and its radius a are assumed to be related to the length Nb of the trapped chain of N effective beads via the simple relation

$$La \simeq Nb^2\,. \tag{2.10}$$

The characteristic time τ_{t} needed for the chain to leave the domain of space of order L can be estimated via

$$\tau_{\mathrm{t}} \sim \frac{L^2}{D_{\mathrm{R}}(N)} \sim \left(\frac{Nb^2}{a}\right)^2 \frac{N\tau_0}{b^2} \sim \tau_0 N^3 \left(\frac{b}{a}\right)^2\,, \tag{2.11}$$

while for the translational self-diffusion coefficient D_{T}, Doi and Edwards (1986) provide an estimate

$$D_{\mathrm{T}} \sim D_{\mathrm{R}} \frac{a}{L} \sim \frac{b^2}{\tau_0 N} \frac{a^2}{Nb^2} \sim \frac{a^2}{\tau_0 N^2}\,. \tag{2.12}$$

The last result is in remarkable agreement with experiments on monodisperse melts while for τ_{t} experimental data suggest $\tau_{\mathrm{t}} \sim N^{3.4}$. There are many attempts to "repair" the simple arguments leading to an estimate of Eq. (2.11). In Sections 6 and 8 we shall discuss in detail some of these attempts, while here we restrict ourselves only by the following remarks. The fact that the chain "cannot intersect the neighboring chains", de Gennes (1990a), makes its "motion" quasi-one-dimensional. The very fact that the "motion" is restricted, naturally breaks the symmetry between the longitudinal and the transversal diffusive motions of the chain (Section 6.3) causing the effective additional stiffness for the longitudinal component of "motion". The mechanism(s) by which the longitudinal "motion" becomes more stiff have both the topological (Kholodenko, 1991), and the geometrical (Kholodenko, 1995, 1996a, 1996b, 1996c), origins. But, irrespective to the underlying mechanism, it is possible to carry out scaling analysis analogous to that given by Eqs. (2.11) and (2.12), which includes the anticipated effects of longitudinal stiffening. This analysis was performed by Tinland et al. (1990) and, independently, by Kholodenko (1991). Stiffening of the longitudinal "motion" was also advocated in more recent papers by Perico and Selifano (1995) and Wang (1995).

To incorporate the stiffness effects into the scaling analysis, we would like to notice that the diffusion coefficient $D_{\mathrm{R}}(N)$ for the Rouse chain, Eq. (2.9), and the translational diffusion coefficient

$D_G(N)$ for the rigid rod

$$D_G(N) \simeq \frac{\ln N}{3\pi\beta\eta_s\hat{b}N} \tag{2.13}$$

will look identical if formally we put b^2/τ_0 in Eq. (2.9) equal to $(\ln N)/3\pi\beta\eta_s\hat{b}$, where β^{-1} is the usual Boltzmann's temperature factor, η_s is the solvent's viscosity and $\hat{b}$ is the diameter of the rod. Now, instead of Eq. (2.11), we can write

$$\tau_t \sim \frac{L^2}{D_G(L)} \sim \frac{\tau_0}{ab^2}\left(\frac{Nb^2}{a}\right)^3 \sim \tau_0 N^3\left(\frac{b}{a}\right)^4, \tag{2.14}$$

where we had assumed, that $D_G^{-1}(L) \simeq L\tau_0/b^2a$. Since, according to Eq. (2.12), the result for D_T is b-independent, the replacement of D_R by D_G will produce no change and, accordingly, the translational self-diffusion coefficient will remain the same, i.e. proportional to N^{-2}. At the same time, Eq. (2.11) will change. Since, according to Eq. (2.13), $b^2 \propto \ln N$. If we now formally put $\ln N = N^{\omega}$, then for experimentally used values of $N(10^5 \leq N \leq 10^6)$ we obtain $0.19 \leq \omega \leq 0.21$. By combining this result with Eq. (2.11), we obtain,

$$\tau \sim \tau_0 N^{3+2\omega}, \tag{2.15}$$

where 2ω lies in the range of $0.38 \leq 2\omega \leq 0.42$. The obtained result is in excellent agreement with the experimental data presented in the book by Doi and Edwards (1986). The extreme case of rigid rod diffusion coefficient given by Eq. (2.13) should not be taken too literally since the stiffness of the chain is scale-dependent property. This means that the effective persistent length $\sim a$ is expected to be larger than b (which is in accord with Doi and Edwards, 1986). If $a/b \gg 1$, then $L/b \ll N$, according to Eq. (2.10) taken from Doi and Edwards (1986).

The results discussed above are also relevant to the description of the viscoelastic properties of crosslinked polymer networks, gels, etc. (de Gennes, 1979) which we would like to discuss briefly now.

2.3. Polymer networks

Study of the role of topology in polymer networks (rubbers, gels, glasses, etc.) was initiated in seminal work by Edwards (1967a,b; 1968). More detailed study of this topic could be found in the subsequent works by Deam and Edwards (1976), and Edwards and Vilgis (1988). More recent developments are summarized in the recent work by Panykov and Rabin (1996), where many additional relevant references could be found.

Polymer melts and polymer networks have many things in common. For example, in both systems there are entanglements which constrain motion of individual chain(s). The presence of entanglements alone is sufficient for the formation of tubes. The concept of a tube had been put forward in the work by Edwards (1967b) in the context of polymer networks and had been successfully used by de Gennes (1971) in connection with the reptation model discussed in Section 2.2. The tube can be formed only if the length of the chain N exceeds some characteristic length N_e (the contour length between two successive entanglements along the polymer's backbone). The parameter N_e is related somehow to the monomer density, as will be explained in

Section 8. The role of topology in both polymer melts and polymer networks is thus effectively reduced to the description of the individual polymer chains inside the fictitious tube. The philosophy of such approach is in complete accord with similar mean field calculations in quantum mechanics, e.g. Hartree or Hartree–Fock type of approximation(s), etc. Unlike the case of quantum mechanics, in the present case the attempts to systematically reduce a well-posed microscopic problem which explicitly accounts for entanglements, e.g. see Deam and Edwards (1976), to the mean field tube model, had only been partially successful.

In Section 8 we provide an alternative treatment of this problem, which takes topological effects explicitly into account, and compare our theoretical results against recent experimental data of Fetters et al. (1994). In case of networks, there is another characteristic length scale N_s (the contour length between two successive crosslinks along the polymer's backbone). Whence, it is reasonable to consider the situations when $N_s > N_e$ and $N_s < N_e$. In the first case the presence of tube(s) should be important (Edwards and Vilgis, 1988), while in the second the effect caused by the tube existence should become unimportant. In reality both N_s and N_e are fluctuating quantities which depend on the polymer/monomer density in a nontrivial way, e.g. see Duering et al. (1994), which most of the time is not well understood. This is caused by the conditions of preparation of the networks, e.g. by vulcanization or by radiation crosslinking. In both cases the final product contains a wide distribution of strand lengths and a large number of dangling ends. The dangling ends are expected to slow down any relaxation significantly, but are not believed to actively support stress. These factors make any attempts of rigorous theoretical treatment quite difficult (Mark and Erman, 1992; Iwata and Edwards, 1988, 1989). The technical complications come as well from the fact that the polymer melt can be viewed as an annealed system while a network is certainly quenched. This means that, in general, one has to use the replica trick methods similar to that used in the theory of spin glasses, Mezard et al. (1988), in order to calculate the observables (Edwards and Vilgis, 1988). Recently, an attempt to by-pass the replica trick procedure was made (Solf and Vilgis, 1995, 1996, 1997). In the regime when $N_e > N_s$ the presence of topological entanglements can be ignored and then the quenched disorder can be dealt with analytically without replicas. Development of these results to the regime $N_s > N_e$ remains a challenging problem.

In order to understand better the complexities associated with entanglements one can, following de Gennes (1979), think of polymer networks made of concatenated rings , the so-called "olympic" gel. In such a system, no permanent crosslinks are present, and the elasticity is determined exclusively by the topology of concatenated rings. The properties of such networks are expected to be (Vilgis and Otto, 1997) very different from that known for the conventional rubbers, Treloar (1975). An "olympic" gel model is a limiting case of a more complicated model proposed by Graessly and Pearson (1977). In this model the network is made out of polymer loops which may be entangled pairwise at random. It is possible to calculate the shear modulus G for such model (see below) even in the presence of the permanent crosslinking since the topological G_t and the crosslinking G_C parts of G are expected to enter into the total modulus G additively (Kramer and Ferry, 1975; Everaers and Kremer, 1996).

The underlying assumptions of Graessly–Pearson (G-P) model are:

(a) the polymer loops are randomly distributed in space so that the number of loops per unit volume is ρ (defined in Eq. (2.3));

(b) the contributions of these loops to the entropy of deformation are independent and pairwise additive;

(c) if $|\mathbf{R}|$ is the distance between the centers of mass of some loop pair, then $f_N(|\mathbf{R}|)$ is the probability of this pair to be linked, and N is the contour length of the polymer, as before;

(d) only the affine deformations are considered so that after the deformation the new displacement vector $\mathbf{R}' = \mathbf{R}$ for all loop pairs.

Whence, if $G = G_t + G_C$, then

$$G_t = F[f(x)]\tilde{\rho}\, k_B T\,, \tag{2.16}$$

where $k_B T$ is the usual temperature factor, $f(x) \equiv f_N(x)$,

$$\tilde{\rho} = 2\pi\rho R_L^3(N)\int_0^\infty \mathrm{d}x\, x^2 f(x)\,, \tag{2.17}$$

$$F[f(x)] = \frac{1}{15}\int_0^\infty \mathrm{d}x\, x^4 (f'(x))^2 [f(x)[1-f(x)]]^{-1} \tag{2.18}$$

while $f'(x) = \mathrm{d}f/\mathrm{d}x$. The entanglement radius, $R_L(N)$ is, to some extent, an adjustable parameter of a G–P model but, according to Everaers and Kremer (1996), can be estimated from the self-consistency equation

$$\frac{4\pi}{3}R_L^3(N) = \frac{1}{2}\int \mathrm{d}^3 r f_N(|\boldsymbol{r}|)\,. \tag{2.19}$$

Whence, if the probability of linking is known, the topological contribution G_t to the elastic sheer modulus can be calculated according to Eq. (2.16). This probability was estimated by Monte Carlo methods by Vologodskii et al. (1975) and was recently reobtained by Everaers and Kremer (1996) who compared their Monte Carlo data for G_t with G–P result, Eq. (2.16). The comparison was made using two independent methods. First, G_t was estimated numerically without any reference to Eq. (2.16). The results of these simulations are nicely summarized by the equation

$$(G - G_C)/\tilde{\rho} = 0.85\, k_B T \tag{2.20}$$

which indicates that the topological contribution to the shear modulus is independent of chain length N. Then, the linking probability $f_N(|\mathbf{R}|)$ was estimated numerically for the simplest link, e.g. see Fig. 10, and is found to be in complete agreement with Vologodskii et al. (1975). It was found that

$$f_N(|\mathbf{R}|) = A\exp\{-c(R/R_L)^\omega\}\,, \tag{2.21}$$

where both A and c are numerical constants, $A \simeq 0.6$ and $c = A/2$, while $R = |\mathbf{R}|$. The exponent ω was found to be equal to 3 but, following G–P, we argue that it can, in principle, have values lower than 3. Substitution of thus obtained $f_N(|\mathbf{R}|)$ into Eq. (2.16) have produced

$$\frac{G - G_C}{\tilde{\rho}} = 1.3\, k_B T \tag{2.22}$$

which is in excellent agreement with the independent result given by Eq. (2.20).

In Section 7 we reobtain the distribution function analytically. In order to compare our results with existing data in literature, several comments need to be made. First, already in the paper by

Graessly and Pearson several trial distribution functions were tested, all in the form of Eq. (2.21), but with the exponent ω ranging between 1 and 3. The exponent 3 was taken from the work of Vologodskii et al. (1975) while the exponent 2 appears in the analytical calculations of Prager and Frisch (1967) of the entanglement probability between the planar Brownian walk and the infinite rod perpendicular to the plane. For arbitrary $\xi \equiv R/R_{\mathrm{R}}$ they obtained $f_N(|\mathbf{R}|) = \mathrm{erf}\, c(\xi)$, which for large ξ's produces $f_N(|\mathbf{R}|) \propto \exp\{-\xi^2\}$. The above result was also independently effectively obtained by Helfand and Pearson (1983) who provided an estimate of the entanglement probability for a closed polymer loop trapped into an array of obstacles (meant to represent other chains). We provide some related results on this subject in Section 8 and Appendix A.1. In Section 7.6 we demonstrate analytically that the exponent ω in Eq. (2.21) can take *only* the values between 2 and 3.

To understand this and other facts discussed in this section, we need to rely on solid mathematical background about knots and links which begins with the next section.

3. Single chain problems which involve entanglements (general considerations)

3.1. Topological persistence length and the probability of knot formation

In his seminal papers, Edwards (1967a,b) had noticed that "treating polymer as a random path clearly must fail at small distances when the precise molecular structure dominates .... It is not clear, however, whether the question of whether random path contain a knot is at all meaningful in the mathematical idealization of infinitesimal steps. One would guess that such questions are not meaningful, getting into unresolved, perhaps unresolvable, questions of measure .... since a random path permitting infinitesimal steps will be 'infinitely knotted' ." With these remarks in mind, it is obvious that the cut-off must somehow be introduced into any kind of discussion which involves *real* polymers which may be topologically entangled.

This cut-off can be introduced both in the continuous and in the lattice polymer models, e.g. see de Gennes (1979). When a flexible polymer is modeled on the lattice, the lattice unit step length can be conveniently chosen to be a unity. In the continuum, such a choice is also permissible if the total polymer length N is being measured in the units of Kuhn's length l. In various models of polymers (Kholodenko, 1995), the role of l is being played by the persistence length $\hat{l}$. More precise definitions will be provided later in the text. Both l and $\hat{l}$ do not have a topological origin, but they do affect the topological properties of polymers. For instance, let us consider a closed random walk on some three-dimensional lattice. It is reasonable to anticipate that there should be a minimal number of steps N_{T} (which depends upon the geometry of lattice) in order for the first non-trivial knot to be formed. Accordingly, for closed walks of less than N_{T} on the lattice, no knots can be formed. The idea about estimating N_{T} originated some time ago in the work by Delbrück (1962), but was rigorously developed only recently. Diao (1993, 1994) using rather sophisticated combinational arguments had found that for a simple cubic lattice $N_{\mathrm{T}} = 24$. In Section 7 we shall provide much simpler derivation of this result using path integrals. In the mean time, we would like to notice that, along with N_{T} which we call "*topological persistence length*", there is a related quantity, ζ_N, which is the probability for a closed walk of N steps to remain unknotted. Frisch and

Wasserman (1961) and Delbrück (1962) put forward a conjecture that

$$\lim_{N\to\infty} P_N \equiv 1 - \zeta_N \to 1\,, \tag{3.1}$$

i.e. for $N \to \infty$ the probability P_N for a closed walk to be knotted tends to unity. This conjecture had been proven only recently by Sumners and Whittington (1988) and by Pippenger (1989). A very nice account of these results could be found in the monograph by Welsh (1993). The above authors had shown that

$$\lim_{N\to\infty} (\zeta_N)^{1/N} = c \tag{3.2}$$

where the constant $c < 1$ had remained undetermined. Recently, Kholodenko (1991, 1994) had been able to provide an estimate of the constant c. By analyzing Monte Carlo data by Windwer (1990), who tried to fit his results for ζ_N by using the ansatz

$$\zeta_N = \tilde{c}\tilde{\mu}^N N^{\alpha} \tag{3.3}$$

with $\alpha = 0$, $\tilde{\mu} = 0.9949$ and $\tilde{c} = 1.2325$, Kholodenko (1991, 1994) had found that it is sufficient to determine only $\tilde{c}$. Indeed, using Eq. (3.3) we obtain

$$1 = \zeta_{N_T} = \tilde{c}\tilde{\mu}^{N_T}\,. \tag{3.4}$$

This produces at once

$$\zeta_N = \tilde{c}\left(\frac{1}{\tilde{c}}\right)^{N/N_T} \tag{3.5}$$

so that if N_T is known, ζ_N is determined by $\tilde{c}$. Eq. (3.5) is in agreement with Eq. (3.2) with c in Eq. (3.2) being $\tilde{c}^{-1}$ in Eq. (3.5) (for $N \to \infty$). In Section 5 the analytical derivation of the result(s) of Eq. (3.3) (or Eq. (3.5)) will be provided.

For completeness, we would like to mention that, in addition to N_T, there is another number, called the edge number, $e(K)$. For a given knot, it is defined as the minimal number of edges required to represent the given knot K as a polygon in three-dimensional space (Randell, 1994). $e(K)$ is a topological invariant similar to the minimal crossing (unknotting) number $u(K)$ to be further discussed in Sections 3.3 and 7.4. Unfortunately, as far as we can see, $e(K)$ is of little importance for polymers. Indeed, it can be shown that for the unknot $e(K) = 3$ and for the trefoil knot $e(K) \leq 6$, etc. To obtain these numbers in the case of polymers, one needs to use rather unrealistic freely jointed chain model of polymers. This model provides satisfactory description of polymers at larger scales (in θ solvent regime), but is much less realistic at the smaller scales where the bond angles and the torsional bond energies should be taken into account. But, unlike N_T, $e(K)$ can be used in the continuum, i.e., in the off-lattice calculations. Whence, if the polymer is made of rather long rigid rods connected by the freely flexible joints, $e(K)$ can be used, in principle.

3.2. Knot complexity and the average writhe

It is rather remarkable that the notion of knot complexity came to knot theory at its birth (Harpe et al., 1986). One of the cofounders of knot theory, Tait, had formulated the main tasks of knot

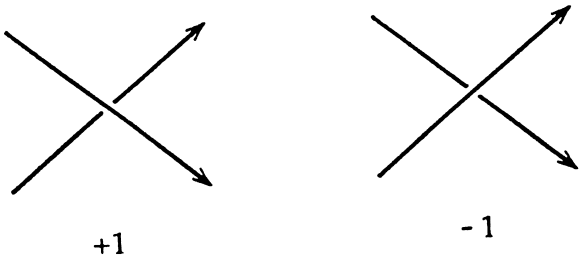

Fig. 2. Sign convention for the oriented crossing.

theory among which he expected "to establish a hierarchy among knots relying on some notion of complexity".

As it will be discussed in Section 4, there are two ways to describe knots: differential-geometric and via planar diagrams. In the last case we are dealing with 4-valent planar graphs where at each crossing the decision should be made about how this crossing must be resolved, e.g. see Fig. 2.

If we disregard this resolution and just count the number of vertices $c(K)$ for a given knot K projection into some plane, we obtain the knot complexity (Kholodenko and Rolfsen, 1996). $c(K)$ is *not* a topological invariant and is *not* the only quantity which measures the knot complexity. Other quantities are discussed in Sections 3.3 and 7. They are all interrelated. For instance, let $\varepsilon(p) = \pm 1$ where p is some vertex in the planar knot diagram. Then, it is possible to define the writhe $W_r[K]$ for a given knot via

$$W_r[K] = \sum_{p \in S(K)} \varepsilon(p)\,, \tag{3.6}$$

where $S[K]$ denotes the set of crossings on some knot diagram K (Kauffman, 1987a).

In case when knots are generated on some 3D lattices, the question arises how the knot complexity $c(K)$ and the writhe $W_r[K]$ of the knot K depend on the number of steps N which are required to form this knot. Evidently, the very same knot can be placed onto the lattice in many ways. Whence, it makes sense to introduce the averaged complexity $\langle c[K]\rangle$ and the averaged writhe $\langle W_r[K]\rangle$ where $\langle \cdots \rangle$ means the averaging over the possible arrangements of a given knot K on the lattice. Alternatively, one can think of generating some knot K and changing the orientations of the plane into which it is projected. This strategy was chosen in the recent numerical simulations by Whittington et al. (1993, 1994a, b). These authors have found that

$$\langle c[K]\rangle \propto N^{\alpha_c}\,, \tag{3.7}$$

where $\alpha_c \simeq 1.122 \pm 0.005$ and

$$\langle |W_r[K]|\rangle \propto N^{\alpha}\,, \tag{3.8}$$

where $\alpha \geq 0.5$. At the same time, $\langle W_r[K]\rangle = 0$, by the symmetry arguments as it will be explained below, in Section 7.2.

The results of Whittington (1994a) indicate that the obtained values for α_c are not sufficiently reliable. These authors argue (without proof!) that actually $1 < \alpha_c < 2$. Recently, Arteca (1994, 1995)

had performed independent detailed numerical simulations and found that $\alpha_c \sim 1.40 \pm 0.04$. The situation with the averaged writhe is more reliable since in Whittington (1993) the exponent α was found analytically to be 0.5. This result is also supported by a completely different calculation by Yor (1992) and by much earlier Monte Carlo results by Chen (1981), Le Bret (1980) and Vologodskii et al. (1979). In Sections 7.2 and 7.3 we shall rederive the results Eqs. (3.7) and (3.8) using path integrals. We shall rigorously demonstrate that $1 < \alpha_c < 1.5$ and that the inclusion of the excluded volume effects lowers the upper bound for α_c from 1.5 to less than 1.4. Obtained results are in excellent agreement with the numerical results of Arteca (1994, 1995).

3.3. The unknotting number and the number of distinct knots for polymer of given length N

From the previous discussion it is intuitively expected that the knot complexity $c(K)$ should be associated with the unknotting number $u(K)$ which is the minimal number of self-crossings which will turn knot into unknot (Kholodenko and Rolfsen, 1996). The question arises how $c[K]$ is related to $u(K)$. Moreover, the unknotting number $u(K)$ is a topological invariant, Rolfsen (1976), while we have noticed that the averaged $c[K]$ is N-dependent. The answer to this question will be provided in Section 7. Here we only notice that $u[K]$ is intrinsically connected with the fact that our knot, i.e. the circle S^1, is embedded into $\mathbf{R}^3$ (or S^3, i.e. $\mathbf{R}^3 \cup \{\infty\}$). If, instead, we would consider the embedding of our knot into $\mathbf{R}^4$ (or S^4), then it can be shown (Bing and Klee, 1964), that any nontrivial knot in $\mathbf{R}^3$ becomes an unknot in $\mathbf{R}^4$. This fact is reminiscent of the fact that any self-avoiding walk in $\mathbf{R}^3$ becomes effectively Gaussian in $\mathbf{R}^4$ (de Gennes, 1979). The above theorem of Bing and Klee makes use of the ε-expansions in knot problems questionable. The relation between $u(K)$ and $c(K)$ is known in literature as Bennequin conjecture (Bennequin, 1983; Menasco, 1994), and mathematically can be stated as

$$\tfrac{1}{2}(|W_{\mathrm{r}}[K]| - \hat{n} + 1) \leq u[K] \leq \tfrac{1}{2}(c[K] - \hat{n} + 1)\,, \tag{3.9}$$

where it is assumed that the knot is made of a closure of a braid of $\hat{n}$ strings (see Section 5 for precise definitions of braids).

The above inequality can be understood using the following arguments (Gilbert and Porter, 1994). Any knot projection can be decomposed into Seifert circles by deleting crossings and glueing the reminding arcs in such a way that they form a set of circles as depicted in Fig. 3. The two arcs and the parts of the crossing removed make up a rectangle. If our knot projection was given an orientation, then the Seifert circles also acquire an orientation as well as the rectangles. Let us now twist these rectangles (as if we would make a Möbius strip) and reglue them back to the circles. Obviously, instead of a knot, this time we shall obtain a surface. The boundary of this surface is our knot K. This surface has a genus $g[K]$ and by means of a very simple argument (Gilbert and Porter, 1994, pp. 92–93), it can be shown that

$$g[K] \leq \tfrac{1}{2}(c[K] - s + 1)\,, \tag{3.10}$$

where s is the number of Seifert circles. In Kholodenko and Rolfsen (1996) it is shown that s and $\hat{n}$ are interrelated (see also Section 4). By comparing inequalities Eqs. (3.9) and (3.10) we conclude that

$$u[K] \simeq g[K] \tag{3.11}$$

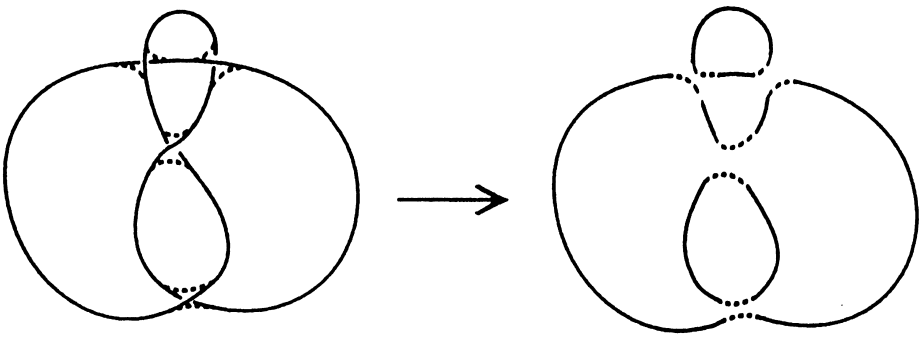

Fig. 3. Formation of Seifert circles for figure-eight knot.

and, since $u[K]$ is a topological invariant, $g[K]$ is also an invariant of a knot K. From the above discussion it follows that the number of distinct knots should somehow be dependent on $u[K]$ (or $g[K]$). According to Tutte (1963), the number $T[n]$ of different planar graphs with n edges is estimated to be

$$T[n] \leq 2 \times 12^n . \tag{3.12}$$

In Freedman et al. (1994) it is argued that the correspondence

$$\{D, n\}\text{crossings} \rightarrow \{G, \text{ with } n \text{ edges}\} \tag{3.13}$$

is at most 2^n to 1. Here, D is a knot diagram while G is a planar graph, so that the number of knot diagrams with exactly n crossings is bounded by $2^n T(n) \leq 2(24^n)$. Given this result, the number $K(n)$ of knot diagrams with at most n crossings must satisfy

$$2^n \leq K(n) \leq 2(24)^n . \tag{3.14}$$

Whence, if n is known then $K(n)$ can be related (identified) with the number of distinct knots for the knot diagram with n crossings. Moreover, since $n \sim c(K)$ as was shown in Freedman et al. (1994), we can replace the above inequality with

$$2^{c[K]} \leq K(n) \leq 2(24)^{c[K]} . \tag{3.15}$$

Whence, knowledge of $c[K]$ provides us with some information about $u[K]$ and $K[n]$. These facts are going to be fully exploited in Section 7.

4. Methods of describing knots (links)

4.1. Differential geometric approach

From the point of view of differential geometry knots are just closed curves in three-dimensional Euclidean space. As is well known, (see, e.g. Dubrovin et al., 1985), every nonplanar curve is being fully described by its local curvature and torsion. Frenchel (1951) had noticed that for any closed

curve (knotted or not) of length N

$$\int_0^N \mathrm{d}\tau\,|k(\tau)| \geq 2\pi\,, \tag{4.1}$$

where $k(\tau)$ is the local curvature of the curve. This result resembles the famous Gauss–Bonnet theorem for surfaces

$$\frac{1}{2\pi}\int_{M^2} K\,\mathrm{d}S = \chi(M^2)\,, \tag{4.2}$$

where $\chi(M^2)$ is the Euler characteristic of the manifold M^2 (Monastyrsky, 1993), and, indeed, was motivated by the result of Eq. (4.2). More surprising is the result of Milnor (1950) who had shown that for the knotted curve

$$\int_0^N \mathrm{d}\tau\,|k(\tau)| > 4\pi\,. \tag{4.3}$$

This result was generalized for surfaces by Langevin and Rosenberg (1976) who had proven that for the unknotted torus

$$\frac{1}{2\pi}\int |K|\,\mathrm{d}S = 4 \tag{4.4}$$

(to be compared with Eq. (4.2)) and if the torus is knotted, then

$$\frac{1}{2\pi}\int |K|\,\mathrm{d}S \geq 8\,. \tag{4.5}$$

This result was subsequently refined by Kuiper and Meeks (1984) and by Willmore (1982) who had demonstrated that if the surface is unknotted and H is the extrinsic curvature (i.e. $H = \frac{1}{2}(k_1 + k_2)$, where k_1 and k_2 are principal curvature radii), then

$$\frac{1}{2\pi}\int_{M^2} H^2\,\mathrm{d}S \geq \pi\,, \tag{4.6}$$

while for the knotted surface

$$\frac{1}{2\pi}\int_{M^2} H^2\,\mathrm{d}S > 4\,. \tag{4.7}$$

Although in this work we shall not touch the topic of knotted surfaces, we believe, that the above results deserve attention, especially in light of the results presented in Section 7.

Besides the result Eq. (4.3), Milnor (1950) had also obtained additional results for closed curves

$$\int_0^N \mathrm{d}\tau\,|k(\tau)| + \int_0^N \mathrm{d}\tau\,|\kappa(\tau)| \geq 2\pi n \tag{4.8}$$

where $\kappa(\tau)$ is the torsion of the curve. For the unknot, $n = 1$. This result along with Eq. (4.3) should be taken into consideration when the path integrals for semi-flexible polymers are calculated

(Kholodenko, 1990, 1995). We shall discuss some of the implications of these constraints on path integrals in Section 7.

Use of these constraints will allow us to calculate the topological persistence length N_T defined in Section 3 and, in principle, affects other observables such as $\langle|W_r[K]|\rangle, \langle c[K]\rangle$, etc. also introduced in Section 3.

4.2. Path integral approach via Abelian and non-Abelian Chern–Simons field theory

Beginning from the seminal works of Edwards (1967a,b, 1968), topological entanglements in polymers are being described by the constrained path integrals which effectively employ the observables of the Abelian Chern–Simons field theory (ACSFT). The non-Abelian variant of these path integral calculations, to our knowledge, was used for polymer problems only in Kholodenko (1994). As was noticed already in Section 3.3, use of the field-theoretic methods for knot problems should be performed with extreme caution since ε-expansions are, strictly speaking, illegitimate for problems which involve knots (links). The most attractive feature of the non-Abelian variant of the Chern–Simons field theory (NACSFT) lies in its ability to connect knots (links) of different complexities via skein (recurrence) relations (Guadagnini, 1993). This allows effectively to disentangle knotted polymer configurations, thus reducing the problem with complicated constraints to that without constraints. This does not imply that the information about entanglements is lost during this disentanglement process. The disentangled partition function will still remember its initial state as it is explained in Section 4.4.

To demonstrate how the above general statements are implemented, let us consider the simplest situation of n interlocked polymer rings. This problem was considered before in Section 2.3, but now we would like to emphasize the mathematical aspects of the problem.

If we ignore the excluded volume effects, the partition function Z for an assembly of simple circular polymer chains in three-dimensions can be written as

$$Z = \int\prod_{i=1}^{n} \mathrm{D}[\boldsymbol{r}(\tau_i)]\delta\left(\int_0^{N_i} \mathrm{d}\tau_i \dot{\boldsymbol{r}}(\tau_i)\right)\exp\left\{-\frac{3}{2\ell}\sum_{i=1}^{n}\int_0^{N_i}\mathrm{d}\tau_i\,\dot{\boldsymbol{r}}^2\right\}. \tag{4.9}$$

where $\dot{\boldsymbol{r}} = \mathrm{d}\boldsymbol{r}/\mathrm{d}\tau$. For an assembly of n interlocked rings we can write, using Eq. (4.9), the following result:

$$Z = \int\prod_{i=1}^{n} \mathrm{D}[\boldsymbol{r}(\tau_i)]\delta\left(\int_0^{N_i} \mathrm{d}\tau_i \dot{\boldsymbol{r}}_i(\tau_i)\right)\exp\left\{-\frac{3}{2l}\sum_{i=1}^{n}\int_0^{N_i}\mathrm{d}\tau_i\,\dot{\boldsymbol{r}}_i^2\right\}$$
$$\times\,\delta\left(c - \sum_{i,j}^{n} lk(i,j)\right), \tag{4.10}$$

where

$$\ell k(i,j) = \frac{1}{4\pi}\oint_{C_i}\mathrm{d}\boldsymbol{l}_i \times \oint_{C_j}\mathrm{d}\boldsymbol{l}_j \boldsymbol{\nabla}_j\left(\left|\frac{1}{\boldsymbol{r}_i - \boldsymbol{r}_j}\right|\right) \tag{4.11}$$

and $\mathrm{d}\boldsymbol{l}_i = \dot{\boldsymbol{r}}_i\,\mathrm{d}\tau_i, \boldsymbol{r}_i = \boldsymbol{r}_i(\tau)$, etc. The constant c in Eq. (4.10) should be an integer thus making the δ-function to be the Kronecker's delta. The microcanonical formulation given by Eq. (4.10) is somewhat inconvenient, because it does not readily allow the standard field-theoretic treatment.

To clarify this point, let us introduce the abelian CS action $S^{\mathrm{A}}_{\mathrm{c-s}}$. Following Guadagnini (1993), we have

$$S^{\mathrm{A}}_{\mathrm{c-s}}[\boldsymbol{A}] = \frac{k}{8\pi}\int_{M^3} \mathrm{d}^3x\, \varepsilon^{\mu\nu\rho} A_\mu \partial_\nu A_\rho\,, \tag{4.12}$$

where the constant prefactor $k/8\pi$ in front of the action is chosen for further convenience and $M^3 = \mathbf{R}^3 \bigcup \{\infty\} = S^3$.

Define now the Abelian Wilson loop $W(C)$ via

$$W(C) = \exp\left\{ \mathrm{i}e \oint \mathrm{d}\boldsymbol{l}\cdot A \right\} \tag{4.13}$$

and consider the average for the set of n loops forming a link L,

$$\langle W(L)\rangle_{\mathrm{c-s}} = \left\langle \prod_{i=1}^{n} \exp\{\mathrm{i}e_i \oint_{C_i} \mathrm{d}\boldsymbol{l}_i \cdot \boldsymbol{A}_i\} \right\rangle_{\mathrm{c-s}} = \left\langle \prod_{i=1}^{n} W(C_i) \right\rangle_{\mathrm{c-s}}, \tag{4.14}$$

where the average $\langle\,\rangle_{\mathrm{c-s}}$ is defined by

$$\langle\,\rangle_{\mathrm{c-s}} = \hat{N}\int \mathrm{D}[\boldsymbol{A}] \exp\{\mathrm{i}S^{\mathrm{A}}_{\mathrm{c-s}}[\boldsymbol{A}]\} \cdots \tag{4.15}$$

with normalization constant $\hat{N}$ being chosen in such a way that $\langle 1\rangle_{\mathrm{c-s}} = 1$. In view of Eq. (4.12), the average in Eq. (4.14) is easily computable since it involves the calculation of Gaussian-like integrals. The result of this averaging procedure produces:

$$\langle W[L]\rangle_{\mathrm{c-s}} = \exp\left\{ -\mathrm{i}\left(\frac{2\pi}{k}\right) \sum_{i,j}^{n} e_i e_j lk(i,j) \right\}. \tag{4.16}$$

The sum in the exponent of Eq. (4.16) contains the "undesirable" self-interaction terms (for $i = j$). Calculation of these terms is nontrivial (Guadagnini, 1993), and the final result depends upon how the limiting procedure $i \to j$ was performed in Eq. (4.11). Let us consider this procedure in some detail since we will use these results in Sections 5–8. For the linking number, given by Eq. (4.11), we can write an equivalent expression as follows:

$$lk(i,j) = \frac{1}{4\pi}\oint_{C_i} \mathrm{d}x^\mu \oint_{C_j} \mathrm{d}y^\nu \varepsilon_{\mu\nu\rho} \frac{(\boldsymbol{x}-\boldsymbol{y})^\rho}{|\boldsymbol{x}-\boldsymbol{y}|^3}\,. \tag{4.17}$$

Let now

$$y^\mu(\tau) = x^\mu(\tau) + \varepsilon n^\mu(\tau), \quad \varepsilon \to 0^+, |\boldsymbol{n}(\tau)| = 1\,. \tag{4.18}$$

By combining Eqs. (4.17) and (4.18) we obtain,

$$lk(i,i) = lk_{\mathrm{f}}(i) = \lim_{\varepsilon\to 0} \frac{1}{4\pi}\int_0^1 \mathrm{d}s \int_0^1 \mathrm{d}\tau\, \varepsilon_{\mu\nu\rho} \dot{x}^\mu (\dot{x}^\nu + \varepsilon \dot{n}^\nu) \frac{(\boldsymbol{x}(s) - \boldsymbol{x}(\tau) - \varepsilon\boldsymbol{n}(\tau))^\rho}{|\boldsymbol{x}(s) - \boldsymbol{x}(\tau) - \varepsilon\boldsymbol{n}(\tau)|^3}\,, \tag{4.19}$$

where the subscript f stands for *framing*. Depending upon the orientation of n^{μ} (Witten, 1989b; Calugareanu, 1961), one may obtain

$$lk_{\mathrm{f}}(i) = 0\,, \tag{4.20}$$

which is known as the *standard*(s) framing, or

$$lk_{\mathrm{f}}(i) = W_{\mathrm{r}}[i]\,, \tag{4.21}$$

where $W_{\mathrm{r}}[i]$ was defined in Section 3 (one should identify i with K). The last case is known as *vertical* (v) framing. More details on the framing procedure can be found in Bar-Natan (1995) and Aldinger et al. (1995). Using these results, one can claim that, *at least for the case of standard framing*, ACSFT can be used to obtain the partition function for the interlocked rings, Eq. (4.10), if instead of the microcanonical the grand canonical ensemble is used. Evidently, in this case, instead of Eq. (4.14), one should write

$$\langle\langle W(L)\rangle_{\mathrm{c-s}}\rangle_{\mathrm{p}} = \left\langle \exp\left\{ -\mathrm{i}\left(\frac{2\pi}{k}\right)\sum_{i,j}^{n} e_i e_j\, lk(i,j)\right\}\right\rangle_{\mathrm{p}} \tag{4.22}$$

with $\langle \cdots \rangle_{\mathrm{p}}$ being defined by

$$\langle \cdots \rangle_{\mathrm{p}} = \int \sum_{i=1}^{n} \mathrm{D}[\boldsymbol{r}_i(\tau_i)] \exp\left\{ -\frac{3}{2l}\sum_{i=0}^{n}\int_0^{N_i} \mathrm{d}\tau_i\, \dot{\boldsymbol{r}}_i^2\right\}\delta\left(\int_0^{N_i}\mathrm{d}\tau_i\,\dot{\boldsymbol{r}}_i(\tau_i)\right)\cdots\,. \tag{4.23}$$

The specifics of polymer problems, as compared with the standard field theory, lies in the fact that it is always necessary to perform a double average as in the case of Eq. (4.22). Moreover, since (for $e_i = e$) the combination $e^2(2\pi/k)$ is not an integer in general (and should be self-consistently determined as it is always done in the grand canonical calculations), the polymer average in Eq. (4.22) is quite nontrivial. We illustrate this by considering an auxiliary problem of calculation of the double average for the polymer ring placed on the multiply connected plane (polymer ring entangled with array of rigid rods of infinite length). This problem is discussed in Appendix A.1 and in Section 8 in connection with the theory of reptation.

Use of ACSFT does not allow us to relate the problem of an assembly of n interlocked rings to that of $n-1$ rings, etc., since it does not involve the skein relations (recursion relations relating knots (links) of different complexity). The situation can be dramatically improved if the NACSFT is considered instead. In this case, instead of the action, given by Eq. (4.12), we have to consider the "improved" action given by (Guadagnini, 1993)

$$S_{\mathrm{c-s}}[\boldsymbol{A}] = \frac{k}{4\pi}\int_{M^3} \mathrm{d}^3x\, \varepsilon^{\mu\nu\rho}\,\mathrm{Tr}\left(A_\mu \partial_\nu A_\rho + \mathrm{i}\frac{2}{3} A_\mu \partial_\nu A_\rho\right), \tag{4.24}$$

where k is some integer and $A_\mu(x) = A_\mu^\alpha T^\alpha$ with T^α being infinitesimal generators of some Lie group G, which obey commutation relations of the corresponding Lie algebra:

$$[T^a, T^b] = \mathrm{i} f^{abc} T^c \tag{4.25}$$

and, in addition,

$$\mathrm{Tr}[T^a T^b] = \tfrac{1}{2}\delta^{ab}\,. \tag{4.26}$$

Instead of the Abelian Wilson loop, Eq. (4.13), now we have to use its non-Abelian generalization given by

$$W_\rho(C) = \mathrm{Tr}\left[P\exp\left\{ \mathrm{i}e \oint_c \mathrm{d}\boldsymbol{l}\cdot\boldsymbol{A} \right\} \right], \tag{4.27}$$

where ρ specifies the type of the representation for T^a's and P denotes the path ordering operator (along the C-curve), while Tr denotes the operation of taking the trace.

Using thus defined $W_\rho(C)$ we can now consider the averaged products, like that given by Eq. (4.14), with the averaging being performed with the help of Eq. (4.15), where, instead of the action given by Eq. (4.12), we have to use now the action given by Eq. (4.24). The most spectacular difference between the Abelian and the non-Abelian variants of Chern–Simons field theory lies in the fact that different link averages in the last case become related to each other. This is the source of various knot polynomials.

4.3. Algebraic (group-theoretic) description of knots (links) via knot polynomials

To understand how the recursion (skein) relations originate, we have to consider in some detail calculation of averaged $W_\rho(C)$ defined by Eq. (4.27). For this purpose we need to expand the exponent in Eq. (4.27) first, thus producing

$$\begin{aligned} W_\rho(C) = \mathrm{Tr}\Bigg[I + \mathrm{i}\oint_C \mathrm{d}x_a^\mu A_\mu - \oint_C \mathrm{d}x^\mu \int^x \mathrm{d}y^\nu A_\mu(\boldsymbol{x})A_\nu(\boldsymbol{y}) \\ - \mathrm{i}\oint_C \mathrm{d}x^\mu \int^x \mathrm{d}y^\nu \int^y \mathrm{d}z^\rho A_\mu(\boldsymbol{x})A_\nu(y)A_\rho(\boldsymbol{z}) + \cdots \Bigg], \end{aligned} \tag{4.28}$$

where

$$\oint_C \mathrm{d}x^\mu \int^x \mathrm{d}y^\nu = \int_o^1 \mathrm{d}s \int_o^s \mathrm{d}\tau\, \dot{x}^\mu(s)\dot{x}^\nu(\tau) = \frac{1}{2}\int_o^1 \mathrm{d}s \int_o^1 \mathrm{d}\tau\, \dot{x}^\mu(s)\dot{x}^\nu(\tau)\,. \tag{4.29}$$

Following Guadagnini et al. (1990), let us choose for G the group $SU(\hat{N})$, then, upon averaging with the help of Eqs. (4.15) and (4.24) we obtain for an assembly of n interlocked loops forming a link L the following perturbative result:

$$\begin{aligned} \langle W(L)\rangle_{\mathrm{f}} = \hat{N}^n \Bigg\{ 1 - \mathrm{i}\left(\frac{2\pi}{k}\right)\left(\frac{\hat{N}^2-1}{2\hat{N}}\right)\sum_{i=1}^n lk_{\mathrm{f}}(C_i) \\ + \left(\frac{2\pi}{k}\right)^2 \hat{N}\left(\frac{\hat{N}^2-1}{2\hat{N}}\right)\sum_{i=1}^n \rho(C_i) - \frac{1}{2}\left(\frac{2\pi}{k}\right)^2\left(\frac{\hat{N}^2-1}{2\hat{N}}\right)^2 \sum_{i=1}^n lk_{\mathrm{f}}^2(C_i) \\ - \left(\frac{2\pi}{k}\right)^2\left(\frac{\hat{N}^2-1}{2\hat{N}}\right)^2 \sum_{i\neq j}^n lk_{\mathrm{f}}^2(C_i) lk_{\mathrm{f}}(C_j) \\ - \left(\frac{2\pi}{k}\right)^2 \frac{1}{2\hat{N}}\left(\frac{\hat{N}^2-1}{2\hat{N}}\right)\sum_{i\neq j}^n lk^2(C_i,C_j) + \mathrm{O}(k^{-3}) \Bigg\}, \end{aligned} \tag{4.30}$$

where f denotes a type of framing: standard(s) or vertical (v).

Here

$$\rho(C_i) = \rho_1(C_i) + \rho_2(C_i)\,, \tag{4.31}$$

where

$$\rho_1(C_i) = -\frac{1}{32\pi^2}\oint_{C_i} \mathrm{d}x^\mu \int^x \mathrm{d}y^\nu \int^y \mathrm{d}z^\rho\, \varepsilon^{\alpha\beta\gamma}\varepsilon_{\mu\alpha\sigma}\varepsilon_{\nu\beta\lambda}\varepsilon_{\rho\gamma\tau}\, I^{\sigma\lambda\tau}(\boldsymbol{x},\boldsymbol{y},\boldsymbol{z})\,, \tag{4.32}$$

$$\rho_2(C_i) = \frac{1}{8\pi^2}\oint_{C_i} \mathrm{d}x^\mu \int^x \mathrm{d}y^\nu \int^y \mathrm{d}z^\rho \int^z \mathrm{d}w^\sigma\, \varepsilon_{\sigma\nu\alpha}\varepsilon_{\rho\mu\beta}\, \frac{(w-y)^\alpha (z-x)^\beta}{|\boldsymbol{w}-\boldsymbol{y}|^3 |\boldsymbol{z}-\boldsymbol{x}|^3} \tag{4.33}$$

with

$$I^{\sigma\lambda\tau}(\boldsymbol{x},\boldsymbol{y},\boldsymbol{z}) = \int \mathrm{d}^3 w \frac{(w-x)^\sigma (w-y)^\lambda (w-z)^\tau}{|\boldsymbol{w}-\boldsymbol{x}|^3 |\boldsymbol{w}-\boldsymbol{y}|^3 |\boldsymbol{w}-\boldsymbol{z}|^3}\,. \tag{4.34}$$

The value of $\rho(C_i)$ is independent of the choice of framing and, in particular, for the unknot U_0, it was explicitly calculated with the result $\rho(U_0) = -\frac{1}{12}$.

For the case of standard framing Eq. (4.30) acquires a much simpler form. In particular, for just one loop, we obtain

$$\langle W(L)\rangle_{\mathrm{s}} = \hat{N}\left\{1 + \left(\frac{2\pi}{k}\right)^2 \left(\frac{\hat{N}^2-1}{2}\right)\rho(L) + \mathrm{O}(k^{-3})\right\}. \tag{4.35}$$

As it was shown by Witten (1989a) and, independently, by Frölich and King (1989), for the case of unknot U_0 the average $\langle W(U_0)\rangle_{\mathrm{s}}$ can be calculated exactly with the result (for $SU(\hat{N})$)

$$\langle W(U_0)\rangle_{\mathrm{s}} = \frac{\sin(\pi\hat{N}/(k+\hat{N}))}{\sin(\pi/(k+\hat{N}))}. \tag{4.36}$$

In the Abelian case, $\hat{N}=1$, and $\langle W(U_0)\rangle_{\mathrm{s}} = 1$. This result is in agreement with Eq. (4.16) in view of Eq. (4.20). To compare Eqs. (4.36) and (4.35) it is sufficient to replace L by U_0 in Eq. (4.35) and use the Taylor series expansion of Eq. (4.36). Through second order in k^{-1} we obtain

$$\langle W(U_0)\rangle_{\mathrm{s}} = \hat{N}\left\{1 - \frac{1}{6}\left(\frac{\pi}{\hat{N}+k}\right)^2 (\hat{N}^2-1) + \mathrm{O}(k^{-2})\right\}. \tag{4.37}$$

If now k is replaced by $k+\hat{N}$ in Eq. (4.35), then the complete agreement is reached between Eqs. (4.35) and (4.37) (since $\rho(U_0) = -\frac{1}{12}$). The need to replace k by $k+\hat{N}$ was shown, e.g. in careful perturbative calculations by Shifman (1991).

Consider now the ratio

$$G_{\mathrm{L}}^{\mathrm{f}} = \frac{\langle W(L)\rangle_{\mathrm{f}}}{\langle W(U_0)\rangle_{\mathrm{f}}} = \hat{N}^{n-1}\Bigg\{1 - \mathrm{i}\left(\frac{2\pi}{k}\right)\left(\frac{\hat{N}^2-1}{2\hat{N}}\right)\sum_{i=1}^{n} lk_{\mathrm{f}}(C_i)$$
$$- \left(\frac{2\pi}{k}\right)^2 \frac{1}{2}\left(\frac{\hat{N}^2-1}{2\hat{N}}\right)^2 \sum_{i=1}^{n} lk_{\mathrm{f}}^2(C_i) - \left(\frac{2\pi}{k}\right)^2 \hat{N}\left(\frac{\hat{N}^2-1}{2}\right)\Bigg[\rho(L_0) - \sum_{i=1}^{n}\rho(C_i)\Bigg]$$
$$- \left(\frac{2\pi}{k}\right)^2 \left(\frac{\hat{N}^2-1}{2\hat{N}}\right)^2 \sum_{i\neq j}^{n} lk_{\mathrm{f}}(c_i) lk_{\mathrm{f}}(C_j) - \left(\frac{2\pi}{k}\right)^2 \frac{1}{2\hat{N}}\left(\frac{\hat{N}^2-1}{2\hat{N}}\right)^2 \sum_{i\neq j}^{n} lk^2(C_i,C_j) + \mathrm{O}(k^{-3})\Bigg\}. \tag{4.38}$$

The higher order terms in the above expansion had been formerly considered by Guadagnini et al. (1989). For two unlocked rings use of the standard framing in Eq. (4.38) produces

$$G_{\mathrm{L}}^{\mathrm{s}} = \hat{N}\left\{1 - \frac{1}{24}\left(\frac{2\pi}{k}\right)^2 (\hat{N}^2-1) + \mathrm{O}(k^{-3})\right\}. \tag{4.39}$$

Comparison between Eqs. (4.39) and (4.36) (with $k \leftrightarrows k + \hat{N}$) immediately produces

$$\langle W(L)\rangle_{\mathrm{s}} = \langle W(U_0)\rangle_{\mathrm{s}} \langle W(U_0)\rangle_{\mathrm{s}} \tag{4.40}$$

in view of Eq. (4.37). Evidently, for n disconnected rings we would obtain

$$\langle W(L)\rangle_{\mathrm{s}} = (\langle W(U_0)\rangle_{\mathrm{s}})^n . \tag{4.41}$$

This result is in agreement with that obtained nonperturbatively by Witten (1989a) and is central for developing the theory of polynomials for knots and links. Indeed, following Harpe et al. (1986) let us consider three oriented knots (links) L_+, L_- and L_0. Their projections onto an arbitrary plane differing from each other by just one crossing is shown in Fig. 4.

Let us define axiomatically a link invariant $P[L]$. Evidently, for the unknot U_0 we should require

$$P[U_0] = \text{const} . \tag{4.42}$$

in view of Eq. (4.36). Let a_+, a_- and a_0 be some, yet undetermined, constants. Then, we impose the condition (skein relation):

$$a_+ P[L_+] + a_- P[L_-] + a_0 P[L_0] = 0 . \tag{4.43}$$

In particular, let L_+,L_- and L_0 be three link projections as depicted in Fig. 5.

Then, using Eq. (4.43) we obtain

$$a_+ P[U_0] + a_- P[U_0] + a_0 P[U_0^2] = 0 , \tag{4.44}$$

where U_0^2 denotes a union of two unlocked rings (i.e. $U_0^2 = U_0 \cup U_0$). By analogy with Eq. (4.40), we can impose a requirement that

$$P[U_0^2] = P[U_0]P[U_0] . \tag{4.45}$$

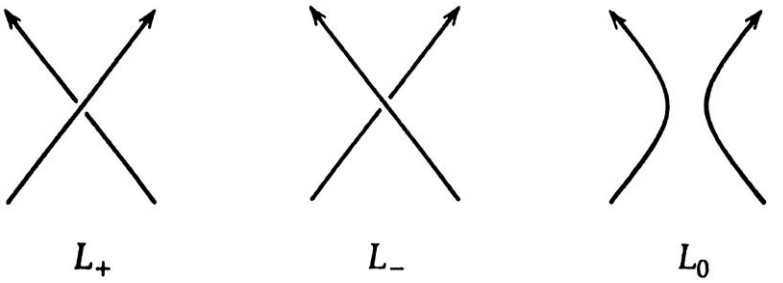

Fig. 4. Projections of three knots (links) which differ by just one crossing.

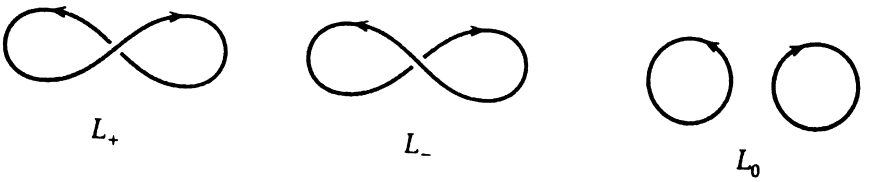

Fig. 5. A special case of three oriented links which differ just by one crossing.

Using this result in Eq. (4.43) we obtain at once

$$P[U_0] = -\frac{a_+ + a_-}{a_0} \equiv \langle W(U_0)\rangle_s \,. \tag{4.46}$$

Comparison with Eq. (4.36) allows us to obtain immediately the skein relation for $P[L]$:

$$\exp\left[-\frac{i\pi\hat{N}}{k+\hat{N}}\right]P[L_+] - \exp\left[+\frac{i\pi\hat{N}}{k+\hat{N}}\right]P[L_-]$$
$$= \left(\exp\left[-\frac{i\pi\hat{N}}{k+\hat{N}}\right] - \exp\left[+\frac{i\pi\hat{N}}{k+\hat{N}}\right]\right)P[L_0] \tag{4.47}$$

which coincides exactly with that obtained by Frölich and King (1989) who used completely different methods to obtain this result. If we divide both sides of this equation by $P[U_0]$ for a single loop, then we obtain the skein relation for the HOMFLY polynomial, $P[L]/P[U_0] = G^s_L$ (Gilbert and Porter, 1994), which can be described axiomatically via a set of relations

$$G^s_{U_0} = 1 \,, \tag{4.48a}$$

$$\omega G^s_{L_+} - \omega^{-1} G^s_{L_-} = z\, G^s_L \,, \tag{4.48b}$$

$$\text{if } G^s_L \sim G^s_{\tilde{L}} \,, \quad \text{then } G^s_L = G^s_{\tilde{L}} \,, \tag{4.48c}$$

where $\sim$ means that two knots L and $\tilde{L}$ are ambient isotopic, i.e. that their projections are invariant with respect to all three Reidemeister moves as depicted in Fig. 6.

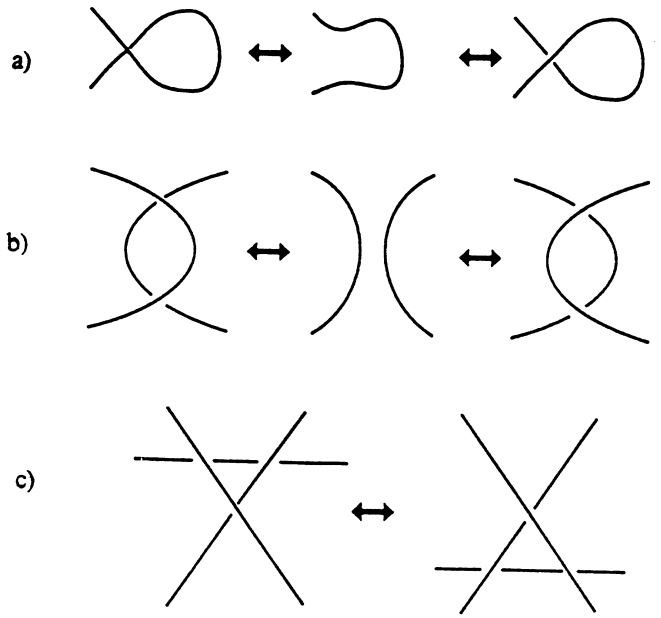

Fig. 6. Three local Reidemeister moves. The variance with respect to moves (b) and (c) guarantees the regular (i.e. in the plane) isotopy, while the invariance with respect to (a) guarantees ambient (i.e. in space) isotopy.

Thus defined HOMFLY polynomials do *not* require NACSFT for their justification, e.g. see Harpe et al. (1986). At the same time, the actual values of constants ω and z in Eq. (4.48b) remain undetermined, while Eq. (4.47) provides

$$\omega = q^{\hat{N}/2}\,, \qquad z = \sqrt{q} - \frac{1}{\sqrt{q}}\,, \qquad q = \exp\left\{ -\mathrm{i}\frac{2\pi}{k+\tilde{N}} \right\}. \tag{4.49}$$

Naively, we can obtain the Jones polynomial V_{L} from HOMFLY if we put $\omega = t^{-1}$ and $z = \sqrt{t} - (1/\sqrt{t})$ in Eq. (4.48b), e.g. see Gilbert and Porter (1994). Thus, we obtain the skein relation,

$$\frac{1}{t}V_{L_+} - \frac{1}{t}V_{L_-} = \left(\sqrt{t} - \frac{1}{\sqrt{t}}\right)V_{L_0} \tag{4.50}$$

supplemented with the normalization condition

$$V_{U_0} = 1\,. \tag{4.51}$$

Comparison with Eq. (4.47) and use of Eq. (4.49) leads us to the only choice: $\hat{N} = 2$ and $\sqrt{t} = -1/\sqrt{q}$. If we recognize that the expansion of Eq. (4.30) can be also considered for the case of vertical framing, then taking into account that $\rho(C_i)$ are framing-independent, and using the definition of $W_{\mathrm{r}}[K]$ given by Eq. (3.6) (along with Eq. (4.21)), we notice the following. For a knot $K = \tilde{K} \cup L_+$ the writhe $W_{\mathrm{r}}[\tilde{K} \cup L_+] = W_{\mathrm{r}}[\tilde{K}] + 1$ while if $K = \tilde{K} \cup L_-$, then $W_{\mathrm{r}}[\tilde{K} \cup L_-] =$

$W_r[\tilde{K}] - 1$. Using these facts, we obtain for the unknot depicted in Fig. 6a,

$$\langle W(U_0)\rangle_{\circlearrowleft} = \alpha \langle W(U_0)\rangle_{\circ}, \tag{4.52}$$

where

$$\alpha = 1 - i\left(\frac{2\pi}{k}\right)\left(\frac{\hat{N}^2-1}{2\hat{N}}\right) - \frac{1}{2}\left(\frac{2\pi}{k}\right)^2\left(\frac{\hat{N}^2-1}{2\hat{N}}\right) + O(k^{-3})$$

$$\approx \exp\left\{-i\frac{2\pi}{k}\left(\frac{\hat{N}^2-1}{2\hat{N}}\right)\right\}. \tag{4.53}$$

Using this result, it can be also shown (Guadagnini, 1990), that, in general,

$$\langle W(L)\rangle_v = \alpha^{W_r[L]}\langle W(L)\rangle_s \tag{4.54}$$

or, in view of Eq. (4.38),

$$G_L^s = \alpha^{-W_r[L]} G_L^v. \tag{4.55}$$

Let us now use this fact and substitute Eq. (4.54) into Eq. (4.48b). We obtain

$$\omega\alpha^{-W_r[L_+]}G^v_{L_+} - \omega^{-1}\alpha^{-W_r[L_-]}G^v_{L_-} = z\alpha^{-W_r[L_0]}G^v_{L_0}. \tag{4.56}$$

Using known properties of $W_r[L]$, just mentioned, we obtain from Eq. (4.56) the following result:

$$\beta G^v_{L_+} - \beta^{-1}G^v_{L_-} = zG^v_{L_0}, \quad \text{where } \beta = \omega\alpha^{-1}. \tag{4.57}$$

This skein relation should be considered along with Eq. (4.52) (and its conjugate), i.e.

$$G^v_{L_+} = \alpha G^v_{L_0}, \tag{4.58a}$$

$$G^v_{L_-} = \alpha^{-1} G^v_{L_0}. \tag{4.58b}$$

The results just obtained are in accord with the results obtained by Cotta-Ramusino et al. (1990). Evidently, by construction, e.g. see Eq. (4.38), $G^v_{U_0} = 1$. Comparison between this result and e.g. Eq. (4.48a) dictates, in view of Eq. (4.55), that for the unknot $W_r(U_0) = 0$. This happens to be a very important fact which allows us to obtain various polynomials using Eqs. (4.57), (4.58a) and (4.58b) and the normalization condition for $G^v_{U_0}$. To make a connection with the field theory, we have to remember that the actual values of constants α, β, ω and z are *not* arbitrary, e.g. see Eq. (4.49). Using Eqs. (4.53) and (4.57) we obtain

$$\alpha = q^{(\hat{N}-1)/2\hat{N}}, \qquad \beta = \omega\alpha^{-1} = q^{1/2\hat{N}}, \qquad z = q^{1/2} - q^{-1/2}. \tag{4.59}$$

To obtain the Jones polynomial, let us consider as before a special case of $SU(2)$, i.e. $\hat{N} = 2$. Then, using Eq. (4.59) we obtain

$$\alpha = q^{3/4}, \qquad \beta = {}^{1/3}, \qquad z = q^{1/2} - q^{-1/2} \tag{4.60}$$

and also, in view of Eq. (4.55), we have

$$V(L, q^{1/2}) = q^{-3W_r[L]/4}G^v_L. \tag{4.61}$$

These results are in complete accord with Guadagnini (1993), where they were obtained in a different way. The important thing to remember is that $V(L, q^{1/2})$ is an invariant of an *ambient*

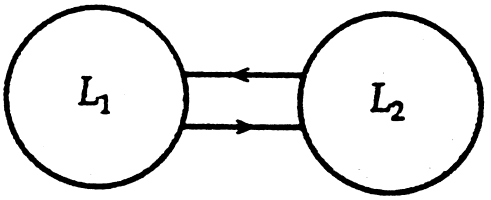

Fig. 7. A projection for the link composition $L_1 \# L_2$.

(i.e. three-dimensional) isotopy while G_L^v is only regular, i.e. two-dimensional (in the plane), isotopy. The differential geometric properties of $W_r[L]$ which can make $V(L, q^{1/2})$ ambient-isotopic will be fully exploited in Sections 6 and 7.

To make our discussion complete, we would like to notice the apparent difference between the field- theoretic and the existing mathematical formulations of various knots (link) polynomials. This difference can be seen most vividly if we return back to our discussion related to the skein relation, Eq. (4.43). In physics literature (Witten, 1989a,b; Guadagnini, 1993), Eq. (4.45) is obtained using the physical arguments (see, e.g. Eqs. (4.39) and (4.40)). At the same time, mathematicians, see, e.g. Harpe et al. (1986) or Lickorish and Millet (1987), discuss a somewhat different relation, e.g.

$$P[L_1 \cup L_2] = -\frac{a_+ + a_-}{a_0} P[L_1]P[L_2]\,. \tag{4.62}$$

If L_1 and L_2 are both unknots, then

$$P[U_0^2] = -\frac{a_+ + a_-}{a_0} \tag{4.63}$$

since, by definition $P[U_0] = 1$. This needs to be contrasted with Eq. (4.45). If we specialize to HOMFLY polynomial, e.g. see Eqs. (4.58a) and (4.48c), then we obtain (Harpe, 1986; Lickorish and Millet, 1987),

$$G_{L_1 \cup L_2} = \frac{\omega - \omega^{-1}}{z} G_{L_1} G_{L_2} \tag{4.64}$$

and

$$G_{L_1 \# L_2} = G_{L_1} G_{L_2}\,, \tag{4.65}$$

where the link composition $\#$ is graphically defined in Fig. 7.

Obviously, both the Eqs. (4.62) and (4.65) are in formal disagreement with Eq. (4.46) for the unknot. Moreover, Eq. (4.63) implies the normalization condition $G_{U_0} = 1$. The factorization property given by Eq. (4.45) and leading to (Eq. (4.46)) is physically very important, Witten (1989a), but formally is in contradiction with Eq. (4.62). To resolve the existing difficulty, let us assume,

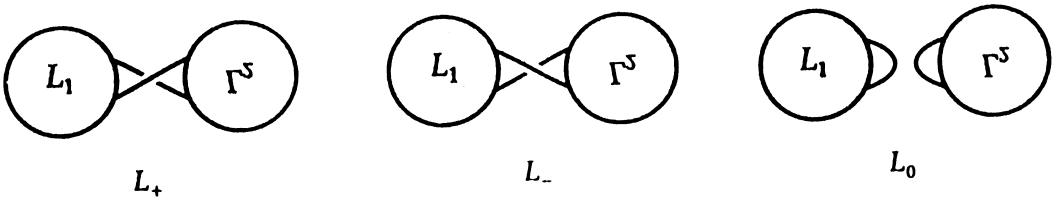

Fig. 8. Three related links.

following Guadagnini (1993) and Witten (1989a) that, instead of Eq. (4.62), the following result is correct

$$P[L_1 \cup L_2] = P[L_1]P[L_2]\,. \tag{4.66}$$

Specializing to HOMFLY skein relation given by Eq. (4.48b) we would obtain for links L_+,L_- and L_0 depicted in Fig. 8 the following result:

$$\omega P(L_1 \# L_2) - \omega^{-1} P(L_1 \# L_2) = zP[L_1 \cup L_2]\,. \tag{4.67}$$

This would immediately imply

$$P(L_1 \# L_2) = \frac{z}{\omega - \omega^{-1}} P[L_1]P[L_2] \tag{4.68}$$

to be compared with Eq. (4.64). Since, according to Eqs. (4.47) and (4.48b) we should have

$$P[U_0] = \frac{\omega - \omega^{-1}}{z}\,, \tag{4.69}$$

this produces our final result:

$$P[U_0]\,P[L_1 \# L_2] = P[L_1]P[L_2] \tag{4.70}$$

which is obviously consistent with Eq. (4.68). For the unknot(s), Eq. (4.70) produces an identity. Evidently, it is possible to change the rest of the arguments, e.g. in Lickorish and Millet (1987), in order to justify the HOMFLY-like skein relation, Eq. (4.48b), but with normalization condition, Eq. (4.48a), being replaced by Eq. (4.69). Eqs. (4.66) and (4.70) are crucial for the applications of NACSFT to polymer problems. Since the Jones polynomial is a special case of HOMFLY, the arguments presented above are related to the Jones polynomial as also can be seen from the work by Witten (1989a) where Eq. (4.70) was also obtained (see, e.g. his Eqs. (4.55) and (4.56)) by using completely different set of arguments.

4.4. Unifying link between different approaches

In Section 3.3 we had shown that the knowledge of the crossing number $c[K]$ allows to estimate the unknotting number $u(K)$ as well as the number of distinct knots with n crossings ($n \sim c[K]$). The question arises: how the crossing number is related to the characteristics of various

polynomials introduced in Section 4.3? In addition, it is of interest to know how the differential-geometric description of knots is related to their group-theoretic (algebraic) description. In this subsection we are going to address mainly the first question, and the detailed answer to the second question will be provided in Section 7.

Consider now once again the HOMFLY polynomial defined by Eqs. (4.48a), (4.48b) and (4.48c). For a given knot (link) L we will obtain (by using the skein relations) the polynomial in z or Laurent polynomial in ω. Let $G_L^s \equiv P_L(\omega, z)$, then we have either

$$P_L(\omega, z) = \sum_{n=m}^{n=M} b_n(\omega) z^n \tag{4.71}$$

or

$$P_L(\omega, z) = \sum_{n=e}^{n=E} a_n(z) \omega^n \,. \tag{4.72}$$

In the first case, by definition, we have $b_m(\omega) \neq 0 \neq b_M(\omega)$ while in the second, $a_e(z) \neq 0 \neq a_E(z)$. Let us define ω-span $(P_L) = E - e$ and z-span $(P_L) = M - m$. Using these definitions it can be shown, Murasugi and Przytycki (1993), that

$$\tfrac{1}{2}[\omega - span\,(P_L)] \leq \beta[L] - 1 \leq \hat{n} - 1 \,, \tag{4.73}$$

where $\hat{n}$ was defined after Eq. (3.9) and $\beta[L]$ is known as the braid index. For the unknot U_0, $\beta[U_0] = 1$, while in general

$$\beta[L] \leq s[D] - ind[D] \,, \tag{4.74}$$

where $s(D)$ is the number of Seifert circles (see, e.g. Eq. (3.10)) for the planar diagram D for some knot (link) L. The index of the diagram D, $ind\,[D]$, is defined in Murasugi and Przytycki (1993) and its general definition is rather complicated. Whence, we would like to avoid its explicit use (Kholodenko and Rolfsen, 1996), by relating the inequality (Eq. (4.73)) to other inequalities whose physical meanings are more transparent. Following Morton (1986), we also have

$$M \leq c[L] - (s[D] - 1) \tag{4.75}$$

while Eq. (4.74) can be rewritten as

$$(\beta[L] - 1) + ind[D] \leq s[D] - 1 \,. \tag{4.76}$$

By rewriting Eq. (4.75) as

$$(s[D] - 1) + M \leq c[L] \tag{4.77}$$

and using Eq. (4.76) we arrive at the inequality

$$(\beta[L] - 1) + ind[D] + M \leq (s[D] - 1) + M \leq c[L] \,. \tag{4.78}$$

This inequality allows us to write

$$ind[D] + M \leq c[L] - (\beta[L] - 1) \,. \tag{4.79}$$

Comparison between this result and the Bennequin's inequality (Eq. (3.9)) and additionally assuming that $ind[D] \leq M$, produces

$$M \leq \tfrac{1}{2}(c[L] - (\beta[L] - 1)) . \tag{4.80}$$

Whence, the Bennequin inequality (Eq. (3.9)) is equivalent to the assertion

$$M \simeq u[L] . \tag{4.81}$$

It is possible actually to prove a stronger result (Kauffman, 1987b; Murasugi, 1987; Thistlethwaite, 1987; Turaev, 1987)

$$z - span(P_L) \leq 4c[L] . \tag{4.82}$$

Moreover, for the alternating knots the above inequality becomes an equality (a knot (link) is considered to be alternating if traveling along the knot diagram one meets crossings alternatively at overpasses and underpasses). Unfortunately, not all knots have an alternating projection diagrams. According to Thistlethwaite (1987) "Amongst the 12 965 unoriented prime knot types of up to 13 crossings, precisely 6236 are non-alternating". For the alternating knots, it is possible to obtain in addition a much stronger result (Murasugi, 1987). Indeed, since the Jones polynomial is a special case of HOMFLY, one can define as well a t-span for V_L defined by Eqs. (4.50) and (4.51). Then, it may be possible to prove that

$$t - span(V_L) = c[L] , \tag{4.83}$$

i.e. the crossing number of an alternating knot (link) is *exactly* the span of its Jones polynomial. This fact is quite remarkable since the Jones polynomial is directly related to the Potts model of statistical mechanics as will be shown in Section 5. This means that, at least for the alternating knots (links), the averaged crossing number, defined by Eq. (3.7) can be sytematically calculated using known tools of statistical mechanics! The "thermodynamic" nature of the crossing number $c[L]$ for the alternating knot (link) can be seen from the following extensive property of $c[L]$ (Murasugi, 1987)

$$c[L_1 \# L_2] = c[L_1] + c[L_2] , \tag{4.84}$$

where the operation $\#$ was defined in Fig. 7. This property means that, at least for the alternating knots (links), one can apply blob-like analysis in the style of de Gennes (1979). Unfortunately, this property no longer holds for the nonalternating knots (Adams, 1994). Some attempts to analyze this, more general, situation are presented in Soteros et al. (1992) in connection with the problem of the proper choice of a good measure for the knot complexity. We urge the interested reader to consult these references for more details.

5. Probability of knotting: the detailed treatment

5.1. Planar Brownian motion in the presence of a single hole. The role of finite size effects

The planar Brownian motion in the presence of a single hole is known in quantum mechanics, e.g. see Kleinert (1995), in connection with the Aharonov–Bohm effect. In the context of polymer

problems related to statistical mechanics of rubber and glasses, the use of the Aharonov–Bohm effect was originally considered by Edwards (1967a,b). Although this single hole problem can be solved exactly, it does not allow a straightforward generalization to the case of Brownian motion in the presence of many (even two!) holes. Some ways of solving this, more general, problem are discussed in Section 8 and Appendix A.1. Here we restrict ourselves only to the one-hole case.

By analogy with Eq. (4.10), we can write down the constraint path integral (Edwards, 1967a,b) as follows:

$$G(\boldsymbol{r}_1,\boldsymbol{r}_2;w)=\int_{\boldsymbol{r}(0)=\boldsymbol{r}_1}^{\boldsymbol{r}(N)=\boldsymbol{r}} D[\boldsymbol{r}(\tau)]\delta\left(w-\frac{1}{2\pi}\int_0^N \mathrm{d}\tau\,\frac{x\dot{y}-y\dot{x}}{x^2+y^2}\right)\exp\left\{-\frac{1}{l}\int_0^N \mathrm{d}\tau\,\dot{\boldsymbol{r}}^2\right\} \tag{5.1}$$

where the winding number w defined by

$$w=\frac{1}{2\pi}\int_0^N \mathrm{d}\tau\,\frac{x\dot{y}-y\dot{x}}{x^2+y^2} \tag{5.2}$$

is the two-dimensional analogue of the linking number $lk(i,j)$ defined in Eq. (4.11) (the hole can be considered as a point of intersection of another closed polymer (of infinite length!) with the plane).

In the absence of a constraint, the path integral of Eq. (5.1) can be easily calculated with the result

$$G_N(r_1,r_2;\theta)=C\exp\left\{-\frac{R^2}{Nl}\right\}, \tag{5.3}$$

where

$$R^2=r_1^2+r_2^2-2r_1r_2\cos\theta \tag{5.4}$$

and the constant C is fixed by normalization. Since it is known that

$$\exp(z\cos\theta)=\sum_{n=-\infty}^{\infty} I_n(z)\mathrm{e}^{\mathrm{i}n\theta}, \tag{5.5}$$

where $I_n(z)$ is the modified Bessel function, $I_n(z)=I_{-n}(z)$, we can rewrite Eq. (5.3) in the following form:

$$G_N(r_1,r_2;\theta)=C\exp\left\{-\frac{r_1^2+r_2^2}{Nl}\right\}\sum_{m=-\infty}^{\infty}\mathrm{e}^{\mathrm{i}m\theta}I_m(z), \tag{5.6}$$

where $z=2r_1r_2/Nl$. To make a connection with the Aharonov–Bohm effect it is sufficient, following Wilczek (1990), to rewrite Eq. (5.6) as follows:

$$G_N^{\hat{a}}(r_1,r_2;\theta)=C\exp\left\{-\frac{r_1^2+r_2^2}{Nl}\right\}\sum_{m=-\infty}^{\infty}\mathrm{e}^{\mathrm{i}m\theta}I_{|m+\hat{a}|}(z). \tag{5.7}$$

When the flux $\hat{a}\neq 0$ and $\hat{a}$ being noninteger the r.h.s. of Eq. (5.7) describes the "free" propagator in the plane in the presence of the "magnetic flux" tube which is perpendicular to the plane and goes through the hole. The presence of an extra "flux", for polymer problems is discussed in Sections 8.2 and 8.3. Here we shall assume that $\hat{a}\to 0$. Following Wilczek (1990), it is convenient to represent

Eq. (5.6) in the equivalent form

$$G_N(r_1, r_2; \theta) = \sum_{m=-\infty}^{\infty} \int \mathrm{d}x \int_{-\infty}^{\infty} \mathrm{d}\lambda\, \delta(\theta - x + 2\pi m) \mathrm{e}^{\mathrm{i}\lambda x} Q_{|\lambda|}(r_1, r_2; N) \tag{5.8}$$

which can be easily obtained with the help of another known identity (Kleinert, 1995):

$$\sum_{m=-\infty}^{\infty} \delta(m - x) = \sum_{m=-\infty}^{\infty} \mathrm{e}^{\mathrm{i}nx2\pi}, \tag{5.9}$$

where

$$Q_{|\lambda|}(r_1, r_2; N) = C \exp\left\{ -\frac{r_1^2 + r_2^2}{Nl} \right\} I_{|\lambda|}(z). \tag{5.10}$$

Using the results just obtained, Eq. (5.6) acquires the following equivalent form:

$$G_N(r_1, r_2; \theta) = \sum_{w=-\infty}^{\infty} G_N(r_1, r_2; \theta, w), \tag{5.11}$$

where

$$G_N(r_1, r_2; \theta, w) = \int_{-\infty}^{\infty} \mathrm{d}\lambda\, \mathrm{e}^{\mathrm{i}\lambda(\theta + 2\pi w)} Q_{|\lambda|}(r_1, r_2; N). \tag{5.12}$$

Following Saito and Chen (1973) this result can be conveniently restated in the form

$$G_N(r_1, r_2; \theta, w), = G_N(r_1, r_2; \theta) f_w(\theta, z), \tag{5.13}$$

with $f_w(\theta,z)$ being given by

$$f_w(\theta, z) = \mathrm{e}^{-z\cos\theta} \int_{-\infty}^{\infty} \mathrm{d}\lambda\, \mathrm{e}^{\mathrm{i}\lambda(\theta + 2\pi w)} I_{|\lambda|}(z). \tag{5.14}$$

Thus defined function $f_w(\theta, z)$ has remarkable properties. In particular, it satisfies the skein relation

$$f_w(\theta + 2\pi, z) = f_{w-1}(\theta, z) \tag{5.15}$$

analogous to the skein relations discussed in Section 4. Successive use of Eq. (5.15) permits us to write as well

$$f_w(\theta, z) = f_0(\theta + 2\pi w, z). \tag{5.16}$$

Whence, in complete agreement with the results of knot theory, *the problem of computation of f_w with arbitrary winding number w can be always reduced to the computation of f_0.*

One of the important quantities of interest is the a priori probability p_w that a ring-shaped polymer is wrapped w times around a hole (or another polymer). This probability can be defined with the help of Eqs. (5.3), (5.11), (5.12) and (5.13). For this purpose we define Z as

$$Z = \int \mathrm{d}\boldsymbol{r}_1 \int \mathrm{d}\boldsymbol{r}_2\, G_N(r_1, r_2; \theta = 2\pi), \tag{5.17}$$

$$Z(w) = \int \mathrm{d}\boldsymbol{r}_1 \int \mathrm{d}\boldsymbol{r}_2\, G_N(r_1, r_2; \theta = 2\pi w), \tag{5.18}$$

so that

$$p_w = \frac{Z(w)}{Z} \tag{5.19}$$

and, by construction,

$$\sum_{w=-\infty}^{\infty} p_w = 1\,. \tag{5.20}$$

Fortunately, it is possible to calculate p_w explicitly. To do so we have to use the known identity

$$\int_0^{\infty} \mathrm{d}x\, \mathrm{e}^{-ax} I_\nu(x) = \frac{1}{\sqrt{a^2-1}}(a + (\sqrt{a^2-1}))^{-\nu}\,. \tag{5.21}$$

By combining Eqs. (5.6), (5.17) and (5.21) we now obtain the following result:

$$\begin{aligned} Z &= \int \mathrm{d}^2 r\, G_N(r_1 = r_2 = r; \theta = 2\pi) \\ &= \lim_{a\to 1^+} \frac{Nl}{2} C \sum_{m=-\infty}^{\infty} \int_0^{\infty} \mathrm{d}x\, \mathrm{e}^{-ax} I_{|m|}(x) \\ &= \frac{Nl}{2} C \sum_{m=-\infty}^{\infty} \frac{1}{\sqrt{2\varepsilon}} (1+\sqrt{2\varepsilon})^{-|m|}, \quad \varepsilon = a-1\,. \end{aligned} \tag{5.22}$$

Similarly, we also obtain

$$\begin{aligned} Z(w) &= \int \mathrm{d}^2 r\, G_N(r_1 = r_2 = r; \theta = 2\pi w) \\ &= \lim_{a\to 1^+} \frac{Nl}{2} C \int_{-\infty}^{\infty} \mathrm{d}\lambda\, \mathrm{e}^{\mathrm{i}\lambda 2\pi w} \int_0^{\infty} \mathrm{d}x\, \mathrm{e}^{-ax} I_{|\lambda|}(x) \\ &= \frac{Nl}{2} \frac{C}{\sqrt{2\varepsilon}} \int_{-\infty}^{\infty} \mathrm{d}\lambda\, \mathrm{e}^{-\mu|\lambda| + \mathrm{i}\lambda 2\pi w}\,, \end{aligned} \tag{5.23}$$

where in the last line we have introduced $\mu = \ln(1+\sqrt{2\varepsilon})$. Using Eqs. (5.23), (5.22) and (5.19) we obtain

$$p_w = \lim_{\varepsilon\to 0^+} \frac{\int_{-\infty}^{\infty} \mathrm{d}\lambda\, \mathrm{e}^{\mathrm{i}\lambda 2\pi w - \mu|\lambda|}}{\sum_{m=-\infty}^{\infty} \mathrm{e}^{-\mu|m|}}\,. \tag{5.24}$$

Use of Eq. (5.8) indicates that p_w obeys the normalization condition given by Eq. (5.20) as required. It is very important to notice that p_w is independent of the length of the chain N as well as of l. This fact underscores the topological nature of p_w. In reality, however, p_w may depend upon the physical characteristics of the polymer involved in our problem. Indeed, let the diameter of our hole be of order l. Then, if the length of the polymer chain is N, the winding number w cannot be larger than N/l. Consider now the denominator of Eq. (5.24) with such restriction. We obtain

$$\sum_m{}' \mathrm{e}^{-\mu|m|} = 1 + 2\frac{\mathrm{e}^{-\mu} - \mathrm{e}^{-\frac{N}{l}\mu}}{1-\mathrm{e}^{-\mu}}\,. \tag{5.25}$$

The limiting procedure $\varepsilon \to 0^+, l \to 0^+$ with the constraint $\mu/l \to c$ so that $Nc \leq 1$ brings the above expression to the following form:

$$\sum_m{}' \, \mathrm{e}^{-\mu|m|} \simeq \frac{2}{\mu}\mathrm{e}^{Nc}(\mathrm{e}^{-Nc} - \mathrm{e}^{-2Nc}) \simeq \frac{2}{\mu}\mathrm{e}^{Nc}\, Nc\,. \tag{5.26}$$

Finally, let us consider p_0 which is the probability that our ring is not entangled with the hole. Evidently p_0 is a two-dimensional analogue of ζ_N introduced in Section 3.1. To calculate p_0 we only have to put $w = 0$ in the numerator of Eq. (5.24) and to combine the result with Eq. (5.26). Whence, we obtain

$$p_0 = \mathrm{e}^{-Nc}/Nc\,. \tag{5.27}$$

Let $-c = \ln\tilde{\mu}$ then we can rewrite p_0 as

$$p_0 = \frac{1}{N\ln(1/\tilde{\mu})}\tilde{\mu}^N \equiv \tilde{c}(N)\tilde{\mu}^N\,. \tag{5.28}$$

This result, indeed, resembles Eq. (3.3) (since $\alpha = 0$ in Eq. (3.3)). The main conclusion of this derivation lies in acknowledging *that the functional form of p_0 reflects the role of the finite size corrections in the topological problem*. We had introduced already N_T in Section 3.1 which is also a nonuniversal and lattice-dependent quantity to be calculated in Section 7. Whence, in dealing with real polymers *the topological and nontopological properties are essentially interrelated*. The result for p_0 obtained above has very suggestive thermodynamic appearance. We would like to demonstrate that, indeed, this expression (as well as Eq. (3.3)) has well-defined thermodynamic (statistical mechanics) meaning. To see this, we need to take another look at the whole problem discussed in Section 5.1.

5.2. Quantum groups and planar Brownian motion

To develop an alternative approach to the whole problem the following identity:

$$\int_0^\infty \mathrm{d}x\, x\mathrm{e}^{-\rho x^2} J_\nu(\alpha x)\, J_\nu(\beta x) = \frac{1}{2\rho}\exp\left\{-\frac{\alpha^2+\beta^2}{4\rho}\right\} I_\nu\left(\frac{\alpha\beta}{2\rho}\right), \tag{5.29}$$

where the modified Bessel function $I_\nu(z)$ is related to the usual Bessel function $J_\nu(z)$ via $I_\nu(z) = \mathrm{e}^{-\mathrm{i}\nu\pi/2}J_\nu(z)$, is the most helpful.

By comparing Eqs. (5.5) and (5.29) we immediately obtain:

$$G_N(r_1, r_2; \theta) = \hat{c}\sum_{m=-\infty}^{\infty} \mathrm{e}^{\mathrm{i}m\theta}\int_0^\infty \mathrm{d}x\, x\mathrm{e}^{-\frac{Nl}{4}x^2} J_m(r_1 x) J_m(r_2 x)\,, \tag{5.30}$$

where, as before, the constant $\hat{c}$ is fixed by normalization. Let us recall (Vilenkin, 1968) that the functions $\mathrm{e}^{\mathrm{i}m\alpha}J_m(Rr)$ are the eigenfunctions of the two-dimensional Laplace operator ∇^2 (written in polar coordinates) corresponding to the eigenvalue $-R^2$. If $Nl/4$ in Eq. (5.30) is interpreted as Euclidean time, then Eq. (5.30) can be interpreted in terms of the usual Green's functions so that

$$Z = 2\pi\int_0^\infty \mathrm{d}r\, r\, G_N(r_1 = r_2 = r; \theta = 2\pi) \tag{5.31}$$

is the partition function in the usual statistical mechanics sense. Whence, *in order to obtain Z it is essential to know the eigenfunctions and the eigenvalues of the corresponding "Hamiltonian" operator which, in turn, can be obtained in a group-theoretic fashion* (Vilenkin, 1968). Such a derivation is in complete accord with the group-theoretic formulation of knot theory (Gilbert and Porter, 1994; Chari and Pressley, 1995).

Let us begin with the observation that each point $p(x,y)$ in two-dimensional plane can be carried by the motion in the plane into the point $p(x^1,y^1)$, where

$$x^1 = x\cos\alpha - y\sin\alpha + a\,, \qquad y^1 = x\sin\alpha + y\cos\alpha + b\,. \tag{5.32}$$

The parameters, a,b,α which uniquely determine the motion are given by

$$-\infty < a < \infty\,, \qquad -\infty < b < \infty\,, \qquad 0 \le \alpha < 2\pi\,.$$

To proceed, we introduce the vectors $\boldsymbol{\xi} = (a,b)$, $\boldsymbol{x} = (x,y)$ and the matrix $\mathbf{A}$ so that Eq. (5.32) can be rewritten as

$$\boldsymbol{x}^1 = \mathbf{A}\boldsymbol{x} + \boldsymbol{\xi}\,. \tag{5.33}$$

The transformation in the plane is fully determined by the pair $(\mathbf{A},\boldsymbol{\xi})$. Consider now two successive transformations in the plane. Then, their composition $\circ$ is given by

$$(\mathbf{A},\boldsymbol{\xi})\circ(\mathbf{B},\boldsymbol{\eta}) = (\mathbf{A}\cdot\mathbf{B}, \boldsymbol{\xi} + \mathbf{A}\cdot\boldsymbol{\eta}) \tag{5.34}$$

which defines a semidirect product of the groups of additive translations E_2 and the group of rotations $SO(2)$ (Vilenkin, 1968). Instead of working with the semidirect product of two groups it is more convenient to enlarge the vector space $\boldsymbol{x}$ to make it three dimensional. For such enlarged space it is possible to introduce the matrix $\mathbf{T}(g)$ given by

$$\mathbf{T}(g) = \begin{pmatrix} \cos\alpha & -\sin\alpha & a \\ \sin\alpha & \cos\alpha & b \\ 0 & 0 & 1 \end{pmatrix}. \tag{5.35}$$

For such a defined matrix $\mathbf{T}(g)$ a usual group composition law holds

$$\mathbf{T}(g_1)\cdot\mathbf{T}(g_2) = \mathbf{T}(g_1\cdot g_2)\,,$$

where $\cdot$ denotes the usual matrix multiplication. The matrix $\mathbf{T}(g)$ provides a representation of the group $M(2)$. If $*$ denotes a semidirect product, then $M(2) = E_2{*}SO(2)$. The Lie algebra of the above group is formed by three elements a_1, a_2 and a_3, which obey the following commutation relations (Vilenkin, 1968):

$$[a_1,a_2] = 0\,, \qquad [a_2,a_3] = a_1\,, \qquad [a_3,a_1] = a_2\,. \tag{5.36}$$

where $[a,b] = ab - ba$, as usual. This Lie algebra is very similar to that used for the angular momentum in quantum mechanics and, whence, the subsequent steps of analysis are the same. One introduces the raising and lowering operators $a^{\pm} = a_1 \pm \mathrm{i}a_2$ so that eigenfunctions can be described in terms of two quantum numbers n and R (see, e.g. Eq. (5.30)), where the quantum number R is defined according to the equation,

$$a^+a^-f_n(R) = -R^2 f_n(R) \tag{5.37}$$

while the quantum number n is defined with the help of

$$a_3 f_n(R) = inf_n(R)\,, \tag{5.38}$$

etc.

The task now is to demonstrate that the commutation relations (*Eq.* (5.36)) *can be obtained from the NACSFT.*

To this purpose, using results of Sections 4.2 and 4.3 and choosing instead of the group $SU(\hat{N})$ another group, e.g. $GSU(2)$, Armand-Ugon et al. (1996), we can obtain, instead of HOMFLY, the Dubrovnik polynomial which is characterized by the following set of skein relations (Kauffman, 1990):

$$D_{\times} - D_{\times} = z\,(D_{\cup} - D_{)(})\,, \tag{5.39}$$

$$D_{\circlearrowleft} = aD_{\cap}\,,\ D_{\circlearrowright} = a^{-1}D_{\cap}\,, \tag{5.40}$$

$$D[U_0] = (a - a^{-1})/z + 1\,. \tag{5.41}$$

Actually, the last result for the unknot is taken from the Armand-Ugon et al. (1996). It is motivated by the same arguments as were presented in Section 4.3, i.e. by the difference in normalization: in mathematics literature (Kauffman, 1990, 1996),

$$D[U_0] = 1\,, \tag{5.42}$$

and in physics literature, see, e.g. Eq. (4.46). Dubrovnik polynomial is an invariant of regular isotopy. As before, see, e.g. Eq. (4.55), one can make an invariant of ambient isotopy using D_K via (Kauffman, 1987)

$$G_K = \alpha^{-W_r[K]} D_K\,. \tag{5.43}$$

Let $W_\rho(c)$ be a Wilson loop operator, e.g. see Eq. (4.27). Following Martin (1989) and Turaev (1989) one can define a Poisson bracket via

$$\{W_\rho(c), W_\rho(c')\}_{\text{P.B.}} = \sum_{c''} S_{cc'}^{c''} W_\rho(c'')\,, \tag{5.44}$$

where, in case of Dubrovnik polynomial, the structure constants $S_{cc'}^{c''}$ are defined by the symbolic rule

$$\{\,/\,,\,\backslash\,\}_{\text{P.B.}} = z\,[\asymp -)(]\,. \tag{5.45}$$

Evidently, Eqs. (5.39) and (5.44) are equivalent and, whence, nonsurprisingly this fact is used in the nonperturbative quantum gravity (Martin, 1989; Armand-Ugon et al., 1996). For us it is important only that one can formally quantize such "*mechanics*" *via the usual rule*

$$\{\,,\}_{\text{P.B.}} \Rightarrow \frac{1}{i\hbar}[\,,\,]\,, \tag{5.46}$$

i.e. it is possible to define a Lie algebra where, instead of the Poisson brackets, the usual commutators are being used. With these remarks, it is easy now to make connection between the

knot polynomials and the commutator algebra given by Eq. (5.36). Indeed, to this purpose, let us consider yet another invariant of regular isotropy, the Kauffman polynomial, which also can be obtained with the help of NACSFT (Guadagnini, 1993). It is defined axiomatically through the following set of skein relations:

$$\langle \times \rangle = A\langle \asymp \rangle + B\langle \,)(\rangle\,, \tag{5.47}$$

$$\langle \times \rangle = B\langle \asymp \rangle + A\langle \,)(\rangle\,, \tag{5.48}$$

$$\langle \bigcirc \cup K \rangle = \tilde{d}\langle K \rangle\,, \tag{5.49}$$

$$\langle \bigcirc \rangle = 1\,. \tag{5.50}$$

The last relation is, of course, unnecessary if the NACSFT is used. The constants $A, B, \tilde{d}$ are arbitrary in the above axiomatic formulation, but are fixed in NACSFT and by the requirements of invariance with respect to the Reidemeister moves, Fig. 6, as will be further explained below in this section. By combining Eqs. (5.47) and (5.48) we obtain

$$\langle \times \rangle - \langle \times \rangle = (A - B)\left[\langle \asymp \rangle - \langle \,)(\rangle\right]. \tag{5.51}$$

This skein relation looks exactly the same as for the Dubrovnik polynomial, Eq. (5.39) so that, indeed these two polynomials are interrelated (Kauffman, 1990). At the same time, by combining Eqs. (5.47) and (5.48) in a different way we obtain as well

$$\frac{1}{B}\langle \times \rangle - \frac{1}{A}\langle \times \rangle = \hat{Z}\langle \asymp \rangle\,, \tag{5.52}$$

$$\frac{1}{A}\langle \times \rangle - \frac{1}{B}\langle \times \rangle = -\hat{Z}\langle \,)(\rangle\,, \tag{5.53}$$

where $\hat{Z} = (A/B - B/A)$. Using results of Eqs. (5.43) and (5.45) we conclude that, upon proper rescaling and quantization, Eqs. (5.52) and (5.53) can be identified with the second and the third of Eq. (5.36). Notice that, on one hand, $[a_1, a_1] = 0$, but, on the other, using the Jacobi identity, we can obtain

$$[a_1,[a_2,a_3]] = -[a_2,[a_3,a_1]] - [a_3,[a_1,a_2]]\,.$$

From here and in view of Eq. (5.36) we conclude that there are two options:

$$[a_1, a_2] = 0 \tag{5.54}$$

or

$$[a_1, a_2] = a_3\,. \tag{5.55}$$

The first option leads to the complete set of commutators given by Eq. (5.36) while the second leads to the Lie algebra $SL(2,C)$, which can be obtained from the Virasoro algebra defined by the set of relations

$$[L_n,L_n] = (n-m)L_{n+m} + \frac{c}{12}(n^3 - n)\delta_{n+m,0}\,. \tag{5.56}$$

The $SL(2,C)$ algebra is obtained from the Virasoro if we put the central charge $c = 0$. In this case, instead of Eq. (5.56) we obtain

$$[L_1, L_0] = L_1 \,, \tag{5.57}$$

$$[L_{-1}, L_0] = -L_{-1} \,, \tag{5.58}$$

$$[L_1, L_{-1}] = 2L_0 \,. \tag{5.59}$$

Let now $a_1 = L_{-1} - L_1, a_2 = -(L_{-1} + L_1)$ and $a_3 = L_0$. Then we obtain

$$[a_2, a_3] = a_1 \,, \qquad [a_3, a_1] = a_2 \,, \qquad [a_1, a_2] = 4a_3 \,. \tag{5.60}$$

This Lie algebra can now be compared with that given by Eq. (5.36). It is actually possible to obtain Eq. (5.36) from Eq. (5.60). To do so, several steps are needed (Vilenkin, 1968), which are similar to that used in the theory of quantum groups (Chari and Pressley, 1995). Notice that if we rescale the operators a_1 and a_2 in Eq. (5.60), e.g. $a_1 \to Aa_1, a_2 \to Aa_2$, then the first two commutators in Eq. (5.60) will not change while the third is going to change into

$$[a_1,a_2] = A^{-2}4a_3 \,. \tag{5.61}$$

Let now $A \to \infty$ so that $A^{-2} = \varepsilon^2 \to 0^+$. Let us introduce $a_1 = a_1^{(0)} + \varepsilon a_1^{(1)}$ and $a_2 = a_2^{(0)} + \varepsilon a_2^{(0)}$. Then, in the limit $\varepsilon \to 0^+$ the operators $a_1^{(0)}$,$a_2^{(0)}$ and a_3 will satisfy the Lie algebra of Eq. (5.36) while the operators $a_1^{(1)}$,$a_2^{(1)}$ and a_3 will obey Eq. (5.60). In the limit $\varepsilon \to 0^+$ their contribution can be ignored.

From the results presented above, several conclusions can be drawn:

(a) the probability p_w given by Eq. (5.24) is of purely topological origin since it is independent of the length of the chain N or the cut-off length l;

(b) the probability p_w can be determined if the eigenfunctions and the eigenvalues of the "topological" Hamiltonian could be obtained in order to construct the statistical mechanics partition function;

(c) the Hamitonian is expected to be some Casimir operator of the corresponding Lie algebra which is directly obtainable by the quantization procedure from the skein relations for some knot polynomials;

(d) in order to utilize the information contained in the partition function, the finite size effects should be properly taken into account.

All the above statements are general enough to be used in more complicated three-dimensional calculations to be discussed below.

5.3. *Jones polynomial, Temperley–Lieb algebra and statistical mechanics of knots* (*links*)

In Section 4.4 we have discussed the remarkable properties of the Jones polynomial which are reflected in Eq. (4.83). We had emphasized that Eq. (4.83) could be very useful in statistical mechanical calculations. Now we would like to develop this statement somewhat deeper. Before doing so, we would like to mention that the property of V_L based on Eq. (4.83) is not the only one which makes V_L so special. Indeed, Jones (1985) (see also Welsh, 1993) had shown that, in addition, V_L has the following basic properties:

(1) For any link L

$$V_L(1) = (-2)^{n(L)-1}\,, \tag{5.62}$$

where $n(L)$ is the number of components of L.

(2) If L is a knot, then

$$V_L(e^{2\pi i/3}) = 1\,. \tag{5.63}$$

(3) If L is a knot, then

$$\left|\frac{dV_L(t)}{dt}\right|_{t=1} = 0\,. \tag{5.64}$$

(4) For the connected sum $L_1 \# L_2$, see e.g. Fig. 7, the polynomial V_L obeys the rule

$$V_{L_1 \# L_2}(t) = V_{L_1}(t) V_{L_2}(t) \tag{5.65}$$

to be compared with Eqs. (4.65) and (4.84).

The above properties of the Jones polynomial should be taken into account in any statistical mechanics application, see, e.g. Wu (1992). To develop statistical mechanics, we shall follow the strategy developed in Section 5.2. Following this strategy, we have to find a set of commutation relations and to look for their representations in order to find the eigenvalues and the eigenfunctions of the corresponding Hamiltonian. Alternatively, we may start with the non-Abelian variant of an expression, like Eq. (4.22), and to use skein relations (and the properties defined by Eqs. (4.66) and (4.70) of knot polynomials) in order to disentangle the Chern–Simons and the polymer averages. After that, we will arrive at some kind of knot polynomial (times the disentangled polymer partition function). Since we will be interested in the ratios, e.g. like that given by Eq. (5.19), the disentangled partition function drops out and we need to analyze only the knot polynomial. Because the Dubrovnik polynomial is related to the Kauffman, we need to study now the Kauffman polynomial.

Let us begin with the observation that the Kauffman polynomial for a given knot K, introduced in the previous section, can be written as (Kauffman, 1990, 1993)

$$\langle K \rangle = \sum_{\{S\}} A^{n_A(S)} B^{n_B(S)} d^{|S|-1} \equiv Z\,, \tag{5.66}$$

where the summation $\{S\}$ takes place over $2^{c(K)}$ states of the planar 4-valent graph with $c(K)$ crossings and $n_A(S), n_B(S)$ correspond to the number of splices of the A- and B-type defined by

$$A\text{-type}: \times \Rightarrow \asymp\,; \quad B\text{-type}: \times \Rightarrow)(\,.$$

Clearly, polynomial $\langle K \rangle$ thus defined has an appearance of the statistical mechanical partition function Z (Baxter, 1982; Wu, 1992), for some two-dimensional spin model defined on such 4-valent graph. The constants A and B in Eq. (5.66) can be considered as some fugacities in the grand canonical formalism. In contrast the partition function Z defined by Eq. (5.31) is written in the canonical formalism. For example, the average winding number $\langle w \rangle$ can be obtained with help of

Eq. (5.19) as

$$\langle w\rangle = \sum_{w=-\infty}^{\infty} w p_w \tag{5.67}$$

while the average number of splices of the A and B-types could be *assigned* by

$$\langle n_A\rangle = A(\partial/\partial A)\ln Z\,, \tag{5.68a}$$

$$\langle n_B\rangle = B(\partial/\partial B)\ln Z\,. \tag{5.68b}$$

So that if $\langle n_A\rangle$ and $\langle n_B\rangle$ are given, then the fugacities A and B are implicitly determined via Eqs. (5.68a) and (5.68b). Unfortunately, the given knot cannot be uniquely characterized by $\langle n_A\rangle$ and $\langle n_B\rangle$ since, as it was discussed in Section 3.3, the combination

$$\langle n_A\rangle + \langle n_B\rangle = c[K] \tag{5.69}$$

is *not* a topological invariant (unlike $u[K]$!). Moreover, as it is written $\langle K\rangle$ is not even an invariant of a regular isotopy. Kauffman (1988) had demonstrated that $\langle K\rangle$ becomes an invariant of a regular isotropy only if $AB = 1$ and $\tilde{d} = -(A^2 + B^2)$. To make an ambient isotopic invariant f out of $\langle K\rangle$ it is sufficient to write

$$f_K(A) = \alpha^{-W_r[K]}\langle K\rangle\,, \quad \alpha = -A^3\,,$$

to be compared with Eq. (4.55). This means, that in case of *standard* framing (see, e.g. Eq. (4.20)) $f_K(A) = \langle K\rangle$. Since, according to Kauffman, the Jones polynomial $V_L(t)$ is related to the Kauffman polynomial via the simple relation

$$V_L(t) = f_K(t^{-1/4})\,, \tag{5.70}$$

one concludes that, at least for the case of standard framing, one can write

$$V_L(t) = \langle K\rangle$$

provided that $AB = 1$, $\tilde{d} = -(A^2 + B^2)$ and $A = t^{-1/4}$. So, formally, by using Eqs. (4.83), (5.68a), (5.68b) and (5.69) we obtain

$$c[K] = t - span\, V(t) = \left(A\frac{\partial}{\partial A} + B\frac{\partial}{\partial B}\right)\ln Z\Big|_{\substack{B=A^{-1}\\ \tilde{d}=-(A^2+B^2)\\ A=t^{-\frac{1}{4}}}} \tag{5.71}$$

In Section 3 we have learned that for a given $c[K]$, the number of possible knots $K(n)$ is bound by the inequality (Eq. (3.14)). Since in Eq. (3.7) we had shown (see also Section 7) that $\langle c[K]\rangle \propto N^{\alpha_c}$ we conclude that by prescribing particular value for $c[K]$, the statistical mechanics of knots becomes quite well defined through Eqs. (5.66), (5.68a), (5.68b), (5.69), (5.70) and (5.71). Eqs. (5.68a) and (5.68b) are three-dimensional analogues of Eq. (5.67). In Section 5.1 we have discussed the role of the finite size effects. They will show up in Eq. (5.67) if we realize that for the polymer chain of length N and Kuhn's length l the winding number cannot take infinite values and

is always restricted by N/l. The quantity $c[K]$ plays *the same role* in three dimensions as N/l in two. This is so because $\langle c[K]\rangle \propto N^{\alpha_c}$, i.e. by assigning the effective polymer length N/N_T, where N_T was defined in Section 3.1, we automatically introduce a physical cut-off into the problem.

The question arises: what is the three-dimensional analogue of p_0 (Eq. (5.28)) and how is it calculated. We claim that ζ_N introduced in Eq. (3.3) is the three-dimensional analog of p_0. To calculate ζ_N, several steps are still required. First, by analogy with Eq. (5.19) we can write

$$\zeta_N = \frac{Z(U_0)}{Z}. \tag{5.72}$$

But $Z(U_0) = V_{U_0} = 1$ according to Eq. (4.51). Whence, we can write as well (for $N \to \infty$)

$$\zeta_N^{-1} = Z. \tag{5.73}$$

Next, following Kauffman (1988), it is convenient to define the bracket polynomial $[K]$ which is related to $\langle K\rangle$ in a straightforward way

$$\langle K\rangle = \tilde{d}^{-1}[K]. \tag{5.74}$$

For this polynomial the relations of Eqs. (5.47), (5.48) and (5.49) hold (with $\langle \cdots \rangle$ being replaced by $[\cdots]$) but Eq. (5.50) is being replaced by

$$[\bigcirc] = \tilde{d}. \tag{5.75}$$

This makes the polynomial $[K]$ more physical, e.g. see the discussion leading to Eq. (4.69), since it can be obtained from the NACSFT. Alternatively, $[K]$ can also be obtained from the graph expansion for the Potts model (Kauffman, 1987a,b). In this case it is sufficient only to assign a particular value to the coefficients A, B and $\tilde{d}$ for the defining relations for the bracket polynomial $[K]$. Specifically, instead of Eqs. (5.47), (5.48), (5.49) and (5.50), following Kauffman (1987a), we write

$$[\rangle\!\langle] = [)(] + q^{-1/2}v\,[][], \tag{5.76}$$

$$[\rangle\!\langle] = q^{-1/2}v\,[)(] + [][], \tag{5.77}$$

$$[\bigcirc K] = -q^{1/2}[K], \qquad [\bigcirc] = -q^{1/2}, \tag{5.78}$$

where in the last two equations we have changed the sign " + " to " − " (as compared to Kauffman, 1987a) for reasons which will become clear shortly below. For an alternative explanation of the switch of signs, please consult Kauffman and Saleur (1993). The physical meaning of constants q and v will also be explained shortly below.

At this stage it is convenient to introduce the concept of braids and braid generators σ_i. Braids are formed when n points on a horizontal line are connected by n "strings" to n points on another horizontal line being directly below the first n points. A general n-braid is constructed from the trivial braid by successive applications of the braid generators σ_i, $i = 1, \ldots, n$. By regarding the trivial n-braid as an identity operator (generator) a set of generators σ_i define the braid group B_n. Given a particular n-braid, some link (or knot) can be formed by tying the opposite ends (i.e. connecting the inputs of the strings with the outputs in some prescribed way: normally the

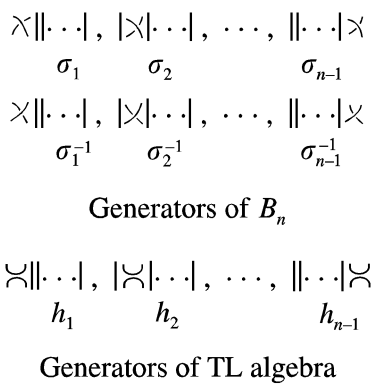

Fig. 9. Diagrammatic representation of the braid group generators σ_i and associated with them the Temperly–Lieb generators h_i.

beginning of a given string is tied with its end, thus forming a closed braid). According to Wadati et al. (1989), any link (knot) can be represented by a closed braid. This representation is highly nonunique, however. The equivalent braids expressing the same link are mutually transformed by successive applications of Markov moves of types I and II, which for braids play the same role as the Reidemeister moves, see, e.g. Fig. 6, for knots. Following Kauffman (1990), it is more useful to introduce a set of generators h_i related to σ_i as it is depicted in Fig. 9. Let b represent some braid and $[b]$ represent the value of the bracket polynomial on a *closed* braid $\bar{b}$, i.e. $[b] = [\bar{b}]$.

Using Eqs. (5.76a) and (5.77a), we obtain

$$\begin{aligned}[\sigma_i] &\equiv [\| \cdots |\rangle\langle| \cdots \|] \\ &= q^{\frac{1}{2}} v\,[\| \cdots |\rangle\!\langle| \cdots \|] + [\| \cdots |\|| \cdots \|] \\ &\equiv q^{\frac{1}{2}} v\,[h_i] + [1_i]\,. \end{aligned} \tag{5.79}$$

With the help of Eq. (5.79) we can write

$$\sigma_i = q^{-1/2} v h_i + 1_i\,, \qquad \sigma_i^{-1} = h_i + q^{-1/2} v 1_i\,. \tag{5.80}$$

The Temperly–Lieb (TL) algebra can now be written as follows:

$$h_i^2 = q^{1/2} h_i\,, \qquad h_i h_{i+1} h_i = h_i\,, \qquad h_i h_j = h_j h_i\,, \quad |i-j| \geq 2\,. \tag{5.81}$$

By simple rescaling of TL generators: $h_i = q^{1/2} e_i$ we arrive at the form of TL algebra discussed by Jones (1985):

$$e_i^2 = e_i\,, \qquad e_i e_{i+1} e_i = (1/q) e_i\,, \qquad e_i e_{j=} e_j e_i\,, \quad |i-j| \geq 2\,. \tag{5.82}$$

The TL algebra, Eq. (5.82), replaces the Lie algebra of the group $M(2)$, Eq. (5.36), and is directly related to the Potts model, (Baxter, 1982; Kauffman and Saleur, 1993), on one hand, and to the Jones polynomial $V_K(t)$, (Jones, 1985) on the other. In particular, following the original work of (Jones, 1985), q^{-1} in the second relation of Eq. (5.82) corresponds to his $t/(t+1)^2$ where variable t is the same as in the skein relation given by Eq. (4.50). At the same time, q represents the number

of states of the Potts model (Baxter, 1982; Kauffman and Saleur, 1993) defined by the following partition function:

$$Z_G(q,v) = \sum_{\{s\}} \exp\left\{K \sum_{\langle i,j\rangle} \delta(s_i, s_j)\right\} = \sum_{\{s\}} \prod_{\langle i,j\rangle} (1 + v\delta(s_i, s_j)) \,, \tag{5.83}$$

where $v = \exp\{K\} - 1$, $\langle i,j\rangle$ denotes the nearest neighbors and $\{s\}$ denotes the summation over q states at each site (vertex) of some planar graph G with the total number of sites $c[K]$. It is possible to introduce an alternating link (knot) associated with G (Kauffman, 1988; Baxter, 1982). In terms of such alternating link (or rather its planar projection), the partition function $Z_G\,(q,v)$ can be written as

$$Z_G(q,v) = q^{c[K]/2}[K(G)] \tag{5.84}$$

with $[K(G)]$ being defined through Eqs. (5.74)–(5.78). Finally, let us recall that, according to the results of Section 4, the NACSFT provides us with the value of $\sqrt{t} = \exp\{i\pi/(k + \hat{N})\}$, see, e.g. Eqs. (4.49) and (4.50). This implies that

$$q = \frac{(1+t)^2}{t} = \left(\sqrt{t} + \frac{1}{\sqrt{t}}\right)^2 = 4\cos^2\left(\frac{\pi}{k+\hat{N}}\right). \tag{5.85}$$

We had shown before, see, e.g. Eqs. (4.47) and (4.49), that $\hat{N} = 2$. Because k can take only integer values (Witten, 1989a), we obtain the following Beraha numbers (Saleur, 1990) for q:

$k = 0, \quad q = 0$ (random resistors network, Wu (1982));
$k = 1, \quad q = 1$ (percolation, Wu (1982));
$k = 2, \quad q = 2$ (Ising model, Wu (1982));
$k \to \infty\,, \quad q = 4$ (four colors problem, Wu (1982)).

In view of Eqs. (5.70), (5.74) and (5.85), we observe that since $V_K(t)$ is the invariant of *ambient* isotopy, we must require $[K(G)]$ to be *at least* an invariant of a *regular* isotopy (i.e. an invariant under the 2nd and 3rd type of Reidemeister moves, e.g. see Fig. 6). Using Eqs. (5.75)–(5.78) we have

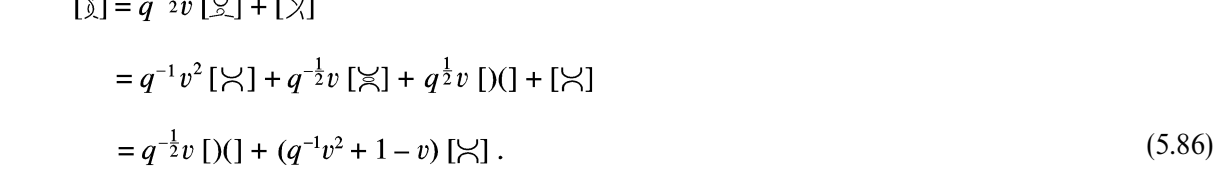

$$= q^{-1}v^2\,[\asymp] + q^{-\frac{1}{2}}v\,[\asymp] + q^{\frac{1}{2}}v\,[)(] + [\asymp]$$

$$= q^{-\frac{1}{2}}v\,[)(] + (q^{-1}v^2 + 1 - v)\,[\asymp]\,. \tag{5.86}$$

The equation obtained leads us to the conclusion that in order for $K[(G)]$ to become an invariant of a regular isotopy, we must require

$$q^{-1}v^2 + 1 - v = 0\,. \tag{5.87}$$

Using methods analogous to that described in Kauffman (1988), it can be also easily shown that the invariance of $[K(G)]$ under the 3rd Reidemeister move will also hold if the requirement of Eq. (5.86)

is satisfied. Using Eq. (5.86) we obtain

$$v^2 - qv + q = 0$$

or

$$v_{1,2} = (q/2) \pm \sqrt{(q^2/4) - q}\,. \tag{5.88}$$

From here, it follows that $q \geq 4$ in order for v to be real. But, according to Eq. (5.85), we have $q \leq 4$. Hence, the only choice we have is $q = 4$. Because of the connection between $[K(G)]$ and the Potts model given by Eq. (5.84), there is yet another reason for q to be equal to 4. For the Potts model, the criticality condition is given by the following equation (Baxter, 1982):

$$q^{-1}v^2 = 1\,. \tag{5.89}$$

Combining Eq. (5.87) with Eq. (5.89) produces $v = 2$ and, whence, according to Eq. (5.89), we obtain again $q = 4$. Notice that the above derivation is possible only with the choice of signs indicated in Eqs. (5.76)–(5.78). From here we conclude that in order for $[K(G)]$ to be a regular isotopy invariant, we have to require $q = 4$ and for the corresponding Potts model to be critical. Moreover, at criticality, in view of Eq. (5.70), the above polynomial is also an invariant of ambient isotopy and, whence, is directly connected with the Jones polynomial. According to Wadati et al. (1989), the restricted 8-vertex SOS model at criticality can also be solved by TL algebra, Eq. (5.82), exhibiting the exponents Δ which are directly obtainable from the Virasoro algebra, Eq. (5.56), with $c = 1 - 6/k(k+1)$ and $\Delta = (p^2 - 1)/2k(k+1)$ with $k = 2, 3, 4 \ldots$; $1 \leq p \leq k - 1$. Whence, in principle, TL and Virasoro algebras are interrelated and, in part, this was demonstrated in Section 5.2. This circumstance allows us to transfer results and the experience of two-dimensional problems discussed in Section 5.2 to three dimensions.

5.4. Probability of knotting and the role of finite size effects

We would like to remind the reader at this point that the probability ζ_N for the closed circular polymer of the effective length N/N_T to remain unknotted was introduced in Section 3 while Eq. (5.73) provides the explicit link with statistical mechanics thus allowing us to calculate ζ_N. Using Eqs. (5.73)–(5.78) we obtain as well

$$\zeta_N^{-1} = \frac{(-1)}{q^{1/2}}[K(G)]\,. \tag{5.90}$$

The factor (-1) is chosen in accord with Eq. (5.78). This means that after unknotting the knot K with the help of skein relations, Eqs. (5.76) and (5.77), we shall obtain a polynomial times the unknot so that the minus sign disappears. More generally, we expect the product of unknots times the polynomial. Each of these unknots will carry a factor of $(-1)q^{1/2}$. For the graph of $c[K]$ vertices we will have a factor of $(-1)^{c[K]}q^{q[K]}$. Looking at Eq. (5.84) and, in view of Eq. (5.83), we know (Adams, 1994; Baxter, 1982), that

$$Z_G(q, v) = q^{c[K]} + \cdots\,. \tag{5.91}$$

This requires us to write, instead of Eq. (5.90),

$$\zeta_N^{-1} = \left.\frac{Z_c(q, v)}{(-1)^{c[K]-1}q^{\frac{c[K]+1}{2}}}\right|_{q=v^2=4}. \tag{5.92}$$

The exact solution for the Potts model at *criticality* (*for* $q = 4$) is known (Baxter, 1982; Wu, 1982). Depending upon the geometry of the lattice we obtain

$$f = \frac{1}{c[K]} \ln Z_G = \begin{cases} \ln\left[\frac{1}{8}\left[\frac{\Gamma(\frac{1}{4})}{\Gamma(\frac{3}{4})}\right]^4\right] & \text{(square lattice)} \\ \ln\left[2\left[\frac{\Gamma(\frac{7}{6})\ \Gamma(\frac{1}{3})}{\Gamma(\frac{2}{3})\ \Gamma(\frac{5}{6})}\right]^3\right] & \text{(triangular lattice)} \end{cases} \tag{5.93}$$

In order to use this result in Eq. (5.92) we have to remember that Eq. (5.93) was actually obtained in the thermodynamic limit, i.e. for $c[K] \to \infty$. In reality, in order to make a comparison with numerical simulations discussed in Section 3, e.g. see Eq. (3.3), Eq. (5.93) should be augumented with the finite size corrections.

Let our lattice contain $c[K] = L \times M$ sites, then the partition function Z_G can be written (Karowski, 1988; William, 1991), as

$$Z_c \simeq \exp\left\{ - LMf + \frac{L}{M}\frac{\pi}{6}c \right\} \tag{5.94}$$

where f is the corresponding free energy defined in Eq. (5.93) while c is the central charge, e.g. see Eq. (5.56), which, for the Potts model with $q = 4$, is equal to one (Dotsenko and Fateev, 1984). If $M \simeq L$, then by combining Eqs. (3.3), (5.92) and (5.94) we obtain,

$$\begin{aligned} \zeta_N &= \sqrt{q}\exp\left\{ - \frac{\pi}{6}c \right\}\exp\left\{ c[K]\left[f + \frac{1}{2}\ln q \right] \right\} \\ &= \sqrt{q}\exp\left\{ - \frac{\pi}{6}c \right\}\tilde{\mu}^{c[K]}. \end{aligned} \tag{5.95}$$

The last equation defines $\tilde{\mu}$. Since $\tilde{\mu}$ can be eliminated according to Eqs. (3.4) and (3.5) we are left with expression for $\tilde{c}$ defined in Eq. (3.3):

$$\tilde{c} = 2\exp\left\{ - \frac{\pi}{6} \right\}. \tag{5.96}$$

The numerical value of $\tilde{c} = 1.1847697$ differs from the numerically obtained $\tilde{c} = 1.2325$ by Windwer (1990) with error of 4%. The result of Eq. (5.96) is in qualitative accord with that obtained by Sumners and Whittington (1988) and by Pippenger, Eq. (3.2). It is documented in Kleinert (1995) and was earlier announced in Kholodenko (1991, 1994).

6. Single chain problems which involve geometrical and topological constraints

6.1. Semi-flexible polymer chain in the nematic environment

The conformational statistics of fully flexible chains is well described by the Klein–Gordon like Gaussian propagators, Zinn-Justin (1993). The situation changes dramatically when the effects of

rigidity should be taken into account. As it was argued in Kholodenko (1995), there is an infinity of propagators which are capable, in principle, of describing semi-flexible chains. Here we shall not go into the full details of this very broad subject. The interested reader may consult Kholodenko (1995) and Ambjorn et al. (1977) and references therein. Here we shall illustrate only some aspects of conformational statistics of semi-flexible chains which involve the geometrical and (or) topological constraints. In particular, we would like to dicuss how the choice of framing affects the conformational statistics of polymers.

To illustrate its effect on chain flexibility, let us recall that the traditionally used Kratky–Porod (KP) model of semiflexible chains (Kleinert, 1995) involves the KP propagator given by

$$G(\boldsymbol{u}_f, \boldsymbol{u}_i; N) = \int_{\boldsymbol{u}(0)=\boldsymbol{u}_i}^{\boldsymbol{u}(N)=\boldsymbol{u}_f} D[\boldsymbol{u}(\tau)]\,\delta(\boldsymbol{u}^2 - 1)\exp\left\{-\frac{\gamma}{2}\int_0^N \mathrm{d}\tau\left(\frac{\mathrm{d}\boldsymbol{u}}{\mathrm{d}\tau}\right)^2\right\} \tag{6.1}$$

with γ being some phenomenological rigidity parameter. The geometrical constraint $\boldsymbol{u}^2 = 1$ in the path integral measure in Eq. (6.1) converts the Brownian motion in $\mathbf{R}^3$ into the Brownian motion on the unit sphere S^2. Analogously to the flat $\mathbf{R}^3$ case, the diffusion on S^2 can be described in terms of the corresponding Schrödinger-like diffusion equation which in quantum mechanics is known as an equation for the rigid rotator. Since we are going to use the results for the rigid rotator in Section 7, we shall describe here the properties of the rigid rotator model which we shall use later. To do so, we would like to simplify our task by considering, instead of the diffusion on the sphere, the diffusion on the circle. In this case the Hamiltonian $\hat{H}_\phi$ is given by (Kholodenko and Vilgis, 1995)

$$\hat{H}_\phi = -\frac{\gamma}{2}\frac{\mathrm{d}^2}{\mathrm{d}\phi^2} \tag{6.2}$$

with dimensionless eigenvalues E_l given by $E_l = \frac{1}{2}l^2$, $l = 0, \pm 1, \pm 2, \ldots$ and eigenfunctions $\psi_l = \dfrac{1}{\sqrt{2\pi}}\exp(\mathrm{i}l\phi)$. This form of the eigenfunctions comes from the periodic boundary condition requirement:

$$\psi_l(\phi + 2\pi) = \psi_l(\phi)\,. \tag{6.3}$$

As we shall see in Section 6.2, there are physical situations when it is possible to generalize the condition of Eq. (6.3) by requiring instead

$$\psi_l(\phi + 2\pi) = \exp(-\mathrm{i}\theta)\psi_l(\phi)\,, \tag{6.4}$$

where $0 \le \theta < 2\pi$. This leads to the wave function

$$\psi_l(\phi) = (1/2\pi)\exp\{\mathrm{i}(l - \theta/2\pi)\phi\} \tag{6.5}$$

which produces the eigenvalue

$$E_l = \tfrac{1}{2}[l - \theta/2\pi]^2\,. \tag{6.6}$$

Instead of dealing with the untraditional boundary condition, e.g. Eq. (6.4), it is possible to replace it by the conventional one, Eq. (6.2), provided that the Hamiltonian of Eq. (6.1) is being replaced by

$$\hat{H}^\theta_\phi = (\gamma/2)[\mathrm{i}(\mathrm{d}/\mathrm{d}\phi) + \theta/2\pi]^2\,. \tag{6.7}$$

At the *classical* level this Hamiltonian comes from the Lagrangian L_θ given by

$$L_\theta = (\gamma/2)[(\mathrm{d}\phi/\mathrm{d}t)^2 + (\theta/2\pi)\mathrm{d}\phi/\mathrm{d}t]\,. \tag{6.8}$$

Since the last term in Eq. (6.8) is a total time derivative, it seems natural that it may be discarded. This is *not* exactly the case at the quantum level in view of Eq. (6.6). The corresponding Euclidean path integral which describes the diffusion on the unit circle is given by

$$G(\boldsymbol{u}_f,\boldsymbol{u}_i;N) = \int_{\boldsymbol{u}(0)=\boldsymbol{u}_i}^{\boldsymbol{u}(N)=\boldsymbol{u}_f} \mathrm{D}[\boldsymbol{u}(\tau)]\,\delta(\boldsymbol{u}^2-1) \times \exp\left\{-\frac{\gamma}{2}\int_0^N \mathrm{d}\tau\left(\frac{\mathrm{d}\boldsymbol{u}}{\mathrm{d}\tau}\right)^2 + \mathrm{i}\frac{\theta}{2\pi}\int_0^N \mathrm{d}\tau\frac{\mathrm{d}}{\mathrm{d}\tau}\tan^{-1}\left[\frac{u_y}{u_x}\right]\right\}. \tag{6.9}$$

The last term in the exponent is just the winding number introduced earlier in Eq. (5.2) as can be easily shown, e.g. see Kholodenko and Vilgis (1994). Since this path integral is related to the completely solvable quantum mechanical problem, see, e.g. Eqs. (6.5) and (6.6), we can analyze its properties in some detail. To this purpose let us introduce the generating function $F(\boldsymbol{p})$ given by

$$F(\boldsymbol{p}) = \left\langle \exp\left(\mathrm{i}\boldsymbol{p}\cdot\int_0^N \boldsymbol{u}(\tau)\,\mathrm{d}\tau\right)\right\rangle, \tag{6.10}$$

where the average $\langle\cdots\rangle$ is performed with help of Eq. (6.9) provided that $\boldsymbol{u}_i = \boldsymbol{u}_f = \boldsymbol{u}$. Using Eq. (6.10) we obtain the following expansion for $F(\boldsymbol{p})$:

$$\begin{aligned} F(\boldsymbol{p}) &= \left\langle \exp\left(\mathrm{i}\boldsymbol{p}\cdot\int_0^N \boldsymbol{u}(\tau)\,\mathrm{d}\tau\right)\right\rangle \\ &= 1 + \mathrm{i}\boldsymbol{p}\cdot\int_0^N \mathrm{d}\tau\langle\boldsymbol{u}(\tau)\rangle - p_\alpha p_\beta\int_0^N \mathrm{d}\tau\int_0^\tau \mathrm{d}\tau'\,\langle u_\alpha(\tau)u_\beta(\tau')\rangle\,. \end{aligned} \tag{6.11}$$

This expansion was analyzed by Polyakov (1990), and additional details are provided in Kholodenko and Vilgis (1995). By symmetry, the first nontrivial term in Eq. (6.11) vanishes while for the second term we have

$$\begin{aligned} \langle u_\alpha(\tau)u_\beta(\tau')\rangle &= \sum_{l\neq 0}\langle 0|u_\alpha|l\rangle\langle|u_\beta|0\rangle \mathrm{e}^{-(E_l-E_0)|\tau-\tau'|\gamma} \\ &= \delta_{\alpha\beta}\sum_{l\neq 0}\frac{1}{l^2}\exp\left\{-\frac{\gamma}{2}l\left(l-\frac{\theta}{\pi}\right)|\tau-\tau'|\right\}. \end{aligned} \tag{6.12}$$

For $\theta = \pm\pi$ and $l = \pm 1$ the term in the exponent vanishes and, for $|\tau-\tau'|\to\infty$ such term becomes the leading term in the series expansion for the correlator. Using this fact Eq. (6.11) produces in this limit:

$$F(\boldsymbol{p}) = \left\langle \exp\left(\mathrm{i}\boldsymbol{p}\cdot\int_0^N \boldsymbol{u}(\tau)\,\mathrm{d}\tau\right)\right\rangle \simeq 1 - \frac{\boldsymbol{p}^2}{2}N^2 + \mathrm{O}(\boldsymbol{p}^4)\,. \tag{6.13}$$

The same result can be obtained following Polyakov's ingenious trick (Polyakov, 1988) which later on was proven rigorously by Alekseev and Shatashvili (1988). The trick lies in the fact that, instead of $\boldsymbol{u}$-averaging, defined in Eq. (6.10), one can perform spin averaging by using the properties of Pauli matrices σ_i. Since

$$\mathrm{Tr}\,\sigma_i = 0 \quad \text{but} \quad \mathrm{Tr}\,\sigma_i^2 = 1$$

we can formally write

$$\left\langle \exp\left(\mathrm{i}\boldsymbol{p}\cdot \int_0^N \boldsymbol{u}(\tau)\,\mathrm{d}\tau \right) \right\rangle \equiv \langle \exp(\mathrm{i}\boldsymbol{p}\cdot\boldsymbol{\sigma}N)\rangle_\sigma\,, \tag{6.14}$$

where $\langle \cdots \rangle_\sigma \equiv \mathrm{Tr}(\cdots)$.

When the r.h.s. of Eq. (6.14) is expanded and the traces over σ_i's are taken, the result of Eq. (6.13) is recovered. The Laplace transform of the r.h.s. of Eq. (6.14) produces

$$\int_0^\infty \mathrm{d}N\,\mathrm{e}^{-sN}\langle \exp(\mathrm{i}\boldsymbol{p}\cdot\boldsymbol{\sigma}N)\rangle_\sigma = \left\langle \frac{1}{\mathrm{i}\boldsymbol{p}\cdot\boldsymbol{\sigma} - s} \right\rangle_\sigma . \tag{6.15}$$

Obviously, Eq. (6.15) describes the Dirac propagator in $d = 2$.

The above analogy with the Dirac propagator exists, however, only for a special value of θ: $\theta = \pi$. For $\theta \neq \pi$ the analogy is lost but the relevant physical results, e.g. that given by Eq. (6.12), are not much affected. Indeed, if we are interested in calculating $\langle \mathbf{R}^2 \rangle$, then using Eq. (6.12) and keeping only the $|l| = 1$ term, which is permissible in the limit $|\tau - \tau'| \to \infty$, we obtain

$$\langle u_\alpha(\tau)u_\beta(0)\rangle \simeq \delta_{\alpha\beta}\,2\exp\{-\gamma/2\}\cosh((\gamma\theta/2)|\tau|)\,. \tag{6.16}$$

The qualitative and quantitative analysis of this result performed in Kholodenko and Vilgis (1995) indicates that the presence of the θ term in Eq. (6.16) makes the chain effectively more stiff. The physical origin of an additional stiffness could be different in general. In this section we shall consider the effects of the nematic environment on a single chain while in Section 6.2 the boundary effects will be considered. In the case of polyelectrolytes, i.e. polymer chains which have charges on their backbones, the stiffness could have an electrostatic origin (Kholodenko, 1995). This is a subject of an ongoing research which we shall not touch in this review.

Warner et al. (1985) (WGB) and independently Rusakov and Shiliomis (1985) have considered the conformational and thermodynamic properties of a single semi-flexible chain inserted into the already existing nematic environment. At the path integral level, the action for such a chain is given by

$$S_{\mathrm{WGB}} = \frac{1}{2}\int_0^N \mathrm{d}\tau\left[\gamma\left(\frac{\mathrm{d}\boldsymbol{u}}{\mathrm{d}\tau}\right)^2 + \tilde{g}[3(u_z)^2 - 1] \right], \tag{6.17}$$

where u_z is the z component of the unit vector $\boldsymbol{u}$. The corresponding Schrödinger-like equation for the propagator of Eq. (6.1) (with action given by Eq. (6.17)) can be written (in dimensionless units) as

$$[\mathrm{d}^2/\mathrm{d}x^2 - g\cos^2 x]\psi = E\psi \quad (d = 2) \tag{6.18}$$

or

$$[\mathrm{d}^2/\mathrm{d}x^2 + \cot x(\mathrm{d}/\mathrm{d}x) - g\cos^2 x]\psi = E\psi \quad (d=3)\,, \tag{6.19}$$

where $0 \le x < \pi$, $x = \phi$.

In both cases the cosine term can be formally expanded and, for $d = 2$, we find a familiar double-well potential characteristic for the hairpin-like problems as discussed by de Gennes (1982). A hairpin is an immediate return (or sharp bend) of a chain in the nematic ordering field. In $d = 3$ the presence of an extra term $(\cot x(\mathrm{d}/\mathrm{d}x))$ formally destroys the nice hairpin picture suggested by de Gennes (1982). Since hairpins were recently observed experimentally (Li et al., 1994), it is essential that the existing models of the semi-flexible chains account for their existence. In Kholodenko and Vilgis (1995) this problem was solved in the following way. By substituting $\psi = z(x)\sqrt{\sin x}$ into Eq. (6.19) it is converted into

$$[\mathrm{d}^2/\mathrm{d}x^2 + \cot x(\mathrm{d}/\mathrm{d}x) - g\cos^2 x - \tfrac{1}{4} - 1/(4\sin x)]\, z(x) = Ez(x)\,. \tag{6.20}$$

This equation differs from Eq. (6.19) considered by WGB by the presence of two extra terms. These two extra terms are *not the artefacts of our substitution*. Indeed, let us consider the three-dimensional version of the path integral given by Eq. (6.9). Following Polyakov (1990) and Kholodenko and Vilgis (1995) the corresponding path integral can be written as follows:

$$G(\boldsymbol{u}_f, \boldsymbol{u}_i; N) = \int_{\boldsymbol{u}(0)=\boldsymbol{u}_i}^{\boldsymbol{u}(N)=\boldsymbol{u}_f} \mathrm{D}[\boldsymbol{u}(\tau)]\delta(\boldsymbol{u}^2 - 1) \times \exp\left\{ -\frac{\gamma}{2}\int_0^N \mathrm{d}\tau \left(\frac{\mathrm{d}\boldsymbol{u}}{\mathrm{d}\tau}\right)^2 + \mathrm{i}\Theta \int_0^N \mathrm{d}\tau\, C[\boldsymbol{u}(\tau)] \right\}, \tag{6.21}$$

where

$$C[\boldsymbol{u}(\tau)] = \int_0^N \mathrm{d}\tau'\, \boldsymbol{u}\cdot\left[\frac{\mathrm{d}\boldsymbol{u}}{\mathrm{d}\tau} \wedge \frac{\mathrm{d}\boldsymbol{u}}{\mathrm{d}\tau'}\right]. \tag{6.22}$$

Unlike the two-dimensional case given by Eq. (6.9), in three dimensions the value of the constant Θ in Eq. (6.21) is not arbitrary. Dirac (1931) had shown that $2\Theta = 0, \pm 1, \pm 2, \pm 3, \ldots$. In Kholodenko and Vilgis (1995) it was shown that for a special value of Θ: $\Theta = 1$, the Schrödinger-like equation for the propagator of Eq. (6.21) can be written as

$$[\mathrm{d}^2/\mathrm{d}x^2 + \cot x(\mathrm{d}/\mathrm{d}x) - \tfrac{1}{4}\cot^2 x]\psi(x) = E\psi(x)\,. \tag{6.23}$$

Eq. (6.23) is directly related to Eq. (6.20) (for $g = 0$) and, hence, the double-well model by de Gennes (1982) *for hairpins is just a special case of the Dirac monopole model in the external field* (Dirac, 1931).

In Section 4 we had considered a problem of "framing" for the self-linking number $lk(i,i)$, e.g. see Eq. (4.19). Using Calugareanu-White theorem, Kauffman (1987a), one can write

$$lk(i,i) = T_w[i] + W_r[i] \tag{6.24}$$

where, according to Pohl (1968),

$$T_w[i] = \frac{-1}{2\pi}\int_0^N \mathrm{d}\tau\, C[\boldsymbol{u}(\tau)] + \text{const.} \tag{6.25}$$

Evidently, Eqs. (6.24) and (6.25) provide the analytical expression for the writhe of the curve:

$$W_{\mathrm{r}}[i] = lk(i,i) - T_w[i]\,. \tag{6.26}$$

More details about the differential-geometric properties and calculation of $W_{\mathrm{r}}[i]$ can be found in Aldinger et al. (1995). Evidently, Eq. (6.25) can be used in the path integral of Eq. (6.21), unlike the formal expression of Eq. (3.6). Nevertheless, both expressions are equivalent. As it was explained in Kholodenko and Rolfsen (1996), $W_{\mathrm{r}}[i]$ also has the meaning of a winding number so that the path integral of Eq. (6.21) is the correct three dimensional extension of the path integral of Eq. (6.9).

To demonstrate that $W_{\mathrm{r}}[i]$ has, indeed the meaning of the winding number, the following arguments are helpful. Let $\boldsymbol{r}(\tau)$ describe an embedding of a circle S^1 into $\mathbf{R}$. For two circles embedded into $\mathbf{R}^3$ one can construct a unit vector

$$\boldsymbol{n}(\tau,\tau') = \frac{\boldsymbol{r}(\tau) - \boldsymbol{r}(\tau')}{|\boldsymbol{r}(\tau) - \boldsymbol{r}(\tau')|} \tag{6.27}$$

which provides a map $S^1 \times S^1 \to S^2$ known as the Gauss map. The degree of such defined Gauss mapping for $S^1 \times S^1$ (diagonal) $\to S^2$ is the winding number which is conventionally known as writhe and is analytically given by

$$W_{\mathrm{r}}[K] = \frac{1}{4\pi}\int_{S^1} \mathrm{d}\tau \int_{S^1} \mathrm{d}\tau' \left(\frac{\mathrm{d}\boldsymbol{r}}{\mathrm{d}\tau} \wedge \frac{\mathrm{d}\boldsymbol{r}}{\mathrm{d}\tau'}\right) \cdot \frac{(\boldsymbol{r}(\tau) - \boldsymbol{r}(\tau'))}{|\boldsymbol{r}(\tau) - \boldsymbol{r}(\tau)'|^3}\,. \tag{6.28}$$

More details on the degree of mapping can be found in Dubrovin et al. (1985).

We shall use the above facts in Section 7 where we are going to calculate the average writhe. Here we only notice that Eq. (6.19) (with monopole term, e.g. like that in Eq. (6.20)) has additional unexpected properties, if besides the nematic perturbation (described by $\cos^2 x$ term), there is a perturbation of nonnematic origin (e.g. constant electric field, polymer in the flow, etc.). In this case, one has to consider an equation of the form

$$[-(\gamma/2)\mathrm{d}^2/\mathrm{d}x^2 + g\cos^2 x + f\cos x]\psi = E\psi \tag{6.29}$$

which is known as Whittaker–Hill (WH) equation. In the context of polymer problems it was first discussed by Jähnig (1979). WH equation has interesting mathematical properties, e.g. see Magnus and Winkler (1966) or Urwin and Arscott (1970). Most important for us is the fact that *for nonzero values of g the force constant f can have only discrete values.* This means that if in the nematic environment we would like to stretch the polymer chain, then the application of a given force will not necessarily cause the stretching, i.e. the stretching will have a stepwise character. Recently, experiments were conducted to check the elastic properties of DNA molecules in solution, see, e.g. Cluzel et al. (1996). In the case of finite DNA concentrations, the experimental force–extension curve (e.g. see Fig. 2B of Cluzel et al.) shows the characteristic stepwise extension in complete agreement with the predictions based on the study of the WH model (Kholodenko and Vilgis, 1995).

6.2. Semi-flexible polymers confined between the parallel plates and in the half space

In Kholodenko et al. (1994) this problem was treated for chains of arbitrary flexibility. Because the obtained results are rather bulky if one is interested in chains of arbitrary flexibility, we provide

here only the summary of the results which are surprisingly *closely connected with that presented in Section* 6.1.

In the presence of some external potential $V(\boldsymbol{r})$ the distribution function G for the Gaussian-like polymer obeys the following equation of "motion":

$$\left[\frac{\partial}{\partial N} - \frac{l}{6}\nabla_r^2 + V(\boldsymbol{r})\right] G(\boldsymbol{r}, \boldsymbol{r}'; N) = \delta(N)\delta(\boldsymbol{r} - \boldsymbol{r}') \,. \tag{6.30}$$

To treat chains of arbitrary flexibility it is sufficient to replace the "non-relativistic" Schrödinger-like Eq. (6.30) with that for the Dirac propagator, as it is explained in Kholodenko et al. (1994) and Kholodenko and Borsali (1995). In the case of half-space it is natural to consider separately the "longitudinal", i.e. perpendicular to the wall, and the "transversal" "motions" of the chain. The longitudinal "motion" is one dimensional. The presence of the surface is being modeled by some sort of δ-like potential, i.e. $V(\boldsymbol{r}) = \delta_0\delta(x)$. With this potential Eq. (6.30) is easily solvable with the result

$$G(x, x'; s) = \frac{1}{2\sqrt{s}}\left[\exp(-\sqrt{s}|x - x'|) - \frac{\delta_0}{\delta_0 + 2\sqrt{s}}\exp(-\sqrt{s}|x| - |x'|\sqrt{s})\right], \tag{6.31}$$

where the Laplace variable s is conjugate to the polymeric length N. The result thus obtained corresponds to the so-called *penetrable* surface model. In this case, the chain can legitimately "tunnel" through the interface, e.g. between two liquids. At the same time, the impenetrable surface restricts the chain to the half-space *regardless* of the strength of the polymer-surface interaction. It can be demonstrated that the propagator for the impenetrable case can be obtained with the help of penetrable, given by Eq. (6.31), with the result (x and $x' > 0$):

$$G(x, x'; s) = \frac{1}{2\sqrt{s}}\left[\mathrm{e}^{-\sqrt{s}|x-x'|} + \frac{\sqrt{s} - \delta}{\sqrt{s} + \delta}\mathrm{e}^{-\sqrt{s}(x+x')}\right], \tag{6.32}$$

where $\delta = \delta_0/2$. Consider now two limiting cases: (a) $\delta_0 \to 0$ and (b) $\delta_0 \to \pm\infty$. In the first and the second case we obtain, respectively,

$$G(x, x'; s) = (1/2\sqrt{s})[\exp(-\sqrt{s}|x - x'|) + \exp(-\sqrt{s}(x + x'))] \,, \tag{6.33a}$$

$$G(x, x'; s) = (1/2\sqrt{s})[\exp(-\sqrt{s}|x - x'|) - \exp(-\sqrt{s}(x + x'))] \,. \tag{6.33b}$$

Comparison with similar problems in quantum mechanics (Kleinert, 1995) indicates that Eq. (6.33a) can be interpreted as a Euclidean-type version of the two-particle relative amplitude for two bosons while Eq. (6.33b) represents the two-particle relative amplitude for fermions. This means *that for the arbitrary strength of the interaction parameter* δ_0 *we have the case of an intermediate* (*or fractional*) *statistics*! This fact is going to be exploited in Section 8. The case of parallel plates can be easily obtained with help of the half-space result, Eq. (6.32), so that we

provide here only the final answer:

$$G_{\|}(x,x';s)=\frac{1}{2\sqrt{s}}\sum_{M=-\infty}^{\infty}\left[\exp(-\sqrt{s}|x-x'-2M\tilde{d}|)\right.$$
$$\left.+\frac{\sqrt{s}-\delta}{\sqrt{s}+\delta}\exp(-\sqrt{s}|x+x'+2M\tilde{d}|)\right], \tag{6.34}$$

where $\tilde{d}$ is the distance between the plates.

Consider now the inverse Laplace transform of the auxiliary Green's function given by

$$\tilde{G}(x,x';s)=\frac{1}{2\sqrt{s}}\sum_{M=-\infty}^{\infty}\exp(-\sqrt{s}|x-x'-2M\tilde{d}|)\,. \tag{6.35}$$

We obtain

$$\tilde{G}(x,x';N)=\frac{1}{2\sqrt{N}}\sum_{M=-\infty}^{\infty}\exp\left\{-\frac{1}{Nl}(x-x'-2M\tilde{d})^2\right\} \tag{6.36}$$
$$\equiv\frac{\sqrt{\pi}}{2\tilde{d}}\Theta(\tilde{x}-\tilde{x}';\mathrm{i}\tau)\,,$$

where $\Theta(x,y)$ is the elliptic theta function (Mumford, 1983) and $\tau=\pi Nl/4\tilde{d}^2$, $\tilde{x}=x/2\tilde{d}$. Whence, at least for $\delta\to 0$ and $\delta\to\pm\infty$, we can write for $G_{\|}(x,x';N)$ the following simple result:

$$2\tilde{d}G_{\|}(x,x';N)=\Theta(\tilde{x}-\tilde{x}',\mathrm{i}\tau)\pm\Theta(\tilde{x}+\tilde{x}'\mathrm{i}\tau)\,. \tag{6.37}$$

But the theta function is just the Green's function for the particle moving on the circle (Kleinert, 1995) which we just had discussed in Section 6.1! This means that the condition for the wave function given by Eq. (6.4) just reflects the strength of the interactions between the polymer and the parallel plates. Whence, we have just demonstrated that

(a) the half-plane and the parallel plates problems are interrelated in the sense that, *at least* for the infinitely repulsive walls, and (or) zero interactions with walls, the parallel plates problems are obtainable from the half-space problem by a simple replacement:

$$(1/\sqrt{\pi N})\exp\{-x^2/Nl\}\to(1/\tilde{d})\Theta(\tilde{x},\mathrm{i}\tau)\,; \tag{6.38}$$

(b) the interaction between the polymer and the walls is responsible for the *fractional statistics* for both the half space and the parallel plates problems;

(c) the explicit connection between the phase θ in Eq. (6.4) and the strength of interaction between the polymer and the wall(s) can be worked out, in principle, based on the work by Gaveau and Schulman (1986). For mathematically rigorous justification of all these results the reader may consult Aldaya et al. (1996).

6.3. *Polymers confined into semi-flexible tubes*

Brownian motion of "particles" on the manifolds was considered by mathematicians some time ago, e.g. see McKean (1969). In physics literature study of this problem was initiated by da Costa

(1981). da Costa had discussed the problem of how to develop the quantum mechanics for "particles" constrained to the manifolds which are embedded into $\mathbf{R}^3$. That is to say: how the extrinsic and intrinsic curvature properties of the manifold affect the Brownian motion. We had discussed already the motion on the circle and on the sphere S^2. Let us now consider, instead of S^2, an arbitrary reasonable smooth surface S which is parametrically given as $\boldsymbol{r} = \boldsymbol{r}(q_1, q_2)$, where q_1 and q_2 are the local coordinates at some point on the surface which has a spatial position $\boldsymbol{r}$. To constrain the "motion" of our ficticious particle to the surface it requires to have some "squeezing" potential. To define such potential, one has to introduce the vector $\boldsymbol{R} = \boldsymbol{R}\,(q_1, q_2, q_3)$ so that

$$\boldsymbol{R}(q_1, q_2, q_3) = \boldsymbol{r}(q_1, q_2) + q_3 \boldsymbol{n}(q_1, q_2)\,, \tag{6.39}$$

where $\boldsymbol{n}$ is the continuous unit vector normal to S. The "squeezing" potential V is evidently a function of q_3, e.g. one may write

$$V(q_3) = \begin{cases} 0\,, & q_3 = 0\,, \\ \infty\,, & q_3 > 0\,. \end{cases} \tag{6.40}$$

If we want to develop quantum mechanics (or statistical physics), such "hard core" potential is somewhat inconvenient. To avoid this problem, the harmonic-like potential is usually used: $V_\lambda(q_3) = \frac{1}{2} m\lambda^2 q_3^2$ where λ is defined through the relation: $\langle q_3^2 \rangle = \hbar/m\lambda$, where $\hbar$ is Planck's constant and m is the mass of the particle. In polymer physics, the above combination may be associated with the tube radius a^2, e.g. see Doi and Edwards (1978) and Section 8. If g_{ij} is the metric tensor of the surface, e.g.

$$g_{ij} = \frac{\partial \boldsymbol{r}}{\partial q_i} \cdot \frac{\partial \boldsymbol{r}}{\partial q_j}, \quad i,j = 1,2 \tag{6.41}$$

and h_{ij} is the second fundamental form of the surface, i.e.

$$h_{ij} = \boldsymbol{n} \cdot \frac{d^2 \boldsymbol{r}}{\partial q_i \partial q_j}, \quad i,j = 1,2\,, \tag{6.42}$$

where the vector $\boldsymbol{n}$ is defined in Eq. (6.39), then for the metric tensor G_{ij} defined by

$$G_{ij} = \frac{\partial \boldsymbol{R}}{\partial q_i} \cdot \frac{\partial \boldsymbol{R}}{\partial q_j}, \quad i,j = 1\text{–}3 \tag{6.43}$$

it is possible to obtain

$$G_{ij} = g_{ij} + [\alpha g + (\alpha g)^{\mathrm{T}}]_{ij}\, q_3 + (\alpha g \alpha^{\mathrm{T}})_{ij}\, q_3^2\,, \tag{6.44}$$

$$G_{i3} = G_{3i} = 0\,, \quad i = 1,2\,, \qquad G_{33} = -1\,, \tag{6.45}$$

where the matrix elements α_{ij} are defined via

$$\alpha_{11} = (1/g)(g_{12} h_{21} - g_{22} h_{11})\,, \tag{6.46}$$

etc. and $g = \det(g_{ij})$.

Using the above results, one can write, in case of polymers, the diffusion equation in the curvilinear coordinates (q_1, q_2, q_3) as follows:

$$\frac{\partial}{\partial N}\Psi = \frac{l}{6}\sum_{i=1}^{3}\frac{1}{\sqrt{G}}\frac{\partial}{\partial q_i}\left(\sqrt{G}(G)^{ij}\frac{\partial}{\partial q_i}\right)\Psi - V_\lambda(q_3)\Psi\,, \tag{6.47}$$

where G^{ij} is defined through the equation

$$\sum_{k=1}^{3} G^{ik}G_{kj} = \delta_j^i\,, \tag{6.48}$$

and $G = \det(G_{ij})$. To proceed, one needs to use Eqs. (6.43), (6.44), (6.45) and (6.46) in Eq. (6.47) and to insure that the function Ψ is properly normalized, i.e. to require

$$\int |\Psi(q_1, q_2, q_3)|^2\,\mathrm{d}V = 1\,, \tag{6.49}$$

where $\mathrm{d}V = \mathrm{d}S f(q_1, q_2, q_3)\,\mathrm{d}q_3$ and

$$f(q_1, q_2, q_3) = 1 + \mathrm{Tr}(\alpha_{ij})q_3 + \det(d_{ij})q_3^2\,, \tag{6.50}$$

$$\mathrm{d}S = \sqrt{g}\;\mathrm{d}q_1\;\mathrm{d}q_2\,. \tag{6.51}$$

By introducing a new "wave" function via $\chi(q_1, q_2, q_3; N) = \sqrt{f}\Psi(q_1, q_2, q_3, N)$ it is possible to rewrite Eq. (6.47) as follows:

$$\frac{l}{6}\sum_{i,j=1}^{2}\frac{1}{\sqrt{g}}\frac{\partial}{\partial q_i}\left(\sqrt{g}g^{ij}\frac{\partial}{\partial q_j}\right)\chi + \frac{l}{6}([\tfrac{1}{2}\mathrm{Tr}(\alpha_{ij})]^2 - \det(\alpha_{ij}))\chi + \frac{l}{6}\frac{\partial^2}{\partial q_3^2}\chi - V_\lambda(q_3)\chi = \frac{\partial\chi}{\partial N}\,. \tag{6.52}$$

This equation naturally admits the separation of variables. By writing $\chi = \chi_\perp\chi_\parallel$ where $\chi_\parallel = \chi_N(q_3)$ and $\chi_\perp = \chi_N(q_1, q_2)$ one obtains easily

$$\frac{\partial}{\partial N}\chi_\parallel = \frac{l}{6}\frac{d^2}{dq_3^2}\chi_\parallel - V_\lambda(q_3)\chi_\parallel$$

and

$$\frac{\partial}{\partial N}\chi_\perp = \frac{l}{6}\sum_{i,j=1}^{2}\frac{1}{\sqrt{g}}\frac{\partial}{\partial g_i}\left(\sqrt{g}g^{ij}\frac{\partial}{\partial g_j}\right)\chi_\perp + \frac{1}{6}([\tfrac{1}{2}\mathrm{Tr}(\alpha_{ij})]^2 - \det(\alpha_{ij}))\chi_\perp\,. \tag{6.53}$$

For the curves (tubes) one needs to replace Eq. (6.39) by

$$\boldsymbol{R}(q_1, q_2, q_3) = \boldsymbol{r}(\boldsymbol{q}_1) + q_2\boldsymbol{n}_2(q_1) + q_3\boldsymbol{n}_3(q_1)\,, \tag{6.54}$$

where $\boldsymbol{n}_2$ and $\boldsymbol{n}_3$ are the usual Serret–Frenet unit vectors, e.g. see Kholodenko (1990). By repeating the same steps as before, for the surfaces, we finally arrive at the desired result:

$$\frac{l}{6}\left(\frac{\partial^2}{\partial q_2^2} + \frac{\partial^2}{\partial q_3^2}\right)\chi_\perp - \frac{w^2}{6}(q_2^2 + q_3^2)\chi_\perp = \frac{\partial}{\partial N}\chi_\perp\,, \tag{6.55}$$

$$\frac{l}{6}\frac{\mathrm{d}^2}{\mathrm{d}q_1^2}\chi_\parallel + k^2(q_1)\chi_\parallel = \frac{\partial\chi_\parallel}{\partial N}\,. \tag{6.56}$$

In arriving at this result we have used the "soft" harmonic oscillator-like confining potential and used w^2, instead of λ, since with this notations Eq. (6.55) coincides exactly with that discussed by Doi and Edwards (1978). Unlike Doi and Edwards (1978), however, the longitudinal part contains an extra potential term which comes from the effects of the local curvature $k(q_1)$ of the tube. Since $k(q_1)$ is, in general, the random variable and since in Eq. (6.56) its contribution always comes with the positive sign, this implies that the presence of the curvature term may lead to the localization. This is obviously an undesirable conclusion which contradicts the main postulates of the reptation theory (Doi and Edwards, 1978) which were briefly discussed in Section 2.2 and will also be discussed in Section 8. To repair the situation, we have to assume that the effects of the local curvature are relatively small, which is possible only *if the tube conformation deviates only slightly from that of the straight line*. This leads to *the effective rigidification of the polymer chain backbone constrained into the tube*. The scaling analysis of such rigidified effective primitive chain (already mentioned in Section 2.2) presented in Kholodenko (1991) is discussed in Section 8 in connection with de Gennes–Doi–Edwards reptation theory (Doi and Edwards, 1978; de Gennes, 1971).

The above derivation of the confining equations developed by da Costa (1981) had been improved by many authors, e.g. see Matsutani (1992), Burgess and Jensen (1993), Kugler and Shtrikman (1988), Ao and Thouless (1994), Maraner (1995), Clark and Bracken (1996), etc. The above cited papers provide some additional condensed matter applications which could be potentially useful in polymer physics. The additional polymer related discussion could also be found in Kholodenko (1996c).

As it follows from Eq. (6.55), the transversal part of the Brownian motion takes place in the oscillator-like potential. This feature is characteristic of the problem about the probability for the random walk of N steps to enclose the prescribed area A. Since we shall employ some of the results related to this problem in Section 8, we would like now to provide some essentials in Section 6.4.

6.4. Configurational statistics of the planar random walks restricted by the area constraint

Following Kholodenko (1996a), let us consider the calculation of the probability density given by

$$P(A,N)=\pi Nl\int_{\boldsymbol{r}(0)=\boldsymbol{r}(N)}\mathrm{D}[\boldsymbol{r}(\tau)]\,\delta\left(A-\frac{1}{2}\left|\int_0^N \mathrm{d}\tau\left(x\frac{\mathrm{d}y}{\mathrm{d}\tau}-y\frac{\mathrm{d}y}{\mathrm{d}\tau}\right)\right|\right)\times\exp\left\{-\frac{1}{l}\int_0^N \mathrm{d}\tau\left(\frac{\mathrm{d}\boldsymbol{r}}{\mathrm{d}\tau}\right)^2\right\} \tag{6.57}$$

to be compared with Eq. (5.1). The algebraic area

$$A=\frac{1}{2}\int_0^N \mathrm{d}\tau\left(x\frac{\mathrm{d}y}{\mathrm{d}\tau}-y\frac{\mathrm{d}x}{\mathrm{d}\tau}\right) \tag{6.58}$$

suffers from several deficiencies. First, unlike the "true", or geometric, area it can be both positive and negative, that is why the modulus sign is included in Eq. (6.57). Second, if the curve which encloses the area A has self-intersections, then the total algebraic area might be much smaller (or even zero!) than the corresponding geometric areas enclosed by the subloops. Levi (1965) had analyzed these problems in connection with computation of $P(A,N)$. He found that although

classically (i.e. geometrically) the area given by Eq. (6.58) is ill-defined, stochastically the area is well defined and leads to meaningful results (e.g. see Theorems 55.1 and 55.2 in his book). Although Levi had solved this problem long ago, in physics this problem was solved even earlier and it is known to be directly connected (Sondheimer and Wilson, 1951), with Landau diamagnetism problem (Landau, 1930).

The probability given by Eq. (6.57) is normalized according to the usual prescription

$$\int_0^\infty \mathrm{d}A\ P(A,N) = 1\,. \tag{6.59}$$

In reality, however, this prescription is physically unrealistic since the polymer chain of length N cannot enclose the area greater than $N^2/4\pi$ (i.e. the area of the circle that has perimeter length equal to N. This means that the correct normalization should be

$$\int_0^{N^2/4\pi} \mathrm{d}A\, P(A,N) = 1\,. \tag{6.60}$$

Moreover, if the modulus sign in Eq. (6.57) is absent, then instead of the normalization defined by Eq. (6.60) another normalization is used (Duplantier, 1989):

$$\int_{-\infty}^{\infty} \mathrm{d}A\, P(A,N) = 1\,. \tag{6.61}$$

The physical consequences of these different normalizations as well as extension of Eq. (6.57) to the case when the circular polymers are of arbitrary rigidity is being treated in Kholodenko (1996a). Here we shall not go into details of these calculations and only restrict ourselves with the results which will be used in Section 8.

It is convenient to introduce the Fourier transform of $P(A,N)$ via

$$P(A,N) = \frac{1}{2\pi}\int_{-\infty}^{\infty} \mathrm{d}k\, P(k,N)\exp(\mathrm{i}kA)\,. \tag{6.62}$$

The modulus sign in Eq. (6.57) can be eliminated with the help of the identity

$$\frac{\mathrm{e}^{-\mathrm{i}\omega|T|}}{2\omega} = \frac{1}{2\pi\mathrm{i}}\int_C \frac{\mathrm{d}k_0}{K^2}\,\mathrm{e}^{-\mathrm{i}k_0 T}\,, \tag{6.63}$$

where $K^2 = \omega^2 - k_0^2$ and C is an appropriately chosen contour in the complex plane. By combining Eqs. (6.57), (6.62) and (6.63) we obtain

$$P(k,N) = \frac{k}{\pi\mathrm{i}G(0,N)}\int_c \frac{\mathrm{d}k_0}{K^2}\int_{r(N)=r(0)} \mathrm{D}[\boldsymbol{r}(\tau)]\exp\left\{-\int_0^N \mathrm{d}\tau\, \mathscr{L}[\boldsymbol{r}(\tau)]\right\}, \tag{6.64}$$

where

$$\mathscr{L}[\boldsymbol{r}(\tau)] = \frac{1}{l}\left(\frac{\mathrm{d}\boldsymbol{r}}{\mathrm{d}\tau}\right)^2 + \frac{\mathrm{i}k_0}{2}\left(x\frac{\mathrm{d}y}{\mathrm{d}\tau} - y\frac{\mathrm{d}y}{\mathrm{d}\tau}\right), \tag{6.65}$$

$K^2 = k^2 - k_0^2$ and $G(0,N) = (\pi N l)^{-1}$.

The path integral of Eq. (6.64) was calculated by Khandekar and Wiegel (1988). However, the same result was obtained much earlier by Sondheimer and Wilson (1951) by recognizing that the Lagrangian of Eq. (6.65) corresponds to that for the particle in the constant magnetic field $\boldsymbol{H}$ such that $\boldsymbol{H} = \nabla \times \boldsymbol{A}$ and

$$\boldsymbol{A} = \{ -(H/2)y, (H/2)x \} . \tag{6.66}$$

With help of this observation, the action in the path integral of Eq. (6.64) can be rewritten as

$$S[\boldsymbol{r}(\tau)] = \int_0^N \mathrm{d}\tau \left\{ \frac{m}{2}\left(\frac{\mathrm{d}\boldsymbol{r}}{\mathrm{d}\tau}\right)^2 + \mathrm{i}e\frac{\mathrm{d}\boldsymbol{r}}{\mathrm{d}\tau}\cdot\boldsymbol{A}[\boldsymbol{r}(\tau)] \right\}, \tag{6.67}$$

where, in case of polymers, the mass $m = 2/l$, the charge $e = 1$, $\hbar = c = 1$ and $H = k_0$. Using such defined dictionary, we can use directly Wilson and Sondheimer's results in order to obtain

$$P(A, N) = (2\pi/Nl)[\cosh(2\pi A/Nl)]^{-2}. \tag{6.68}$$

The average area can now be obtained as

$$\langle A \rangle = \int_0^\infty \mathrm{d}A\, P(A, N) = (Nl/2\pi)\ln 2 . \tag{6.69}$$

In principle, we can calculate any moment, e.g. $\langle A^n \rangle$ since we have closed form explicit expression for $P(A, N)$ given by Eq. (6.68). More interesting, however, is to calculate the generating function

$$F(\mu) = \int_0^\infty \mathrm{d}A\, \mathrm{e}^{-\mu A} P(A, N) \tag{6.70}$$

which is just the Laplace transform of $P(A, N)$. If we combine Eqs. (6.57) and (6.70), we immediately discover that the delta function in Eq. (6.57) disappears, and the problem of calculation of $F(\mu)$ is reduced to that given by Eq. (6.64) (with k being replaced by μ). It was shown in Kholodenko (1996a,b) that the constant μ has also a physical meaning: $-\mu = \Delta p$, where Δp is the pressure difference between the inside and outside of the two dimensional vesicle (circle). Whence, one can think about calculating $\langle A \rangle$ for the prescribed pressure difference Δp. In this case, one obtains after some calculation the following result for $\langle A \rangle$:

$$\langle A \rangle = 1/\Delta p - (Nl/2)\cot(\Delta p Nl/2) . \tag{6.71}$$

This result is going to be used in Section 8.

7. Knot complexity – detailed treatment

7.1. Calculation of the topological persistence length

The topological persistence length N_{T} was introduced in Section 3.1. It is defined as a minimal number of steps on some three-dimensional lattice required for the first nontrivial knot to be formed. Evidently, N_{T} is non-universal quantity which depends on the lattice type.

In this section we shall provide an estimate of N_T using the existing path integrals for semi-flexible polymers, e.g. that given by Eq. (6.1). Since N_T is a lattice-dependent quantity, while the path integral is defined in the continuum, our result for N_T will depend upon the discretization procedure which is used to arrive at the continuum limit for the path integral we are going to use (Kholodenko, 1995). Such dependence, however, is not too strong as we shall demonstrate shortly.

In order to obtain the result for N_T we need to use the Milnor's inequality given by Eq. (4.3). This inequality should be combined with the Schwarz inequality (Frenchel, 1951) valid for any closed curve, and given by

$$(2\pi)^2 \leq \left(\int_0^N d\tau\,|k(\tau)|\right)^2 \leq N\int_0^N d\tau\,k^2(\tau)\,, \tag{7.1}$$

where $k(\tau)$, as before, is the local curvature of the curve. If we think of the curve as made of real physical material, e.g. polymer, then using polymer methodology, e.g. see Section 6, we have to perform the statistical average of Eq. (7.1) with help of the path integral(s) for the semi-flexible chains. The statistical average $\langle\cdots\rangle$ in terms of such path integral(s) can be in the simplest case defined as

$$\langle\cdots\rangle = \tilde{N}\int_{\boldsymbol{u}(0)=\boldsymbol{u}(N)} D[\boldsymbol{u}(\tau)]\delta(\boldsymbol{u}^2-1)\exp\left\{-\frac{\gamma}{2}\int_0^N d\tau\left(\frac{d\boldsymbol{u}}{d\tau}\right)^2\right\}\cdots\,, \tag{7.2}$$

where the normalization constant $\tilde{N}$ is chosen in such a way that $\langle 1\rangle = 1$ and the constant γ was defined in Eq. (6.1). In the fully flexible limit, $\gamma \to 0$, the polymer chain behaves as Gaussian. It is known (Kholodenko, 1993) that in this limit the polymer Kuhn's step length $l = 2\gamma$. We can associate the length l with the unit step length of the random walk on some regular (e.g. cubic) three-dimensional lattice (de Gennes, 1979). Such identification should be done with some caution, however, since the discrete analogue of the path integral of Eq. (7.2) is expected to exist and to be well defined. As results of Kholodenko (1995) indicate, the lattice-dependent factors (like $\sqrt{2}$ for cubic lattice, etc.) are likely to occur when the identification between the discrete and the continuum formulations are made. These factors are responsible for some numerical differences in final results for N_T. From the experimental point of view, the measured combination $2\gamma N = lN = \langle \boldsymbol{R}^2\rangle$ does not allow to measure separately l and N in one measurement. Some independent measurements are required (Kholodenko, 1993; Hickl et al., 1997), which inevitably introduce some errors. Whence, *both* the discrete and the continuum formulations can provide only the upper and the lower bounds for N_T as will be further explained below.

By combining Eqs. (7.1) and (7.2) we obtain

$$(2\pi)^2 \leq \left\langle\left(\int_0^N d\tau|k(\tau)|\right)^2\right\rangle \leq N\left\langle\int_0^N d\tau\,k^2(\tau)\right\rangle\,. \tag{7.3}$$

This inequality should be valid for *any closed* polymer configuration. At the same time, by combining inequalities Eqs. (4.3), (7.1) and (7.3) we obtain the following result for the *knotted* curves:

$$(4\pi)^2 \leq \left\langle\left(\int_0^N d\tau|k(\tau)|\right)^2\right\rangle \leq N\left\langle\int_0^N d\tau\,k^2(\tau)\right\rangle\,. \tag{7.4}$$

Since any three-dimensional curve is being characterized by the local curvature $k(\tau)$ and torsion $\kappa(\tau)$ (Kholodenko, 1990), it is not a priori clear that the path integral of Eq. (7.2) contains knotted three-dimensional configurations (at least within the semiclassical level of approximation) since the action in the path integral contains only the curvature part. Fortunately, Langer and Singer (1984a,b) and subsequently Bryant and Griffiths (1986), and, even more recently, Kholodenko and Nesterenko (1995), have shown that this is indeed the case. More specifically, Langer and Singer (1984a,b) had considered a three-dimensional variational problem for the functional of the type

$$F_{\mathrm{LS}}[C] = \int_0^N \mathrm{d}s\,(k^2(s) + m^2)\,, \tag{7.5}$$

where $\mathrm{d}s$ is the length element along the contour C and the Lagrange multiplier m^2 accounts for the fact that the length of the curve is fixed. Kholodenko and Nesterenko (1995) had shown that the variational problem for the functional $F_{\mathrm{LS}}[c]$ produces trajectories which are *identical* to those obtained from the functional

$$F_{\mathrm{KN}}[c] = \frac{1}{2}\int_0^N \mathrm{d}s\,k^2(s) \tag{7.6}$$

defined on the space of constant curvature (e.g. sphere). This result is in accord with those obtained earlier by Griffiths (1983). The numerical value of the constant curvature is directly related to m^2, (Kholodenko and Nesterenko, 1995). Langer and Singer (1984a,b) had demonstrated that "*there is a countable infinity of* (*similarity classes of*) *closed nonplanar elasic curves in* $\mathbf{R}^3$. All such elasicae are embedded and lie on the embedded tori of revolution (see, e.g. Fig. 23) infinitely many are knotted and the knot types which occur are precisely the (n, m) torus knots (see, e.g. Fig. 23 and Rolfsen, 1976) satisfying $m > n$. The integers m and n determine the elasticae uniquely (up to similarity)."

To actually perform the averaging, several steps are required. First, we would like to notice that for the semi-flexible polymers it is the dimensionless combination N/γ which actually determines how stiff the polymer chain is. In terms of the Kuhn's length, we have $\omega = N/l = N/2\gamma$. Using this result, the action functional in Eq. (7.2) can be rewritten as

$$S = \frac{\gamma}{2}\int_0^N \mathrm{d}\tau\,k^2(\tau) = \frac{1}{4\omega}\int_0^1 \mathrm{d}\tau\,k^2(\tau)\,, \tag{7.7}$$

where in arriving at the last equality we have taken into account that in the case of natural parametrization, $\boldsymbol{n}^2 = 1$, we have $k^2(\tau) = (\mathrm{d}\boldsymbol{n}/\mathrm{d}\tau)^2$ and $\boldsymbol{n} = \mathrm{d}\boldsymbol{r}/\mathrm{d}\tau$ where $\boldsymbol{r}(\tau)$ is the spatial position of the polymer segment at contour position τ. By combining Eq. (7.2) with Eqs. (7.4) and (7.7) we obtain,

$$N\left\langle \int_0^N \mathrm{d}\tau\,k^2(\tau)\right\rangle = \left\langle \int_0^1 \mathrm{d}\tau\,k^2(\tau)\right\rangle = -4\frac{\partial}{\partial\omega^{-1}}\ln I[\omega]\,, \tag{7.8}$$

where

$$I[\omega] = \int d\boldsymbol{u} \int_{\boldsymbol{u}_i = \boldsymbol{u}_f = \boldsymbol{u}} D[\boldsymbol{u}(\tau)]\, \delta(\boldsymbol{u}^2 - 1) \exp\left\{ -\frac{1}{4\omega} \int_0^1 d\tau\, k^2(\tau) \right\}$$

$$= \sum_{n=0}^{\infty} (2n+1) \exp(-\omega(n+1)n) . \tag{7.9}$$

In arriving at the last line in Eq. (7.9), we have used the results of Kholodenko and Vilgis (1996). As in this reference, we would like to replace the summation by integration (which corresponds to the semi-classical approximation) in the last line. This then produces:

$$I[\omega] \simeq \int_0^{\infty} dx\, 2x \exp(-\omega x^2) . \tag{7.10}$$

Combining Eq. (7.8) with Eq. (7.10) produces (within the approximations made)

$$\left\langle \int_0^1 d\tau\, k^2(\tau) \right\rangle = 4\omega . \tag{7.11}$$

Combining this result with the inequality (Eq. (7.4)) we obtain

$$(4\pi)^2 \leq 4\omega$$

or

$$(2\pi)^2 \leq \omega . \tag{7.12}$$

Since $(2\pi)^2 \approx 40$ and since ω is the effective number of steps on the lattice we obtain

$$\omega \geq 40 . \tag{7.13}$$

This result is in excellent agreement with the numerical results of Windwer (1990), see, e.g. Eq. (3.4). Indeed, by using the experimental values for $\tilde{\mu}$ and $\tilde{c}$ in Eq. (3.4) one obtains $\omega = 40.884$. At the same time, if we would choose the rescaled length: $N \to N\sqrt{2}$ (or, equivalently, the rescaled Kuhn's length $l \to l/2$) we would obtain instead

$$\omega \geq 28 \tag{7.14}$$

which is in very good agreement with Diao's rigorous calculations, (Diao, 1993, 1994) which provide $N_T = 24$ for knots on the cubic lattice. Since factors like $\sqrt{2}$ reflect the symmetry of the cubic lattice and naturally emerge in the discretized models for the semi-flexible polymers (Kholodenko, 1995), the results of Eqs. (7.13) and (7.14) represent the upper and the lower bound estimates for N_T on the cubic lattice. Evidently, if we would choose a different lattice, the results for N_T might be somewhat different.

7.2. Calculation of the averaged writhe

In Section 3.2 we had discussed the numerical simulations which produce for the averaged writhe the result given by Eq. (3.8). To obtain this result analytically, i.e. with help of the existing

path integral methods, we have to use Eq. (6.24) along with the auxiliary Eqs. (6.24)–(6.28). Use of these equations permits us to write the partition function $Z(g)$ which is very similar to that given by Eq. (7.9), i.e.,

$$Z[g] = \int \mathrm{d}\boldsymbol{u} \int_{\boldsymbol{u}_i(0)=\boldsymbol{u}_f(N)=\boldsymbol{u}} \mathrm{D}[\boldsymbol{u}(\tau)]\delta(\boldsymbol{u}^2 - 1) \times \exp\left\{ -\frac{1}{4\omega}\int_0^1 \mathrm{d}\tau\,[k^2(\tau) + \mathrm{i}g\,W_{\mathrm{r}}[\boldsymbol{u}(\tau)]]\right\}. \tag{7.15}$$

With the help of such defined partition function we can obtain the averaged writhe according to the usual rule:

$$\langle W_{\mathrm{r}}[K]\rangle = \frac{1}{\mathrm{i}}\frac{\delta \ln Z(g)}{\delta g}. \tag{7.16}$$

The imaginary factor $\mathrm{i} = \sqrt{-1}$ in Eq. (7.15) is introduced for the sake of convenience: to show the correspondence with the exactly solvable quantum problem. Thus defined average writhe is nonzero only for the fixed orientation of the closed curve C. This means that it can be both positive or negative depending upon the orientation of the curve (e.g. see the definition of $W_{\mathrm{r}}[K]$ given by Eq. (3.6)). In those cases, when in simulations *both* orientations of the curve are being considered (Whittington et al., 1993, 1994a,b), one needs to calculate $\langle |W_{\mathrm{r}}[K]| \rangle$ instead of Eq. (7.16). This causes us to replace $W_{\mathrm{r}}[\boldsymbol{u}(\tau)]$ in the exponent of Eq. (7.15) by the value of its modulus. The presence of the modulus sign in the exponent of the partition function in Eq. (7.15) causes no additional computational problems since the identity, Eq. (6.63), allows us to reduce this, apparently more complicated problem, to that without the modulus sign which is known to be soluble (Kholodenko and Vilgis, 1996). Indeed, in Section 6.1 we had mentioned already, that the propagator of Eq. (6.21) can be obtained by solving the Schrödinger-like Eq. (6.23) for the Dirac monopole (Dirac, 1931). In Kholodenko and Vilgis (1995, 1996) we had provided all technical details needed for proof of this fact.

Additional details can be found in the paper by Dunne (1992) and Aitchinson (1987). To calculate $Z(g)$ given by Eq. (7.15) we need to know only the spectrum of the corresponding Schrödinger-like operator and its degeneracy. Following Dunne (1992), we easily obtain

$$Z[g] = \sum_{n=0}^{\infty} (2|g| + 2n + 1)\exp\{-\omega E(n)\}, \tag{7.17}$$

where $E(n)$ is given by

$$E(n) = n(n+1) + |g|(2n+1). \tag{7.18}$$

For $g = 0$ we obtain back the result Eq. (7.9) as required. For $g \neq 0$ we have to use formally Eq. (7.16). This leads us to the problem. Eq. (7.17) does not contain an imaginary part while Eq. (7.16) contains the imaginary factor of i so that, if we formally use Eq. (7.17) in Eq. (7.16) we will obtain, seemingly, physically wrong imaginary result for the averaged writhe. The mistake in performing such formal manipulation lies in our so far formal treatment of the path integral of Eq. (7.15). Much more careful treatment, see, e.g. Kholodenko and Vilgis (1995, 1996) reveals that

the imaginary i-factor in Eq. (7.15) is not an artefact but an essential ingredient of the whole Dirac monopole problem. This can be seen already from our treatment of the two-dimensional analogue of the Dirac monopole problem discussed in Section 6.1. The transition from two to three dimensions is *not* merely a replacement of the winding number, Eq. (5.2), by that given by Eq. (6.28). It also involves the quantization of the coupling constant g in Eq. (7.15) known already to Dirac (1931). In three dimensions $g = 2\pi\Theta$ where $2\Theta = 0, \pm 1, \pm 2, \ldots$. Since g is quantized, the differentiation, e.g. like that given in Eq. (7.16), should be performed with some caution. The same caution should be exercised in view of the modulus sign for g in Eq. (7.15). The existence of this sign can be naturally associated with the possibility to have two orientations for the closed contour C as we have mentioned already. If the orientation of the contour is fixed, then by choosing e.g., $g > 0$, we can formally define the average writhe as

$$\langle |W_{\mathrm{r}}[K]| \rangle = \frac{1}{Z[g]} \left[2 \sum_{n=0}^{\infty} \exp\{ -\omega E(n) \} + \sum_{n=0}^{\infty} (2n+1)(2g+1+2n) \exp\{ -\omega E(n) \} \right]. \quad (7.19)$$

To compare this result with Eq. (3.8), it is sufficient now to let $g \to 0^+$ and to replace the summation by integration, e.g. as it was done in Eq. (7.10). This then produces

$$\langle |W_{\mathrm{r}}[K]| \rangle = \frac{N}{2\gamma} \left[\sqrt{\frac{2\gamma\pi}{N}} + \text{const.} \frac{\gamma^{3/2}}{N^{3/2}} \right] \propto \sqrt{\frac{N}{\gamma}} + \mathrm{O}\left(\frac{1}{\sqrt{N}} \right). \quad (7.20)$$

In arriving at this result we have used the definition of ω, Eq. (7.7), and required $g \to 0^+$ to reach an agreement with the numerical result of Eq. (3.8). Should we choose instead $g \to 0^-$, we would obtain, instead of Eq. (7.20), $\langle |W_{\mathrm{r}}[K]| \rangle \propto -\sqrt{N}$ so that, indeed, the algebraic sum of this result and that given by Eq. (7.20) produces zero in complete agreement with writhe definition given in Section 3.2. The fact that only one result was considered, while Eq. (7.19) provides the results for arbitrary (albeit discrete!) values of g, is associated with the specificity of the numerical simulations leading to the result of Eq. (3.8). In the limit $g \to 0^+$ the average, Eq. (7.16), represents a kind of Kubo-like result, where the average is made over the unperturbed "equilibrium" system. In the future numerical simulations one might be willing to study the general case: when both ω and g are allowed to wary. This could be especially relevant for studying the supercoiled DNA, etc.

7.3. Calculation of the knot complexity

We had defined the knot complexity in Section 3.2 as a number of vertices $c[K]$ in the planar graph for a given knot K. If the vertices are not resolved, e.g. like indicated in Fig. 2, then different knots could have, in principle, the same complexity. Whence, $c[K]$ is not a topological invariant for a given knot K. At the same time, the unknotting number $u[K]$ is. Use of the Bennequin conjecture, Eq. (3.9), allows to provide some bounds for $u[K]$ if both $W_{\mathrm{r}}[K]$ and $c[K]$ are known. Using the definition of $W_{\mathrm{r}}[K]$ given by Eq. (3.6) we can define $c[K]$ via

$$c[K] = \sum_{p \in S(K)|} |\varepsilon(p)| . \quad (7.21)$$

At the same time, using the definition of $W_r[K]$ given by Eq. (6.28), we can write as well

$$c[K] = \frac{1}{4\pi}\int_{S^1} d\tau \int_{S^1} d\tau^1 \left| \left(\frac{d\boldsymbol{r}}{d\tau} \wedge \frac{d\boldsymbol{r}}{d\tau^1} \right) \cdot \frac{(\boldsymbol{r}(\tau) - \boldsymbol{r}(\tau^1))}{|\boldsymbol{r}(\tau) - \boldsymbol{r}(\tau^1)|^3} \right| . \tag{7.22}$$

Such defined analytical expression for the knot complexity $c[K]$ is in agreement with that proposed by Arnold (1986). One may naively think that if one substitutes Eq. (7.22) into Eq. (7.15) (instead of $W_r[U(\tau)]$) the corresponding path integral could be easily solved as well. Unfortunately, use of the identity, Eq. (6.63), cannot help in this case so that to obtain the Schrödinger-like expression for the partition function $Z[g]$ is not an easy task. Instead, there is another method of computation (Freedman et al., 1994; Freedman and Z-Hu 1991) which uses the notion of the knot energy. The knot energy $E[K]$ can be defined as follows:

$$E[K] = \int_{-N/2}^{N/2} d\tau \int_{\tau - N/2}^{r + N/2} d\tau' \left\{ \frac{1}{|\boldsymbol{r}(\tau) - \boldsymbol{r}(\tau')|^\alpha} - \frac{1}{|\tau - \tau'|^\alpha} \right\} , \tag{7.23}$$

where the arch-length parametrization is used (i.e. $|d\boldsymbol{r}/d\tau| = 1$) and α is some constant, $1 < \alpha \leq 3$. As the above authors had shown,

$$c[K] + 2/\pi \leq (1/2\pi) E[K] . \tag{7.24}$$

The constant $2/\pi$ is obtained only for a special value of α: $\alpha = 2$. This value of α has some physical significance associated with the reparametrization invariance of the r.h.s. of Eq. (7.23). To see this, let us consider a special case of an unknot U_0: a circle γ_0 of radius R. Then, the energy of a circle can be calculated as

$$E[\gamma_0] = R^2 \int_{-\pi}^{\pi} d\tau \int_{-\tau-\pi}^{\tau+\pi} d\tau' \left\{ \frac{1}{[2R \sin|\tau - \tau'|/2]^\alpha} - \frac{1}{[R|\tau - \tau'|]^\alpha} \right\} . \tag{7.25}$$

For $\alpha = 2, E[\gamma_0]$ becomes independent of the radius R and, whence, of the length of the curve N. For any other α we obtain evidently

$$E[\gamma_0] \propto R^{2-\alpha} \propto N^{2-\alpha} . \tag{7.26}$$

If we assume that the above N-dependence persists also for more complicated (knotted) situations, then using Eq. (7.24) and ignoring the factor of $2/\pi$ (for large N) we obtain

$$c[K] \leq N^{2-\alpha} \tag{7.27}$$

which would require α to be less than or equal to one in order to be in qualitative agreement with the result of Eq. (3.7). This, however, is not permissible in view of the definition of $E[K]$, Eq. (7.23), which requires α to be between 1 and 3.

The resolution of this contradiction can be found if we analyze the averaged value of $E[K]$. The averaged knot energy is defined by

$$\langle E[K] \rangle = \int_0^N d\tau \int_0^N d\tau' \left\langle \frac{1}{|\boldsymbol{r}(\tau) - \boldsymbol{r}(\tau')|^\alpha} \right\rangle , \tag{7.28}$$

where we have disregarded the singular counterterm present in Eq. (7.23) for reasons which will become clear shortly below. To this purpose we have to decide what kind of the averaging

procedure can be used in Eq. (7.28). For $N \gg N_T$ we know from Section 5 that, most likely, our closed curve will be knotted and, because $N_T \gg l$ it can be also considered as very flexible. In this case, instead of the averaging defined by Eq. (7.2) we can use a simpler one, e.g. that for Gaussian-like chains:

$$\langle \cdots \rangle = N_G \int d\boldsymbol{r} \int_{\boldsymbol{r}(0)=\boldsymbol{r}(N)=\boldsymbol{r}} D[\boldsymbol{r}(\tau)] \exp\left\{ -\frac{3}{2l} \int_0^N d\tau \left(\frac{d\boldsymbol{r}}{d\tau} \right)^2 \right\} \cdots . \tag{7.29}$$

The normalization constant N_G is chosen, as before, to satisfy $\langle 1 \rangle = 1$. Replacement of Eq. (7.2) by Eq. (7.29) is done mainly for technical (computational) reasons. Evidently, Eq. (7.2) (or more complicated path integral for semiflexible chains) can be used as well, in principle. Our choice of averaging allows us to disregard the singular counterterm present in Eq. (7.23), since the averages of the type given by the r.h.s. of Eq. (7.28) are known in literature (Feynman, 1972; Kholodenko, 1992).

Before we engage ourself into calculation of the averaged knot energy, we would like to provide some justification for the word "energy" used by mathematicians. To this purpose, let us rewrite $E[K]$, given by Eq. (7.23), into the following equivalent form:

$$E[K] = \int_0^N d\tau f(\tau) , \tag{7.30}$$

where

$$f(\tau) = \int_0^N d\tau' \left\{ \frac{1}{|\boldsymbol{r}(\tau) - \boldsymbol{r}(\tau')|^\alpha} - \frac{1}{|\tau - \tau'|^\alpha} \right\} . \tag{7.31}$$

For a very large and very stiff circle, at least locally, the conformation of the contour is very close to the rigid rod limit (i.e. $k(\tau) \to 0$). In this case our problem resembles that known in the theory of polyelectrolyte chains (Kholodenko, 1995), i.e. polymer chains which carry some charges along their contours. When charges are unscreened, the cumulative electrostatic repulsion between the different segments along the chain is given by Eq. (7.30) with $\alpha = 1$. In the case of knots, $\alpha > 1$, and the electrostatic analogy cannot be used straightforwardly. Nevertheless, we can employ similar methods of analysis of $E[K]$. To this purpose, for $k(\tau) \to 0$, we can use the following Taylor series expansion

$$\boldsymbol{r}(\tau') = \boldsymbol{r}(\tau) + \frac{d\boldsymbol{r}}{d\tau}(\tau - \tau') + \frac{1}{2}\frac{d^2\boldsymbol{r}}{d\tau^2}(\tau - \tau')^2 + \cdots . \tag{7.32}$$

Use of the Secret–Frenet formulas from the differential geometry of estaic curves (Dubrovin et al., 1995; Kholodenko, 1990), allows us to obtain after some algebra

$$|\boldsymbol{r}(\tau) - \boldsymbol{r}(\tau')| \simeq s \left[1 - \frac{s^2}{12} k^2(\tau) \right]^{1/2} , \tag{7.33}$$

where $s = |\tau - \tau'|$. For $s \ll \sqrt{12}/|k(\tau)|$ we obtain

$$\frac{1}{|\boldsymbol{r}(\tau) - \boldsymbol{r}(\tau')|^\alpha} \simeq \frac{1}{s^\alpha} \left(1 + \frac{s^2}{12} k^2(\tau) \right)^{\alpha/2} \approx \frac{1}{s^\alpha} + \frac{\alpha}{24} s^{2-\alpha} k^2(\tau) + \cdots . \tag{7.34}$$

The first term in this expansion cancels with second (counter) term in Eq. (7.31) while the second term for $\alpha = 2$ becomes s-independent. In *this* limit we can safely write

$$E[K] = \frac{N}{12}\int_0^N d\tau\, k^2(\tau) \tag{7.35}$$

to be compared with Eq. (7.7). Obviously, for $\alpha = 2$ the knot energy has the same physical meaning as the elastic bending energy. For the unknot U_0, Freedman et al. (1994) had calculated $E[K]$ and found (for $\alpha = 2$): $E[U_0] = 6\pi + 4 = 22.84964$. Whence, we can write also for the unknot:

$$E[U_0] = \frac{N}{12}\int_0^N d\tau\, k^2(\tau) \approx 22.84954\,. \tag{7.36}$$

When this result is combined with the inequality Eq. (7.3) and Eq. (7.7) we obtain

$$6\pi + 4 = E[U_0] \geq \frac{1}{12}\int_0^1 d\tau\, k^2(\tau) \geq \frac{\pi^2}{3} \tag{7.37}$$

in complete agreement with the results discussed in Section 7.1.

With these observations we are ready now to calculate the averaged knot energy given by Eq. (7.28). To perform an average in Eq. (7.28), let us formally define the Fourier transform of the potential $|\boldsymbol{r}|^{-\alpha}$ via

$$v_\alpha(\boldsymbol{k}) = \int d\boldsymbol{r}|\boldsymbol{r}|^{-\alpha} e^{i\boldsymbol{k}\cdot\boldsymbol{r}} = \frac{4\pi}{k}\int_0^\infty dr\, r^{1-\alpha}\sin kr = \frac{4\pi}{k^{3-\alpha}}\,\mathrm{const}(\alpha)\,, \tag{7.38}$$

where $\mathrm{const}(\alpha) = \int_0^\infty dx\, x^{1-\alpha}\sin x$.

The const(α) is well defined only for $1 < \alpha < 3$, and this result is in a complete agreement with Freedman et al. (1994), where the same bounds were obtained by using completely different arguments. Using Eq. (7.28) we can write as well

$$v_\alpha(\boldsymbol{r}) = \frac{1}{|\boldsymbol{r}|^\alpha} = \frac{1}{(2\pi)^3}\int d\boldsymbol{k}\, e^{-i\boldsymbol{k}\cdot\boldsymbol{r}} v_\alpha(\boldsymbol{k})\,. \tag{7.39}$$

By combining Eq. (7.28) with Eq. (7.39), we obtain

$$\langle E[K]\rangle = \frac{1}{(2\pi)^3}\int d\boldsymbol{k}\, v_\alpha(\boldsymbol{k})\, S(\boldsymbol{k})\,, \tag{7.40}$$

where $S(\boldsymbol{k})$ is defined by

$$S(\boldsymbol{k}) = \int_0^N d\tau \int_0^N d\tau' \langle e^{-i\boldsymbol{k}\cdot(\boldsymbol{r}(\tau)-\boldsymbol{r}(\tau'))}\rangle\,. \tag{7.41}$$

This quantity (up to numerical prefactor) is the static scattering form-factor for the circular Gaussian-like polymers. This quantity was calculated by Casassa (1965), and it is for this reason we have chosen the averaging procedure specified by Eq. (7.29). The action in the exponent of Eq. (7.29) is *not* reparametrization-invariant while the energy, Eq. (7.23), is (for $\alpha = 2$).

The lack of reparametrization invariance for this and related action(s), and its consequences for the calculation of physical observables was recently discussed in Kholodenko (1995). The experience with flexible polymers suggests, nevertheless, that for a large ω the Gaussian approximation defined by Eq. (7.29) is quite adequate (the excluded volume effects can be easily incorporated into Eq. (7.29), if necessary, as it is explained below). For large ω the difference between the circular and the linear polymers becomes unimportant when computing $S(\boldsymbol{k})$, see, e.g. Feynman (1972). This fact allows us to write at once the result for $S(\boldsymbol{k})$:

$$S(\boldsymbol{k}) = N^2 \int_0^1 \mathrm{d}y \int_0^1 \mathrm{d}y' \, \mathrm{e}^{-(lN/6)|y-y'|} . \tag{7.42}$$

Combining this result with Eq. (7.40) we obtain,

$$\begin{aligned} \langle E[K] \rangle &= \frac{N^2}{(2\pi)^3} (4\pi)^2 \mathrm{const}(\alpha) \int_0^\infty \mathrm{d}k \, k^{\alpha-1} \int_0^1 \mathrm{d}y \int_0^1 \mathrm{d}y' \, \mathrm{e}^{-(lN/6)|y-y'|k^2} \\ &= \mathrm{const}'(\alpha) N^{2-\alpha/2} , \end{aligned} \tag{7.43}$$

where $\mathrm{const}'(\alpha)$ is defined by the first line of Eq. (7.43) (with appropriately rescaled k). The result of Eq. (7.43) should be compared against Eq. (7.26) and against the numerical result given by Eq. (3.7) (in view of Eq. (7.24)). For $\alpha \simeq 1$ we have $\langle E[K] \rangle \propto N^{3/2}$ while for $\alpha = 3$ we obtain $\langle E[K] \rangle \propto N^{1/2}$. While the first value lies within the domain of the expected values of α_c, see, e.g. Eq. (3.7), the second value is considerably lower. To sharpen our estimates, let us take now a closer look at the value of $\mathrm{const}'(\alpha)$ in Eq. (7.43). We have, upon proper rescaling,

$$\begin{aligned} \mathrm{const}'(\alpha) &\propto 2 \int_0^\infty \mathrm{d}k \, k^{\alpha-1} \int_0^1 \mathrm{d}y \int_0^1 \mathrm{d}y' \, \mathrm{e}^{-k^2|y-y'|} \\ &\propto \int_0^1 \mathrm{d}y \int_0^1 \mathrm{d}y' \frac{1}{|y-y'|^{\alpha/2}} \int_0^\infty \mathrm{d}k \, k^{\alpha-1} \, \mathrm{e}^{-k^2} . \end{aligned} \tag{7.44}$$

The last integral is manifestly nonsingular only for $1 < \alpha < 2$ which produces at once

$$c_\alpha N \le \langle E[K] \rangle \le c'_\alpha N^{3/2} , \tag{7.45}$$

where c_α and c'_α are some constants depending on α. Using Eq. (7.24) and ignoring the factor of $2/\pi$ which is permissible for large N's we obtain

$$\langle c[K] \rangle \le \frac{1}{2\pi} \langle E[K] \rangle . \tag{7.46}$$

By combining Eqs. (7.45) and (7.46) we conclude that the observed value(s) of α_c, defined by Eq. (3.7), should lie within the following bounds:

$$1 + \delta < \alpha_c < 1.5 - \delta \tag{7.47}$$

with $\delta \to 0^+$. The lower bound for α_c is also in accord with the result of Eq. (4.84) for the alternating knot(s) (link(s)).

The above bounds are obtained without taking account of the excluded volume effects. The experience with similar types of calculations (Kholodenko, 1992), suggests that the upper bound in Eq. (7.47) can be noticeably lowered thus bringing our estimate for $\langle c[K]\rangle$ closer to the experimentally observed, see, e.g. Eq. (3.7), and the discussion related to it. To this purpose we would like to recall that the mean end-to-end distance $\langle \boldsymbol{R}^2\rangle$ scales like $N^{2\nu}$ where $\nu = \frac{1}{2}$ for Gaussian chains and $\nu \simeq \frac{3}{5}$ for the chains with excluded volume (de Gennes, 1979). Whence, the result of Eq. (7.43) can be equivalently rewritten (for the Gaussian chains) as

$$\langle E[K]\rangle \propto N^{2-\alpha\nu} \equiv N^{\alpha_c} \tag{7.48}$$

and, by continuity, we expect it to be correct also in the good solvent regime. For α close to 1 this would produce

$$\alpha_c = 2 - \alpha\nu < 1.4 \tag{7.49}$$

while for the upper permissible value of $\alpha = 2$, the lower bound for the exponent α_c should remain unchanged, i.e. $\alpha_c = 1$, in view of Eq. (7.44). Hence, account for the excluded volume effects, brings our results much closer to the experimentally observed (Arteca, 1994, 1995).

7.4. Calculation of the unknotting number and the number of distinct knots as a function of polymer length N

The unknotting number of $u[K]$ was defined in Section 3.2 as the minimal number of self-crossings which will turn knot K into an unknot. Unfortunately, there is no known analytical expression for $u[K]$. The Bennequin inequality (conjecture) Eq. (3.9) provides some bounds for $u[K]$. We had demonstrated in Section 4.4 that $u[K]$ is of the order of the highest degree of the corresponding HOMFLY polynomial. By combining the inequality Eq. (4.80) with the conjecture Eq. (4.81), we obtain

$$M \simeq u[K] \leq \tfrac{1}{2}c[K]\,. \tag{7.50}$$

Accordingly, for the averaged quantities we obtain

$$u[K] \leq \frac{1}{4\pi}\langle E[K]\rangle \tag{7.51}$$

where we have used the fact that $u[K]$ is a topological invariant while $c[K]$ is not and its average is bound by $\langle E[K]\rangle$ according to the inequality (7.46). Obtained estimate for $u[K]$ deserves some additional comments. Indeed, since for a given knot K, $u[K]$ is a topological invariant, it should be independent of the polymer length N. At the same time, the average knot complexity $\langle c[K]\rangle$ as well as $\langle E[K]\rangle$ exhibit strong N-dependence. Moreover, the averaged $\langle c[K]\rangle$ *makes physical sense only with respect to the length of the polymer*. This can be seen already from our calculations of N_T. For $N < N_T$ we may still anticipate to observe crossings in knot projection(s) onto some chosen plane(s). The minimal number of crossings to produce a non-trivial knot should be at least 3 (Rolfsen, 1976). Whence, for $N \simeq N_T$ we expect to have *at least* 3 crossings. This naturally reintroduces the lower cut off into the knot problem. At the same time, if the number of crossings $c[K] \simeq n$ is *fixed* but $N \to \infty$, then the knot complexity $\langle c[K]\rangle \simeq n$ does not mean much, because $n/N \to 0$. By performing the average in Eq. (7.51) we actually replace the problem related to a *given*

knot K to that related to *all* possible knots of length N. Since $\langle c[K]\rangle$ grows faster than the length N, using the results of the previous subsection we obtain $n/N \sim N^{\alpha_c - 1} \to \infty$. The obtained infinity is not physically relevant, however. Indeed, if we would ignore (for the moment only), the excluded volume effects, then we would need to consider $\langle c[K]\rangle$ crossings in the volume $V \sim [\sqrt{\langle \boldsymbol{R}^2\rangle}]^3 \sim N^{3/2}$. This creates the ratio

$$P = \langle c[K]\rangle / N^{3\nu} \sim N^{2-\nu(3+\alpha)} \tag{7.52}$$

(with $\nu = \frac{1}{2}$ in the absence of excluded volume effects) which we shall call the "*packing capacity*" of a knot. According to our estimate, Eq. (7.47), this ratio will go to *at most* a constant for $\alpha = 1$. This would require to have no more than one crossing per unit volume (if we use the system of units where $l = 1$) which is physically sensible. Whence, the lower bound for the exponent α, $\alpha = 1$, can be obtained based on simple physical arguments. The upper bound for α can be also simply obtained if we formally consider the collapsed state for which $\sqrt{\langle \boldsymbol{R}^2\rangle} \propto N^{1/3}$, i.e. $\nu = \frac{1}{3}$. Using this result in Eq. (7.52) and requiring P to be a constant, we obtain $\alpha = 3$ in complete accord with Eq. (7.23).

Consider now the problem of calculation of the number of distinct knots for the polymer of length N. If the given knot K has n crossings, $n = c[K]$, then, according to Eq. (3.15), the average number of different knots $\langle K(n)\rangle$ with n crossings is bound by

$$2^{\langle c[K]\rangle} \leq \langle K(n)\rangle \leq 2(24)^{\langle c[K]\rangle}, \tag{7.53}$$

where $\langle c[K]\rangle$ was estimated in Section 7.3. Use of this result allows us to introduce an additional entropy term (not present for the linear polymers) via

$$S[K] = k_B \ln \langle K(n)\rangle, \tag{7.54}$$

where k_B is Boltzmann's constant. This extra entropy term leads to some measurable effects discussed in the next subsection.

7.5. Some physical applications

Roovers and Toporowski (1983) and Roovers (1985) have found that ring polystyrene in cyclohexane has a relatively large second virial coefficient A_2 at Θ temperature compared to the *linear* polymers of the same chemical composition. At the same time, they found that Θ temperature for the ring polymers (Θ_r) is noticeably *lower* than that for the linear polymers of *the same* chemical composition. These effects can be qualitatively explained with help of the entropic contribution defined by Eq. (7.54). Following Grosberg and Khokhlov (1989), one can introduce the swelling ratio $\delta = \sqrt{\langle R^2\rangle}/lN$. For the linear chain the free energy can be written as

$$\frac{F_{\text{linear}}}{k_B T} \approx \delta^2 + \frac{1}{\delta^2} + \left(\frac{B\sqrt{N}}{l^3}\right)\delta^{-3} + \left(\frac{C}{l^6}\right)\delta^{-6}, \tag{7.55}$$

where $B \propto (T - \Theta)/\Theta$ and the constant C is responsible for the strength of 3-body interactions. It is important to realize that Θ temperature can be defined in several ways (Kholodenko and Freed, 1984b). For example, it can be defined as a temperature at which the chain is exactly Gaussian, or

as a temperature at which the second virial coefficient A_2 vanishes. Since in the experiments by Roovers and Toporowski (1983), Roovers (1985) the second definition is used, we shall adopt it in this work too.

Minimization of the free energy with respect to δ produces the following equation for the linear chain:

$$\delta^5 - \delta = x + y\,\delta^{-3}\,, \tag{7.56}$$

where $x = B\sqrt{N/l^3}$ and $y = C/l^6$. This equation produces physically meaningful qualitative results in good, Θ and poor solvent regimes (Grosberg and Khokhlov, 1989). In particular, under Θ-conditions, if we choose $\delta = 1$ as a solution to Eq. (7.56) (which corresponds to the onset of collapse, Kholodenko and Freed, 1984b), this would require us to write $x = -y$, or

$$B = -C/l^3 1/\sqrt{N}\,. \tag{7.57}$$

Using the definition of B, we obtain the known shift of the Θ-temperature (without the logarithmic corrections, which only could be obtained field-theoretically, see, e.g. Kholodenko and Freed, 1984b):

$$\Theta - T \propto N^{-1/2}\,. \tag{7.58}$$

For rings we have to account for the extra entropy term introduced in Eq. (7.54). Since the entropy is always defined up to an additive constant, it is convenient to measure entropy with respect to Θ conditions. In this case, repeating the same steps as for the linear polymers, we arrive at the following equation:

$$\delta^5 - \delta = x + y\delta^{-3} + \text{const.}\,\delta^{\omega+3}\,, \tag{7.59}$$

where $\omega = \alpha_c/\nu$, in view of Eq. (7.48), and the actual value of non-negative const. is unimportant in these qualitative calculations. For $\delta = 1$ we have now $x = -y - \text{const.}$, or

$$B = -(C/l^3 + l^3\text{const.})1/\sqrt{N}\,. \tag{7.60}$$

This result indicates that the rings should have *lower* temperature Θ_r at which they behave as ideal. This means that at Θ temperature for the *linear* polymers, the *ring* polymers will have $\delta > 1$, i.e. the topological entropy, Eq. (7.54), produces the same effect on rings as if they would have an additional excluded volume-type interaction which makes the second virial coefficient for rings effectively larger than that for the linear polymers. This is in complete accord with the observations by Roovers and Toporowski (1983). Our explanation of these effects differs, however, from that provided by Iwata (1989).

Consider now another application. Our calculation of the averaged knot energy, Eq. (7.28), is very similar to the calculation of the diffusion coefficient D for the individual polymer chain. Within the Kirkwood approximation the calculation of D involves the averages like

$$D = \frac{k_B T}{6\pi\eta_s}\int_0^N \frac{d\tau}{N}\int_0^N \frac{d\tau'}{N}\left\langle \frac{1}{|\boldsymbol{r}(\tau) - \boldsymbol{r}(\tau')|}\right\rangle, \tag{7.61}$$

see, e.g. Kholodenko (1992). Here, η_s is the viscosity of the solvent. For the Gaussian-like chains the average in Eq. (7.61) is easily computable with the result (for D):

$$D = \frac{k_B T}{6\pi\eta_s \sqrt{\langle \boldsymbol{R}^2 \rangle}}, \tag{7.62}$$

where $\langle \boldsymbol{R}^2 \rangle \propto N$. Hence, the diffusion coefficient for polymers formally resembles that for the hard spheres if the sphere radius R is approximated by $\sqrt{\langle \boldsymbol{R}^2 \rangle}$. Not surprisingly, the porocity (the packing capacity, P which we had introduced earlier in Eq. (7.52)) indicates that, indeed, at Θ conditions our ring polymer acts as if it is a hard impenetrable sphere. This result, surprisingly, comes also from the completely different type of calculations performed by Oono and Kohmoto (1982). Evidently in solvents other than Θ-solvents the concept of porocity can be used as well. In detailed calculations Wiegel (1980) and later Starting and Wiegel (1994) had shown how to perform calculations for solutions of polymers modelled as porous hard spheres. The central idea for these calculations is a phenomenological Darcy's law which can be written as

$$\boldsymbol{F} = -\frac{\eta_s}{k}\boldsymbol{V}, \tag{7.63}$$

where $\boldsymbol{F}$ is the force exerted by the fluid on the medium (per unit volume) and $\boldsymbol{V}$ is the velocity of fluid while the phenomenological constant k is related to our porocity $\boldsymbol{P}$ as can be seen from Wiegel (1980). The microscopic origin of the Darcy law is studied in some detail by Bear (1972). Unlike Wiegel's work in which the porocity was introduced as a phenomenological parameter, in the present case its origin is known so that the additional refinements could be made, see, e.g. the results by Quake (1994) discussed in Section 2.

Finally, let us notice, following Delbrück (1962), that the difference between the truly circular and the linear polymers is not so significant, at least at Θ conditions where $\sqrt{\langle \boldsymbol{R}^2 \rangle} \simeq \sqrt{N}$ so that the ratio $\sqrt{\langle \boldsymbol{R}^2 \rangle}/N \to 0$, for $N \to 0$. I.e. the distance between the ends of an open polymer chain is much smaller than the contour distance. Under these conditions, the rapid temperature quench could bring our polymer into one of $\langle K(n) \rangle$ globular-like (glassy) states as was first noticed by de Gennes (1984). Since, nevertheless, such a glassy state is not a state of true equilibrium, there is a difference between the kinetics of collapse for linear and circular polymers (de Gennes, 1985; Grosberg et al., 1988; Ma et al., 1995).

Still, additional applications of the obtained results could be made for problems which involve vortices in superfluid helium, classical turbulence, superconductivity, etc., see, e.g. Akao (1996). We deliberately avoid discussions of these applications with hope that the interested reader can easily restore the details, based on the results which we describe in this review, if necessary.

7.6. Link energy and the probability of entanglement between two ring polymers

The formalism developed above can be easily extended for the links. In case of links, new questions could be posed (as discussed in Section 2) in addition to that presented in the previous subsection. Vologodskii et al. (1975) being influenced by much earlier work by Frisch and Wasserman (1961), had discussed the following problem. Consider two closed random walks which are independently generated on some cubic lattice. For each walk the position of center of mass (for

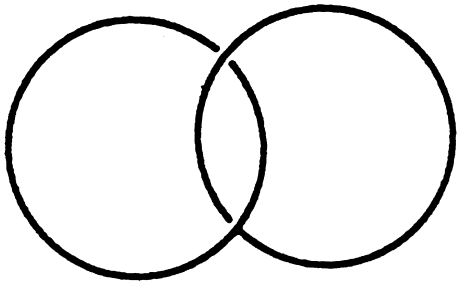

Fig. 10. The simplest (Hopf) link considered by Vologodskii et al. (1975) in connection with calculation of the probability $P_2(R)$.

unit masses at the ends of each bond segment) was determined with respect to some coordinate system. Then, thus generated "polymer" rings were brought to the proximity of each other so that the distance between their centers becomes R. This motion of one ring with respect to other was made by means of a simple parallel translations (i.e. without deforming "polymer chains") so that one ring could go through another without the excluded volume restrictions (phantom chains). The probability $P_0(R)$ that the rings are *not* entangled was determined as well as the probability $P_i(R)$ of entanglement into a topological state i (where i was determined through usage of knot polynomials (e.g. see Section 4)). The possibility of having rings both knotted and entangled was disregarded, and only entanglements *between* rings were counted. As a result of these numerical simulations, $P_0(R)$ was determined to behave as

$$P_0(R) = 1 - A_0 \exp(-\alpha_0 R^3)\,, \tag{7.64}$$

where A_0 is some constant (of order unity for long chains) and $\alpha_0 \propto N^{-1.7}$. For the simplest link depicted in Fig. 10 the results of computer simulation had produced the following result for $P_2(R)$:

$$P_2(R) = A_2 \exp(-\alpha_2 R^3)\,, \tag{7.65}$$

where the polymer length dependence of constants A_2 and α_2 was not given explicitly. This dependence was estimated only quite recently by Everaers and Kremer (1996) who found $\alpha_2 \approx \alpha/2R_L^3$ with $\alpha \simeq 0.6$ and $R_L \simeq \sqrt{N}$. These results are going to be reproduced below with help of the link energy E_L (Freedman et al., 1994), defined by (for the n-component link)

$$E_L \equiv E(\{K_i\}) = \sum_{i=1}^{n} E[K_i,K_i] + \frac{1}{2}\sum_{\substack{i,j=1\\ i\neq j}}^{n} E[K_i,K_j]\,, \tag{7.66}$$

where

$$E[K_i,K_i] \equiv E[K_i]\,, \tag{7.67}$$

with $E[K_i]$ being defined in Eq. (7.23), while $E[K_i,K_j]$ is being defined as

$$E[K_i,K_j] = \int_0^N d\tau_i \int_0^N d\tau_j \frac{1}{|\boldsymbol{r}(\tau_i) - \boldsymbol{r}(\tau_j)|^{\alpha}}\,. \tag{7.68}$$

The arch-length parametrization is being used here in complete agreement with Eq. (7.23). Since, according to Vologodskii et al. (1975), the individual rings are assumed to be knotless, the first form

in Eq. (7.66) can be omitted. As before, we need to calculate the averaged link energy. This averaging can be performed with help of the averaging procedure defined by Eq. (7.29) (this time, for two ring-type polymers). The reason why we are interested in the averaged link energy could be seen from the standard statistical mechanics arguments, Hill (1956), which connects the pair correlation function $g(\boldsymbol{r}_1, \boldsymbol{r}_2) = g(|\boldsymbol{r}_1 - \boldsymbol{r}_2|)$ with the potential of the mean force $U(|\boldsymbol{r}_1 - \boldsymbol{r}_2|)$:

$$g(|\boldsymbol{r}_1 - \boldsymbol{r}_2|) = \exp\left(- \frac{U(|\boldsymbol{r}_1 - \boldsymbol{r}_2|)}{k_{\mathrm{B}} T} \right), \tag{7.69}$$

where, in case of m point-like interacting particles, $U(|\boldsymbol{r}_1 - \boldsymbol{r}_2|)$ is given by

$$U(|\boldsymbol{r}_1 - \boldsymbol{r}_2|) = \frac{1}{Z} \int \prod_{i=1}^{m} \mathrm{d}\boldsymbol{r}_{i+2} \sum_{i,j}^{m'} V(|\boldsymbol{r}_i - \boldsymbol{r}_j|) \exp\left\{ - \frac{\sum'_{i,j=1} V(|\boldsymbol{r}_i - \boldsymbol{r}_j|)}{k_{\mathrm{B}} T} \right\} \tag{7.70}$$

with $V(|\boldsymbol{r}_i - \boldsymbol{r}_j|)$ being the microscopic (two-body) potential and Z is just the partition function itself. The prime(s) indicate the absence of self-interaction terms, i.e. $i \neq j$, in Eq. (7.70).

In case of the entangled polymers, the correlation function $g(|\boldsymbol{r}_1 - \boldsymbol{r}_2|) \equiv g(R)$ can be identified with $P_i(R)$ introduced earlier. *This is effectively done in* Vologodskii et al. (1975). Whence, calculation of $P_i(R)$ is reduced to the calculation of the potential of the "mean force", i.e. to the calculation of the averaged link energy. The attempts to perform such calculation (but *without* use of Eq. (7.68)!) were made in the past, see, e.g. Tanaka (1982) or Iwata and Kimura (1981). No agreement has been reached between these calculations and Monte Carlo simulations by Vologodskii et al. (1975). The calculation of the averaged link energy is very similar to the calculation of the second virial coefficient A_2 for the dilute polymer solutions, see, e.g. Kholodenko and Freed (1983). The only novelty of the present calculation, as compared to the calculation of A_2, lies in the additional constraint

$$\boldsymbol{R} - \frac{1}{N} \int_0^N \mathrm{d}\tau_1 \, \boldsymbol{r}(\tau_1) + \frac{1}{N} \int_0^N \mathrm{d}\tau_2 \, \boldsymbol{r}(\tau_2) = 0 \tag{7.71}$$

which needs to be inserted into the corresponding path integral measure thus reflecting the fact that the distance between the center of masses of rings should be equal to $\boldsymbol{R}$. The calculation of A_2 involves the Feynman diagram depicted in Fig. 11. Here the solid closed line(s) indicate(s) the propagator(s) for the ring polymer(s), the wavy line indicates the interaction between the polymers and the volume factor V^{-1} is needed to make A_2 volume-independent.

For completeness, we provide some details of this simpler calculation which are needed in the more difficult case involving the constraint, Eq. (7.71). In the system of units, in which the Kuhn's lenth l is chosen to be $2d$, the propagator $G_0(\boldsymbol{R}, \tau)$ for the open chain can be written as

$$G_0(\boldsymbol{R}, \tau) = \int \frac{\mathrm{d}^d k}{(2\pi)^d} \mathrm{e}^{-k^2 \tau + \mathrm{i} \boldsymbol{k} \cdot \boldsymbol{R}} . \tag{7.72}$$

Since the calculation of the loop(s) in the denominator of Fig. 11 involves integrals like $\int \mathrm{d}^d R \, G_0(\boldsymbol{R}, N)$, we obtain two volume factors coming from two rings. In the numerator the extra volume factor will come because of the translational invariance of the interaction potential. These considerations explain the presence of the volume factor in Fig. 11. Calculation of the numerator

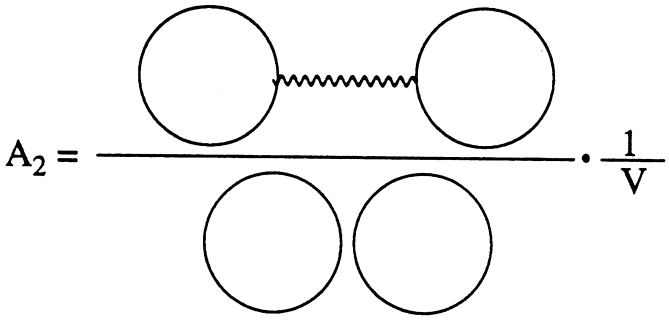

Fig. 11. Feynman diagram for the calculation of the second virial coefficient A_2.

involves calculation of the following expression:

$$I = \int_0^N d\tau \int_0^N d\tau' \int d\boldsymbol{r}_1 \int d\boldsymbol{r}_2 \int d\boldsymbol{r}'_1 \int d\boldsymbol{r}'_2 \, G_0(\boldsymbol{r}_1 - \boldsymbol{r}_2, \tau) \times G_0(\boldsymbol{r}_2 - \boldsymbol{r}_1, N - \tau) V(|\boldsymbol{r}_2(\tau) - \boldsymbol{r}'_2(\tau')|) \times G_0(\boldsymbol{r}'_1 - \boldsymbol{r}'_2, \tau') G_0(\boldsymbol{r}'_2 - \boldsymbol{r}'_1, N - \tau') \,, \tag{7.73}$$

where $V(|\boldsymbol{r}_1 - \boldsymbol{r}_2|)$ is the polymer–polymer interaction potential. Substitution of Eq. (7.72) into Eq. (7.73) and account of translational invariance immediately produce the following result for I:

$$I = N^2 [G_0(0,N)]^2 V^3 \int d\boldsymbol{R} \, V(|\boldsymbol{R}|) \tag{7.74}$$

so that the result for A_2 follows:

$$A_2 = N^2 V(\boldsymbol{k} = \boldsymbol{0}) \,, \tag{7.75}$$

where $V(\boldsymbol{k} = \boldsymbol{0})$ is obtained by noticing that

$$V(\boldsymbol{k}) = \int d\boldsymbol{R} \, e^{i\boldsymbol{k}\cdot\boldsymbol{R}} V(|\boldsymbol{R}|) \,. \tag{7.76}$$

To account for the constraint given by Eq. (7.71) it is useful to recalculate I using a different method, Feynman (1972). For this purpose, we have to consider the calculation of the following auxiliary functional integral for the closed path:

$$\hat{I} = \int_0^N d\tau \int_{r(0)=r(N)} D[\boldsymbol{r}(\tau')] \exp\left\{ -\frac{1}{4} \int_0^N d\tau' \dot{\boldsymbol{r}}^2 + i\boldsymbol{k}\cdot\boldsymbol{r}(\tau) \right\} . \tag{7.77}$$

To calculate such an integral it is very useful to introduce the following Fourier decomposition of $\boldsymbol{r}(\tau)$:

$$\boldsymbol{r}(\tau) = \boldsymbol{a}_0 + \sum_{n=1}^{\infty} \boldsymbol{a}_n \cos\left(\frac{n\pi\tau}{N}\right) . \tag{7.78}$$

Using this decomposition the action in the exponent of the path integral of Eq. (7.77) can be written as (Kholodenko and Quian, 1988)

$$S = \frac{\pi^2}{8N}\sum_{n=1}^{\infty} \boldsymbol{a}_n^2\, n^2 - \mathrm{i}\boldsymbol{k}\cdot\sum_{n=0}^{\infty}\boldsymbol{a}_n \cos\left(\frac{n\pi\tau}{N}\right). \tag{7.79}$$

The integral over the zero mode $\boldsymbol{a}_0$ produces $\delta(\boldsymbol{k})$ so that the second term in Eq. (7.79) (with components $\boldsymbol{a}_n$ other than zero) vanishes upon $\boldsymbol{k}$-integration. The first term in Eq. (7.79) has the same structure as that calculated for the closed paths (Feynman, 1972), and, whence will produce the same result as Eq. (7.72) (for $\boldsymbol{R} = \boldsymbol{0}$). The presence of $\delta(\boldsymbol{k})$ is important since if we represent the interaction potential as

$$V(\boldsymbol{r}_1, \boldsymbol{r}_2) = \int\frac{\mathrm{d}^d k}{(2\pi)^d}\int\frac{\mathrm{d}^d k'}{(2\pi)^d}\mathrm{e}^{\mathrm{i}\boldsymbol{k}\cdot\boldsymbol{r}_1 + \mathrm{i}\boldsymbol{k}'\cdot\boldsymbol{r}_2}V(\boldsymbol{k},\boldsymbol{k}') \tag{7.80}$$

so that $V(\boldsymbol{k},\boldsymbol{k}') = V(\boldsymbol{k})\delta(\boldsymbol{k}+\boldsymbol{k}')$, then evidently, zero modes coming from two rings will remove $\boldsymbol{k}$ and $\boldsymbol{k}'$ integrations in Eq. (7.80) thus producing the volume factor $\delta(\boldsymbol{0})$ coming from $\delta(\boldsymbol{k}+\boldsymbol{k}')$. Collecting all terms together, we arrive again at the result of Eq. (7.75) as required.

Consider now the more complicated case which involves the constraint of Eq. (7.71). In this case, we have to substitute into the path integral measure the δ-factor given by

$$\delta = \int\frac{\mathrm{d}^3 K}{(2\pi)^3}\exp\left[\mathrm{i}\boldsymbol{K}\cdot\left(\boldsymbol{R} - 1/N\int_0^N \mathrm{d}\tau\,\boldsymbol{r}(\tau) + 1/N\int_0^N \mathrm{d}\tau'\boldsymbol{r}(\tau')\right)\right]. \tag{7.81}$$

The presence of this factor changes the action in the exponent of Eq. (7.77) into

$$S = \frac{1}{4}\int_0^N \mathrm{d}\tau'\dot{\boldsymbol{r}}^2 - \mathrm{i}\boldsymbol{k}\cdot\boldsymbol{r}(\tau) + \mathrm{i}\,\boldsymbol{K}\cdot\frac{1}{N}\int_0^N \mathrm{d}\tau'\,\boldsymbol{r}(\tau'). \tag{7.82}$$

Use of the Fourier expansion, Eq. (7.78), converts the above action into

$$S' = \frac{\pi^2}{8N}\sum_{n=1}^{\infty}\boldsymbol{a}_n^2 n^2 - \mathrm{i}\boldsymbol{k}\cdot\sum_{n=0}^{\infty}\boldsymbol{a}_n\cos\left(\frac{n\pi\tau}{N}\right) + \mathrm{i}\,\boldsymbol{K}\cdot\boldsymbol{a}_0\,. \tag{7.83}$$

Integration of the zero mode produces now the δ-constraint: $\delta(\boldsymbol{k}-\boldsymbol{K})$. By integrating over $\boldsymbol{k}$ (see, e.g. Eq. (7.80)) we are left with the following action:

$$S' = \frac{\pi^2}{8N}\sum_{n=1}^{\infty}\left[\boldsymbol{a}_n^2\, n^2 - \mathrm{i}\,\boldsymbol{K}\cdot\boldsymbol{a}_n\cos\left(\frac{n\pi\tau}{N}\right)\right]. \tag{7.84}$$

Performing the Gaussian integration over each of $\boldsymbol{a}_n$ modes we obtain now the following result including both rings and discarding factors like $\delta(\boldsymbol{0})$:

$$\frac{U(|\boldsymbol{R}|)}{k_{\mathrm{B}}T} = \int\frac{\mathrm{d}^3 K}{(2\pi)^3}\mathrm{e}^{\mathrm{i}\boldsymbol{K}\cdot\boldsymbol{R}}V_{\alpha}(\boldsymbol{K})\int_0^N \mathrm{d}\tau\int_0^N \mathrm{d}\tau'$$
$$\times\exp\left\{-\frac{2NK^2}{\pi^2}\sum_{n=1}^{\infty}\frac{1}{n^2}\left[\cos^2\left(\frac{n\pi\tau}{N}\right) + \cos^2\left(\frac{n\pi\tau'}{N}\right)\right]\right\}. \tag{7.85}$$

Following Feynman (1972), we can replace the summation in the exponent of Eq. (7.85) by the integration via the rule:

$$\sum_{n=1}^{\infty} \cdots \to \frac{N}{\pi}\int_0^{\infty} \mathrm{d}x \cdots . \tag{7.86}$$

This produces after a little calculation (upon completion of τ integrations and rescaling):

$$\frac{U(|\boldsymbol{R}|)}{k_{\mathrm{B}}T} = \frac{2\,\mathrm{const}\,(\alpha)}{\pi}\left(\frac{R}{\sqrt{N}}\right)^{4-\alpha}\int_0^{\infty} \mathrm{d}x\, x^{\alpha-5}(1-\mathrm{e}^{-x^2/R^2})^2\left(\frac{\sin xy}{xy}\right), \tag{7.87}$$

where const(α) was defined after Eq. (7.38) and $y^{-1} = \sqrt{N}$. Straightforward convergence analysis indicates that the obtained integral is convergent for $1 \le \alpha \le 3$ in complete agreement with the results of Section 7.3. In order to actualy use Eq. (7.87) we notice that for $y \ll 1$ we can subdivide the domain of x-integration into two parts, e.g. from 0 to 1 and from 1 to ∞. We then can appropriately Taylor series expand the integrand in each subdomain of integration by taking into account that (in chosen system of units) $R^2 \ge 1$. For $\alpha = 1$ and $R \ll N$ we obtain, in view of Eq. (7.69), the result of Everaers and Kremer (1996) given by Eq. (7.65) while for $\alpha = 2$ we obtain the result of Helfand and Pearson (1983). Comparison between these results and Eq. (7.44) indicates that the exponent α in Eq. (7.87) is likely to be bounded by the inequality $1 \le \alpha \le 2$ for any kind of entanglement of a given polymer with other polymers (or with itself). This observation leads us to Eq. (2.21) where, accordingly, we obtain $2 \le \omega \le 3$.

Obtained results allow us to calculate several additional quantities. For example, in view of Eq. (7.64), one can calculate the topological second virial coefficient A_2^{T} between two non-entangled polymers. Following Vologodskii et al. (1975), we obtain

$$A_2^{\mathrm{T}} = \frac{1}{2}\int \mathrm{d}^3 r\left[1 - \exp\left(-\frac{F_0(R)}{k_{\mathrm{B}}T}\right)\right], \tag{7.88}$$

where $F_0(R)$ is related to $P_0(R)$ via

$$F_0 = -k_{\mathrm{B}}T \ln P_0(R)\,. \tag{7.89}$$

Substitution of Eq. (7.89) into Eq. (7.88) produces, in view of Eqs. (7.64) and (2.21), the following result for A_2^{T} (for $\alpha \simeq 1$):

$$A_2^{\mathrm{T}} = \tfrac{4}{3}\pi R_{\mathrm{L}}^3\,. \tag{7.90}$$

It is quite remarkable that this result was obtained with help of only qualitative arguments by Frisch and Wasserman (1961) as discussed in Section 2. The existence of non-negative A_2^{T} causes additional repulsion between the polymer rings (not to be confused with depression of Θ temperature discussed in Section 7.5) thus leading to the effective reduction of their sizes. More quantitative analysis of this phenomenon is provided in Section 8.

8. Polymer dynamics: an interplay between topology and geometry

8.1. Statistical mechanics of a melt of polymer rings

Already in Section 2 we have noticed that in the melt of linear polymers of length N the ratio $\sqrt{\langle R^2\rangle}/N \to 0$ for $N \to \infty$. I.e. dynamically, for times $\tau < \tau_t$ the melt of polymer rings and linear polymers should behave very similar which is indeed the case, see, e.g. McKena et al. (1989) (especially Fig. 20 of this reference). This experimental observation is very important for the development of the dynamics of polymer melts of both linear and ring polymers. The entanglements which are inevitably present in such melts in the form of (quasi) links are not only responsible for the formation of the effective tube which surrounds the given polymer chain (which is well documented experimentally, Straube et al., 1995) but affect also the stiffness of the trapped chain. We have discussed this fact, in part, in Section 6.3 from the geometrical point of view. Here we would like to discuss the same problem from the topological point of view.

To this purpose, let us consider again the partition function given by Eq. (4.10). Following the work of Brereton and Vilgis (1995), we shall concentrate our attention on a single ring placed in a melt of other rings. The many body problem which involves different rings is going to be reduced effectively to the one-body problem for the ring which is being singled out. To this purpose, let us rewrite Eq. (4.10) in the following form:

$$Z(\{c_\alpha\},\{m_{\beta\beta'}\}) = \left\langle \prod_{\beta\neq\alpha}^{n} \delta(lk(\alpha,\beta),m_{\alpha\beta}) \prod_{\beta>\beta'\neq\alpha}^{n} \delta(lk(\beta,\beta'),m_{\beta\beta'}) \right\rangle \tag{8.1}$$

where $\delta(x,y)$ is, as before, the Kroneker's delta and $\langle \cdots \rangle$ denotes the polymer averaging, e.g. like that given by Eq. (7.29), of all $n-1$ chains, except one, which we denote as α. Since the Kroneker's delta can be written as

$$\delta(x,y) = \int_0^{2\pi} \frac{\mathrm{d}g}{2\pi} \exp\{\mathrm{i}g(x-y)\}, \tag{8.2}$$

Eq. (8.1) can be equivalently rewritten according to Brereton and Vilgis (1995) as

$$Z(\{c_\alpha\};\{m_{\beta\beta'}\}) = \prod_{\beta\beta'=1}^{n} \int_0^{2\pi} \frac{\mathrm{d}g_{\beta\beta'}}{2\pi} Z(\{c_\alpha\};\{g_{\beta\beta'}\}) \exp\{-\mathrm{i}g_{\beta\beta'}m_{\beta\beta'}\} \tag{8.3}$$

where

$$Z(\{c_\alpha\},\{g_{\beta\beta'}\}) = \left\langle \exp\left\{\frac{1}{\Omega}\sum_{\beta\neq\alpha}(g_{\alpha\beta}+g_{\beta\alpha})\frac{(\boldsymbol{u}^\alpha(\boldsymbol{q})\times\boldsymbol{u}^\beta(-\boldsymbol{q}))\cdot\boldsymbol{q}}{\boldsymbol{q}^2}\right\} \times \exp\left\{\frac{1}{\Omega}\sum_{\beta\beta'\neq\alpha} g_{\beta\beta'}\frac{(\boldsymbol{u}^\beta(\boldsymbol{q})\times\boldsymbol{u}^{\beta'}(-\boldsymbol{q}))\cdot\boldsymbol{q}}{\boldsymbol{q}^2}\right\}\right\rangle, \tag{8.4}$$

and Ω is the volume of the system. In arriving at the result given by Eq. (8.3) the linking number, defined by Eq. (4.11), has been transformed with help of identities

$$\boldsymbol{u}^\alpha(\boldsymbol{r}) = \oint_{c_\alpha} \mathrm{d}\boldsymbol{l}^\alpha \delta(\boldsymbol{r}^\alpha - \boldsymbol{r}), \tag{8.5}$$

$$\frac{r^k}{|\boldsymbol{r}|^3} = \frac{1}{2\pi^2\mathrm{i}}\int \mathrm{d}^3q \frac{q^k}{q^2}\exp(\mathrm{i}\boldsymbol{q}\cdot\boldsymbol{r}). \tag{8.6}$$

Such transformation allows to calculate the partition function, Eq. (8.1), in formally closed form given by

$$Z(\{c_\alpha\};\{m_{\beta\beta'}\}) = \prod_{\beta\beta'=1}^{n} \frac{1}{\pi^2}\int_0^{\pi} \mathrm{d}a_{\beta\beta'} \int_{a_{\beta\beta'}}^{2\pi - a_{\beta\beta'}} \mathrm{d}s_{\beta\beta'} \exp\{\mathrm{i}2 s_{\beta\beta'} m_{\beta\beta'}\}$$
$$\times \exp\left\{ -\frac{1}{\Omega}\sum_{\boldsymbol{q}} [A_{\alpha\alpha}(\boldsymbol{q};\{s_{\beta\beta}\}) l(\boldsymbol{q};\{c_\beta\}) - B_{\alpha\alpha}(\boldsymbol{q};\{s_{\beta\beta'}\})\phi(\boldsymbol{q};\{c_\alpha\})]\right\} \tag{8.7}$$

where the matrices

$$A_{\alpha\alpha}(\boldsymbol{q};\{s_{\beta\beta'}\}) = \frac{n}{\gamma(\boldsymbol{q})}\left\{ \Gamma^2 \left[1 + \frac{\Gamma^2}{q^2}\right]^{-1}\right\}_{\alpha\alpha},$$
$$B_{\alpha\alpha}(\boldsymbol{q};\{s_{\beta\beta'}\}) = \frac{n}{\gamma(\boldsymbol{q})}\left\{ \frac{\Gamma^3}{q^2} \left[1 + \frac{\Gamma^2}{q^2}\right]^{-1}\right\}_{\alpha\alpha}, \tag{8.8}$$

with matrix $\Gamma_{\alpha\beta}$ being given by

$$\Gamma_{\alpha\beta} \equiv [\Gamma(\boldsymbol{q})]_{\alpha\beta} = (1/n) s_{\alpha\beta}\gamma(\boldsymbol{q}); \tag{8.9}$$

while

$$\gamma(\boldsymbol{q}) = \rho \oint_{c_\alpha}\oint_{c_\alpha} \mathrm{d}\boldsymbol{l}\cdot\mathrm{d}\boldsymbol{l}' \langle \exp\{\mathrm{i}\boldsymbol{q}\cdot(\boldsymbol{r}-\boldsymbol{r}')\}\rangle, \tag{8.10}$$

$$l(\boldsymbol{q};\{c_\alpha\}) = \oint_{c_\alpha}\oint_{c_\alpha} \mathrm{d}\boldsymbol{l}\cdot\mathrm{d}\boldsymbol{l}' \frac{\exp\{i\boldsymbol{q}\cdot(\boldsymbol{r}(l)-\boldsymbol{r}(l'))\}}{q^2}, \tag{8.11}$$

$$\phi(\boldsymbol{q};\{c_\alpha\}) = \oint_{c_\alpha}\oint_{c_\alpha} \mathrm{d}\boldsymbol{l}\times\mathrm{d}\boldsymbol{l}'\cdot\boldsymbol{q} \frac{\exp\{\mathrm{i}\boldsymbol{q}\cdot(\boldsymbol{r}(l)-\boldsymbol{r}(l'))\}}{q^2} \tag{8.12}$$

with $\rho = Nn/\Omega$.

Evidently, in order to calculate Eq. (8.7) explicitly, some approximations should be made. These are discussed in Brereton and Vilgis (1995). The results can be considerably simplified if all linking numbers $m_{\alpha\beta}$ in Eq. (8.1) are being put equal to zero which corresponds to the description of the melt of unlinked rings. In this case, after some algebra, one arrives at the result

$$Z(\{c_\alpha\},\{0\}) = \exp\{\mathrm{i}\pi lk(\alpha,\alpha)\}\exp[-(1/l_{\mathrm{eff}})E[\{c_\alpha\}]] \tag{8.13}$$

with the self-linking number $lk(\alpha,\alpha)$ being defined by Eq. (4.19) while the knot energy $E(\{c_\alpha\})$ is being given by

$$E[\{c_\alpha\}] = \lim_{\varepsilon\to 0}\oint_{c_\alpha}\oint_{c_\alpha} \frac{\mathrm{d}\boldsymbol{l}\cdot\mathrm{d}\boldsymbol{l}'}{|\boldsymbol{r}(l)-\boldsymbol{r}(l')|^{1+\varepsilon}}$$

with $l_{\mathrm{eff}} = l(6/\rho l^3\pi^2)$. In the original paper of Brereton and Vilgis (1995) a different terminology for $E[\{c_\alpha\}]$ is being used (they call it the "self-inductance"). This choice of terminology is due to chronological reasons: the paper by Brereton and Vilgis had appeared in 1995 while Kholodenko

and Rolfsen's had been published in 1996. Both terms in the exponents of Eq. (8.13) were already discussed earlier in this work. The first term is associated with the choice of framing, see, e.g. Section 4.2, and causes the polymer chain to be more stiff, Section 6.1. The presence of the second term is essential if the polymer chain is effectively knotted as discussed in Sections 3, 5 and 7. Implicitly, it can also be associated with the probability for a given chain *not* to be entangled with other chains as discussed in Section 7.6. When the r.h.s. of Eq. (8.13) is substituted into the path integral, e.g. Eq. (7.2), for the ring C_∞, this leads to the delicate competition between the stiffening and softening. In Kholodenko (1991) only the stiffening effect was taken into account which amounts to the assumption (also implicitly present in de Gennes (1971) and Doi and Edwards (1978) treatment of reptation) that the chain trapped into the tube is knotless. If the rigidity wins, then one can use the scaling analysis of Section 2.2 in order to arrive at famous result: $\tau_t \propto N^{3.4}$ for the viscosity. Since, however, according to Eqs. (3.5) and (5.95), for $N \to \infty$ the fraction of the unknotted rings is completely negligible, the presence of the second term in the exponent of Eq. (8.13) is quite natural and effectively counterbalances the stiffening leading to the noticeable contraction of the ring in the polymer melt (Müller et al. 1996), in qualitative accord with calculations of Brereton and Vilgis (1995). Since the topological effects alone are unable to make the trapped polymer backbone more stiff, the geometrical factors discussed in Section 6.3 should be taken into account. They are responsible for making the longitudinal part of the trapped polymer motion more stiff so that the scaling analysis of Section 2.2 could be used. The transversal part of this motion requires additional discussion since it is responsible for the transition from the Rouse to the reptation regime of the dynamics of polymer melts (Kholodenko, 1996b,c; Kholodenko and Vilgis, 1994).

8.2. Statistical mechanics of planar rings in an array of obstacles (the replica approach)

The transversal motion of the trapped polymer is usually described by the oscillator-like Schrödinger equation, see, e.g. Doi and Edwards (1978) and Eq. (6.55). We have demonstrated in Kholodenko and Vilgis (1994), that this oscillator-like Schrödinger problem can be reinterpreted in terms of magnetic language. In this language we are dealing with the quantum Landau-diamagnetism-like problem about the planar "motion" of charged particles placed in the constant magnetic field. Such reinterpretation allows us to look at the whole problem of chain confinement from a much wider perspective. In Kholodenko (1996a,b) it was shown that the Landau diamagnetism problem is also isomorphic to the problem about the planar random walk which encloses the fixed prescribed area A, see, e.g. Section 6.4. Now, we want to introduce some complications into this problem. Specifically, let us assume that our closed planar walk takes place at the punctured plane where the punctures are meant to represent the cross sections of other chains, or tubes. In the case of chains the punctures have infinitely small radius while in the case of tubes they have a finite radius. Topologically, however, this fact makes no difference, see, e.g. Kholodenko (1996b,c) and Appendix A.1. Whence, we may want to calculate the probability of enclosing a given area A by the planar random walk of N steps in the presence of impurities with some prescribed surface density $\hat{\rho} = n_t/A$ where n_t is the total number of cross sections (punctures). We would like to impose an additional constraint that *no impurities are allowed to be inside the contour which encloses the area A*. The presence of randomly distributed impurities introduces some sort of quenched (or annealed) disorder into the problem which is normally being treated with the use of replicas. Use of

replicas can be bypassed based on topological considerations, see, e.g. Kholodenko (1996b,c) and below, but it is of interest to compare the observables which can be calculated in both ways. To this purpose, we would like to consider a closely related problem about the properties of the closed planar walk of N steps which is entangled with a random array of cross sections, e.g. two-dimensional analogue of Eq. (4.10) where the constant c is now a random variable with prescribed probability distribution. This problem was considered by Tanaka (1984) and, more recently, by Otto and Vilgis (1996). Related results were earlier obtained by Nechaev and Rostiashvili (1993) and Rostiachvili et al. (1993) based on the fundamental earlier work by Brereton and Shah (1980).

To develop our results, let us recall a useful identity (Fulton, 1995),

$$\begin{aligned} \mathrm{d}\ln z = \frac{\mathrm{d}z}{z} &= \frac{\mathrm{d}x + \mathrm{i}\,\mathrm{d}y}{x + \mathrm{i}y} = \frac{x\,\mathrm{d}x + y\,\mathrm{d}y}{x^2 + y^2} + \mathrm{i}\frac{-y\,\mathrm{d}x + x\,\mathrm{d}y}{x^2 + y^2} \\ &\equiv \mathrm{d}\ln r + \mathrm{i}\,\mathrm{d}w(\theta)\,, \end{aligned} \tag{8.14}$$

where, according to Eq. (5.2), $\int_0^N \mathrm{d}w(\theta) = w$ and we used polar coordinates: $x = r\cos\theta, y = r\sin\theta$ in the last of our equations.

Evidently, we can consider as well a combination $\sum_{i=1}^{n_t} \mathrm{d}\ln(z - a_i)$ which would place singularities (punctures) of the complex z-plane at points a_i. Obviously, the total winding number w^t can be written now as (Fulton, 1995),

$$\begin{aligned} w^t &= \sum_{i=1}^{n_t} \left[\mathrm{Im} \int_0^N \mathrm{d}\tau\, \mathrm{d}\ln(z - a_i) \right] \\ &\equiv \int_0^N \mathrm{d}\tau\, \dot{\boldsymbol{r}}(\tau) \cdot \boldsymbol{A}[\boldsymbol{r}(\tau)]\,, \end{aligned} \tag{8.15}$$

where the vector potential $\boldsymbol{A}[r(\tau)]$ is given by $\boldsymbol{A} = (A_x, A_y)$ with

$$A_x = -\sum_{i=1}^{n_t} (y - a_{x_i}) r_i^{-1}, \qquad A_y = \sum_{i=1}^{n_t} (x - a_{y_i}) r_i^{-1} \quad \text{and} \quad r_i^2 = (x - a_{x_i})^2 + (y - a_{y_i})^2\,.$$

For a single closed polymer chain of length N which is entangled with punctures the partition function $Z(c)$ (with account of the excluded volume effects) can be written as

$$Z(c) = \int D[\boldsymbol{r}(\tau)]\delta\left(\int_0^N \mathrm{d}\tau\, \dot{\boldsymbol{r}}\right)\delta\left(c - \int_0^N \mathrm{d}\tau\, \dot{\boldsymbol{r}} \cdot \boldsymbol{A}[\boldsymbol{r}(\tau)]\right) \exp\{-S[\boldsymbol{r}(\tau)]\}\,, \tag{8.16}$$

where

$$S[\boldsymbol{r}(\tau)] = \frac{1}{l^2}\int_0^N \mathrm{d}\tau\, \dot{\boldsymbol{r}}^2 + \frac{a^2}{2}\int_0^N \mathrm{d}\tau \int_0^N \mathrm{d}\tau' \delta(\boldsymbol{r}(\tau) - \boldsymbol{r}(\tau'))$$

with a^2 being the two-dimensional excluded volume parameter.

Since both the locations a_i of punctures as well as the total winding number $w^t \equiv c$ are fluctuating variables it is necessary to perform some sort of averaging of $Z(c)$ in order to calculate the obsevables (e.g. $\langle \boldsymbol{R}^2 \rangle$, etc.). It is assumed, that the disorder associated with the location of punctures could be considered as *annealed* while the disorder associated with w^t as *quenched*. To

perform the average for the case of quenched disorder normally requires the use of replicas. This can be accomplished in several steps. First, we can rewrite the annealed average of $Z(c)$ as

$$\langle Z(g)\rangle_A = \int \mathrm{D}[\boldsymbol{A}]\delta(\nabla\cdot\boldsymbol{A})\int \mathrm{D}[\boldsymbol{r}(\tau)]\delta\left(\int_0^N \mathrm{d}\tau\,\dot{\boldsymbol{r}}\right)$$
$$\times\exp\left\{-\frac{1}{2\varphi_0}\int \mathrm{d}^2x(\nabla\times\boldsymbol{A})^2 - \mathrm{i}g\int_0^N \mathrm{d}\tau\,\dot{\boldsymbol{r}}\cdot\boldsymbol{A} - S[\boldsymbol{r}(\tau)]\right\}, \tag{8.17}$$

where the parameter φ_0 is related to the distribution of obstacles which is assumed to be Gaussian-like. The function $Z(g)$ is related to $Z(c)$ via Fourier transform:

$$Z(c) = \int_{-\infty}^{\infty}\frac{\mathrm{d}g}{2\pi}\exp\{\mathrm{i}gc\}\langle Z(g)\rangle_A\,. \tag{8.18}$$

Second, upon introduction of the "current" $\boldsymbol{J}$ via

$$\boldsymbol{J}(\boldsymbol{r}) = \int_0^N \mathrm{d}\tau\,\dot{\boldsymbol{r}}(\tau)\delta(\boldsymbol{r}-\boldsymbol{r}(\tau))$$

use of the Hubbard–Stratonovich transformation in Eq. (8.17) allows us to eliminate the $\boldsymbol{A}$-field. This produces the following result for $\langle Z(g)\rangle_A$:

$$\langle Z(g)\rangle_A = \int \mathrm{D}[\boldsymbol{r}(\tau)]\delta\left(\int_0^N \mathrm{d}\tau\,\dot{\boldsymbol{r}}\right)\exp\left\{-S[\boldsymbol{r}(\tau)] - \frac{\varphi_0 g^2}{2}A[\boldsymbol{r}(\tau)]\right\}. \tag{8.19}$$

Here, following Cardy (1994), we have introduced an area

$$A[\boldsymbol{r}(\tau)] = \int \mathrm{d}^2r\int \mathrm{d}^2r'\langle A_\mu(\boldsymbol{r})A_\mu(\boldsymbol{r}')\rangle J_\mu(\boldsymbol{r})J_\mu(\boldsymbol{r}') \tag{8.20}$$

which has the same meaning as the expression introduced earlier, see, e.g. Eq. (6.58). Upon the substitution of an identity $1 = \int \mathrm{d}A\,\delta(A - A[\boldsymbol{r}(\tau)])$ inside the path integral, Eq. (8.19) it is possible to rearrange terms so that the result for $\langle Z(g)\rangle_A$ now looks like this

$$\langle Z(g)\rangle_A = \int \mathrm{D}[\boldsymbol{A}]\delta(\nabla\cdot\boldsymbol{A})\int \mathrm{d}A\int \mathrm{d}\tilde{\alpha}\exp\left\{-\frac{1}{2}\int \mathrm{d}^2x(\nabla\times\boldsymbol{A})^2 - \left(\frac{\varphi_0 g^2}{2} - \mathrm{i}\tilde{\alpha}\right)A\right\}$$
$$\times Z(e,\boldsymbol{A})\,, \tag{8.21}$$

where $Z(e,\boldsymbol{A})$ is defined by

$$Z(e,\boldsymbol{A}) = \int \mathrm{D}[\boldsymbol{r}(\tau)]\exp\left\{-S[\boldsymbol{r}(\tau)] - \mathrm{i}e\int \mathrm{d}^2r\,\boldsymbol{A}[\boldsymbol{r}(\tau)]\cdot\boldsymbol{J}(\boldsymbol{r}(\tau))\right\}. \tag{8.22}$$

with $e = \sqrt{2\mathrm{i}\tilde{\alpha}}$. Following Nechaev and Rostiashvili (1993), the last expression can be rewritten with the help of replicas in terms of the n-component complex scalar field theory path integral:

$$Z(e,\boldsymbol{A}) = \lim_{n\to 0}\int \mathrm{D}\boldsymbol{\varphi}\int \mathrm{D}\boldsymbol{\varphi}^*\exp\{-S[\boldsymbol{\varphi},\boldsymbol{\varphi}^*]\}\,, \tag{8.23}$$

where $\boldsymbol{\varphi} = \{\varphi_1, \ldots, \varphi_n\}$ and

$$S[\boldsymbol{\varphi}, \boldsymbol{\varphi}^*] = \sum_{i=1}^{n} \varphi_i^* \left(m^2 - \frac{l^2}{4}(\nabla - \mathrm{i}e\boldsymbol{A})^2 \right) \varphi_i + \frac{La^2}{4} \sum_{i.j=i}^{n} |\varphi_i|^2 |\varphi_j|^2 .$$

In this expression the mass variable m^2 is $\sim N^{-1}$ while L is the average size of the polymer in the direction perpendicular to the plane. Substitution of Eq. (8.23) into Eq. (8.21) and integration over the field A produces in the replica symmetric approximation, i.e. $\sum_i^n |\varphi_i|^2 = n|\varphi|^2$, the following final result:

$$\langle Z(e, A) \rangle_A = \exp\left\{ - n \int \mathrm{d}^2 r \, L_{\mathrm{eff}} \right\}, \tag{8.24}$$

where

$$L_{\mathrm{eff}} = \mathrm{i}\tilde{\alpha}\left(- \frac{l^2}{4\pi} |\varphi|^2 \ln\left(\frac{|\varphi|^2}{M^2} \right) + \frac{l^2}{2\pi} |\varphi|^2 \right) + (m^2 - La^2 M^2)|\varphi|^2 + \frac{La^2}{4} |\varphi|^4$$

with M^2 being an arbitrary mass which appears as a result of regularization of the one-loop corrections coming from $\boldsymbol{A}$-integration. By introduction of the "free energy" $f(\tilde{\alpha})$ via

$$f(\tilde{\alpha}) = \frac{1}{V} \frac{\partial}{\partial n} \left[\int \mathrm{d}^2 r \, L_{\mathrm{eff}} \right] = L_{\mathrm{eff}} \tag{8.25}$$

if it is possible to rewrite Eq. (8.21) as

$$\langle Z(g) \rangle_A = \int \mathrm{d}A \, \delta\left(A + \frac{l^2}{4\pi} V |\varphi|^2 \ln\left(\frac{|\varphi|^2}{M^2} \right) - \frac{l^2}{2\pi} V |\varphi|^2 \right) \mathrm{e}^{-Vf(A,g)} \tag{8.26}$$

where $V = \int \mathrm{d}^2 r$ and $f(A,g)$ is defined by

$$f(A,g) = (\varphi_0 g^2 / 2V)/A + (m^2 - La^2 M^2)|\varphi|^2 + (La^2/4)|\varphi|^4 . \tag{8.27}$$

Use of this result in Eq. (8.18) with account that c is Gaussianly distributed random variable allows to calculate the average $Z(c)$. Actual calculations of this quantity can be only performed with help of the saddle point approximation which produces the following consistency conditions:

$$\rho_{\mathrm{c}} = (L/a)^2 (l^2/4\pi)(\varphi_0/\Delta_{\mathrm{c}})(1 - c_0^2/\Delta_{\mathrm{c}}) , \tag{8.28}$$

$$1/N_{\mathrm{c}} = (La^2/2)\rho_{\mathrm{c}} \ln[L^3 \rho_{\mathrm{c}}], \quad L^3 \rho_{\mathrm{c}} > 1 , \tag{8.29}$$

and

$$A_{\mathrm{c}} = (V/2\pi)\rho_{\mathrm{c}}(1 - \tfrac{1}{2}\ln[L^3 \rho_{\mathrm{c}}]) \tag{8.30}$$

with $\rho = |\varphi|^2$ and parameters Δ_{c} and c_0 characterizing the average total winding number (c_0 is the mean winding number) and Δ_{c} is the dispersion of the winding number while φ_0 is the mean density of obstacles. For the fixed value of parameters φ_0, c_0 and Δ_{c} the above results determine the critical length N_{c} so that below the critical length the polymer acts as if it is still fully flexible (Gaussian-like) while above N_{c} it collapses to the conformational state of branched polymer. Indeed,

according to Eq. (8.26), we have

$$A = V(l^2/2\pi)(\rho - (1/2)\rho\ln(\rho L^3)) . \tag{8.31}$$

If now we take into account that $\rho = N/V$, this result can be written as (for $N > N_c$):

$$\begin{aligned} A &= (l^2/2\pi)N(1 - \tfrac{1}{2}\ln N + \cdots) \\ &\simeq (l^2/2\pi)\, N^{1-1/2} . \end{aligned} \tag{8.32}$$

Since $A \sim \langle \boldsymbol{R}^2 \rangle$ we obtain immediately $\sqrt{\langle \boldsymbol{R}^2 \rangle} \propto lN^{1/4}$ which is the scaling law for the branched polymer without excluded volume.

The main conclusions of the calculations just presented could be summarized as follows:

1. The problem about conformational properties of a planar ring trapped (entangled) in an array of obstacles was actually reduced to the problem about the calculation of the effective area which such a ring encloses.

2. It was shown that the problem is well defined only above a certain threshold (in parameter space).

3. Below this threshold the ring polymer collapses and acquires the shape of the branched polymer (the last result is being independently used by Obukhov et al. (1994) to describe the dynamics of rings in gels as discussed in Section 2).

Below we shall reproduce these results using completely different (topological) methods which do not rely on use of replicas. By doing this some new aspects of the "trapping problem" will be revealed.

8.3. Statistical mechanics of planar rings in an array of obstacles (the Riemann surface approach)

In Section 6.4 we had discussed configurational statistics of the planar random walks restricted by the area constraint. Surprisingly, the problem about the random entanglements considered in Section 8.2 happens to be very closely related to this area problem. In this section we will try to clarify why, indeed, such connections exist.

As it was already noticed in Section 6.4, the planar area constraint problem is essentially equivalent to the standard Landau diamagnetism problem (Landau, 1930), in case the plane is not punctured. In such a (standard) case, the problem lies in quantum (and statistical mechanics) treatment of motion of the electron in the presence of constant magnetic field H defined by the vector potential $\boldsymbol{A}$, see, e.g. Eq. (6.66). In Kholodenko (1996a) full analysis of this problem is given for both nonrelativistic and relativistic electrons (since this problem happens to be isomorphic to the problem of statistical description of deformable planar droplets of arbitrary rigidity). We shall discuss only the nonrelativistic limit in this review. The relativistic effects are briefly discussed in Kholodenko (1996a). In the nonrelativistic limit the solution is reduced to that known for the quantum harmonic oscillator with frequency depending upon the strength of the magnetic field H. Whence, for *arbitrary small H we still have an infinite tower of equidistant discrete energy levels*. The situation changes dramatically if the motion of an electron is considered on the punctured plane. In this case we may have, *depending upon the surface density* $\hat{\rho}$ of punctures, a finite number of bound states or even no bound states at all (Kholodenko, 1996b,c). Whence, we may anticipate, that there is some threshold $\hat{\rho}_c$ so that above (below) $\hat{\rho}_c$ there will (will not) be bound states. The above picture

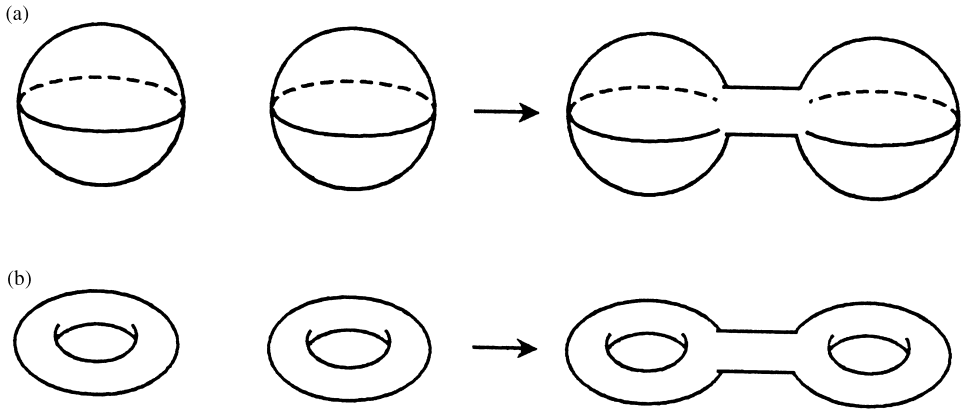

Fig. 12. (a) Fusion of two punctured spheres produces a sphere again. (b) Fusion of two punctured tori produces a new surface of genus 2.

can be now recast into polymer language (Kholodenko and Vilgis, 1994; Kholodenko, 1996c). The transversal part of the diffusive motion, Eq. (6.55), is isomorphic to the Landau diamagnetism problem (Kholodenko and Vilgis, 1994). In the presence of planar punctures Eq. (6.55) should be modified. Upon such modification the tube existence and stability will be determined by the number of available bound states. The transition from zero to finite number of bound states is *discontinuous*. We formulate our results in such a way that the numerical predictions of our theory related to the onset of tube creation (destruction) associated with transition from the Rouse (no tubes) to the reptation (tube assisted) regime could be directly compared with experimental data (Kholodenko, 1996c), and demonstrate very satisfactory agreement with the experiment. Quantitative results obtained below are in qualitative accord with the results of Otto and Vilgis (1996) discussed in Section 8.2.

Let us begin with the following auxiliary example. Following Arnold (1978) (see, e.g. Appendix A.1), let us consider the classical motion of a particle in a square with periodic boundary conditions (i.e. on the torus). We shall complicate matters by putting inside a square another circle (hole) so that our particle can elastically scatter out of this hole and the walls of the square. The classical motion in such billard takes place actually on a Riemann surface which is known as a double torus (i.e. sphere with two handles). The double torus is obtained by gluing two copies of the usual torus with a hole in it as depicted in Fig. 12. The gluing is done around the circumference of a hole. It is well known that the Riemann surfaces represent the case of surfaces of *constant negative* curvature. The *classical* motion on such surfaces is chaotic (Arnold, 1978). To bring this auxiliary problem closer to our original tube problem, let us consider, instead of just one hole, many (with some surface density $\hat{\rho}$ introduced in Section 8.2). Then, it is intuitively clear that we will end up with the Riemann surface of genus g (sphere with g handles) where the genus g is determined by the density of obstacles (holes). All this can be made quite rigorous by considering homotopy of the paths on the punctured plane with periodic boundary conditions and by using the van Kampen theorem as explained, e.g., in Massey (1967), Gilbert and Porter (1994) or Fulton (1995). We deliberately would like to avoid all these mathematical complications unfamiliar to most of the readers trained in

polymer physics. Instead, we would like to use more intuitive examples (including that of Arnold) which have some physical appeal. But since the van Kampen theorem tells us that the punctured plane *is* effectively the Riemann surface (irrespective of the classical mechanics example discussed above), one can exploit this fact "quantum mechanically".

Let us recall that the conformational properties of flexible chains in the external random potential V are described with the help of the end-to-end distribution function $G(\boldsymbol{r},\boldsymbol{r}';N)$ which obeys the "equation of motion" (in three dimensions)

$$\left(\frac{\partial}{\partial N}-\frac{l}{6}\nabla_r^2+V(\boldsymbol{r})\right)G(\boldsymbol{r},\boldsymbol{r}';N)=\delta(\boldsymbol{r}-\boldsymbol{r}')\delta(N)\,. \tag{8.33}$$

Upon the decomposition of this equation into longitudinal and transversal parts (as discussed in Section 6.3) we are left with effectively two independent Schrödinger-like equations. The transversal (planar) problem could be treated, in principle, with the help of the methods described in Section 8.2. Following the seminal work of de Gennes (1971) on reptation (see, e.g. his Eqs. (2.4) and (2.5)), the random environment can be modeled, however, with the help of a Smoluchovski-type equation for G given by

$$\frac{\partial}{\partial N}G=D\frac{\partial}{\partial r^2}G-c\frac{\partial}{\partial r}G\,. \tag{8.34}$$

The actual values of constants D and c depend on the microscopic model used to arrive at Eq. (8.34), For example, in Nechaev et al. (1987) the "motion"on the regular lattice is considered (see also Nechaev (1990)) while in Nechaev (1988) "motion" on the Bethe lattice is being considered. Eq. (8.34) appears to be universal (Helfand and Pearson, 1983; Rubinstein and Helfand, 1985; Mehta et al. 1991) and independent of the dimensionality of the embedding space. In case the "motion" takes place on the regular lattice $D=2pq, c=q-p, p=z^{-1}, q=1-p$ and z is the coordination number of the lattice. The above equation should be actually supplemented with initial and boundary conditions, e.g.

$$G(r,N=0)=\delta(r)\,,\qquad \mathrm{D}(\partial G/\partial r)|_{r=0}-cG(0,N)=0\,. \tag{8.35}$$

As it was argued in Kholodenko (1996b), to obtain the general solution of Eq. (8.35) it is permissible initially to ignore the boundary conditions: once the general solution is obtained, it will be forced to satisfy the specific boundary conditions. So far, we have not made any connection(s) between Eq. (8.34) and the topological properties of the underlying two-dimensional punctured plane. To do so, we would like to pose the question: *is it possible to rewrite Eq.* (8.34) *in the form of diffusion-type equation on some curved manifold?* The answer to this question is "yes". To prove this, let us first bring Eq. (8.34) to the dimensionless form. If one chooses $\alpha=D/c^2$ and $\beta=D/c$, then one obtains the dimensionless analogue of Eq. (8.34) given by

$$\frac{\partial}{\partial\tau}G(x,\tau)=\frac{\partial^2}{\partial x^2}G-\frac{\partial}{\partial x}G\,. \tag{8.36}$$

Let us demonstrate that this equation can be rewritten in an equivalent form as

$$(\partial/\partial\tau)G=(1/\sqrt{g})\partial_\alpha(g^{\alpha\beta}\sqrt{g}\partial_\beta)G \tag{8.37}$$

for some metric tensor $g_{\alpha\beta}$. If we choose: $g_{xx}=1$, $g_{\varphi x}=g_{x\varphi}=0$, $g_{\varphi\varphi}=\mathrm{e}^{-2x}$, then we can obtain: $g=\mathrm{e}^{-2x}, g^{\varphi\varphi}=1, g^{xx}=\mathrm{e}^{2x}$ so that we get

$$\frac{1}{g}\partial_\alpha(g_{\alpha\beta}\sqrt{g}\partial_\beta\cdots)=\mathrm{e}^x\frac{\partial}{\partial x}\left(\mathrm{e}^x\frac{\partial}{\partial x}\cdots\right)+\mathrm{e}^x\frac{\partial}{\partial\varphi}\left(\mathrm{e}^x\frac{\partial}{\partial\varphi}\cdots\right). \tag{8.38}$$

If $G(r,\tau)$ is φ-independent, then use of Eq. (8.38) in Eq. (8.37) produces back Eq. (8.36) as required. Once we have obtained the metric tensor $g_{\alpha\beta}$ of surface, we can find out what kind of surface it determines.

The first fundamental form of the surface (the length) can be written now, based on the above results, as

$$\mathrm{d}s^2=\mathrm{d}x^2+\mathrm{e}^{-2x}\mathrm{d}\varphi^2\,. \tag{8.39}$$

By introducing a new variable $y=\mathrm{e}^x$ we obtain $\mathrm{d}y=\mathrm{e}^x\,\mathrm{d}x$ and, therefore, Eq. (8.39) can be rewritten as

$$\mathrm{d}s^2=\mathrm{d}x^2+\mathrm{e}^{-2x}\,\mathrm{d}\varphi^2=(\mathrm{d}y^2+\mathrm{d}\varphi^2)/y^2\,. \tag{8.40}$$

In mathematical literature the metric given by the last expression of Eq. (8.40) is known as the hyperbolic metric (Arnold, 1978; Stillwell, 1992). The Poincaré model H consists of a subset of the complex plane C defined by

$$H=\{z=\varphi+\mathrm{i}y\in C|y>0\} \tag{8.41}$$

supplemented with hyperbolic metrics given by Eq. (8.40) (Poincare, 1882; Buser, 1992). If we would use complex variables z and $\bar{z}$, then Eq. (8.40) could be rewritten as

$$\mathrm{d}s^2=(\mathrm{d}z)^2/(\mathrm{Im}\,z)^2\,. \tag{8.42}$$

For finite distances d between z and z' in this model we could obtain with the help of Eq. (8.42) the following result:

$$\cosh d(z,z')=1+\frac{|z-z'|^2}{2\,\mathrm{Im}\,z\,\mathrm{Im}\,z'} \tag{8.43}$$

to be compared with the usual Euclidean distance

$$d_{\mathrm{E}}(z,z')=|z-z'|\,. \tag{8.44}$$

With the help of d just defined, the solution of Eq. (8.36) (without boundary effects) is known to be (Buser, 1992; Kholodenko, 1996b)

$$G_{\mathrm{H}}(z,z';\tau)=\frac{1}{2(2\pi\tau)^{1/2}}\,\mathrm{e}^{-\tau/4}\int_{d(z,z')}^{\infty}\frac{\mathrm{d}x\,x\,\mathrm{e}^{-x^2/4\tau}}{\sqrt{\cosh x-\cosh d(z,z')}}\,. \tag{8.45}$$

Earlier, when we have discussed Arnold's billiard, the claim was made that the actual motion takes place on the Riemann surface (i.e. sphere with g handles) instead of H-plane (also known as the Lobachevski plane). There is no contradiction, however, between the earlier claim and the results just obtained since the Lobachevski plane is the universal covering surface for the Riemann

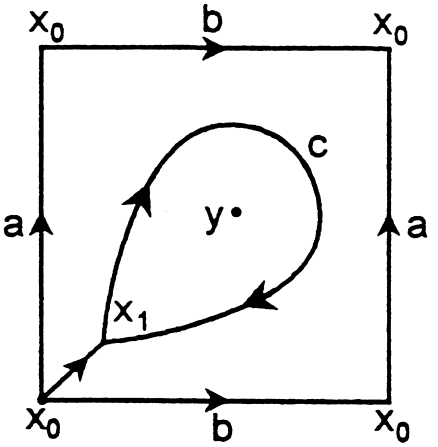

Fig. 13. The planar representation of a torus is just a square with opposite sides properly identified. In this representation the homotopy of paths around a puncture inside a square is equivalent to the homotopy of paths around a puncture near one of the corners.

surface of any genus $g > 1$, Stillwell (1992). The notion of the covering surface could be easily understood using the following example. Let Γ be a discrete translation in the complex plane C (or $\mathbf{R}^2$), then a given square S_q can be obtained as an image of some *fundamental* square $\hat{S}_q$ upon translation, i.e. $S_q = \Gamma\hat{S}_q$. The torus can be obtained as a quotient $\mathbf{R}^2/\Gamma$ so that $\mathbf{R}^2$ is the universal covering surface for the torus. Analogously, every Riemann surface can be constructed from some fundamental $4g$-gon on the H-plane ($g > 1$), see, e.g. Figs. 13 and 14 for $g = 2$ surfaces. Whence, any Riemann surface is just a quotient H/Γ where Γ is some generator of discrete translations in H-plane (Buser, 1992). The genus g of the surface is directly connected with the number of punctures in the plane and this fact is *completely independent of whether these punctures are frozen or not. Moreover, the hyperbolicity will remain* even if we remove the restriction that the motion should be strictly planar: because tubes are entangled in three dimensions (Kholodenko and Vilgis, 1994), and form quasi-knotted configurations, Brownian motion in the presence of such quasi-knots will remain hyperbolic (Thurston, 1979). To understand intuitively how this happens we refer the reader to the Appendix.

For the moment, let us consider again the simplest Arnold's billiard which is just a union of two punctured toruses glued along the circumference of the punctures, see, e.g. Fig. 12. To construct such a billiard we need two copies of the Riemann sphere each having three holes. We can glue together two holes on each sphere thus converting it into punctured torus and, then, we can glue the resulting objects together to make the final product. It can be shown (Buser, 1992) that *every Riemann surface of genus $g > 1$ is just a collection of thrice punctured spheres along with the gluing prescription, which is used for their assembly.* Once we recognized this fact, we can construct a finite square lattice made of m^2 copies of the Arnold square. By gluing these squares together it is possible to insert yet another set of k holes into this lattice (Buser, 1992), thus forming a surface of genus

$$g = 1 + \tfrac{1}{2}(m^2 + k)\,, \tag{8.46}$$

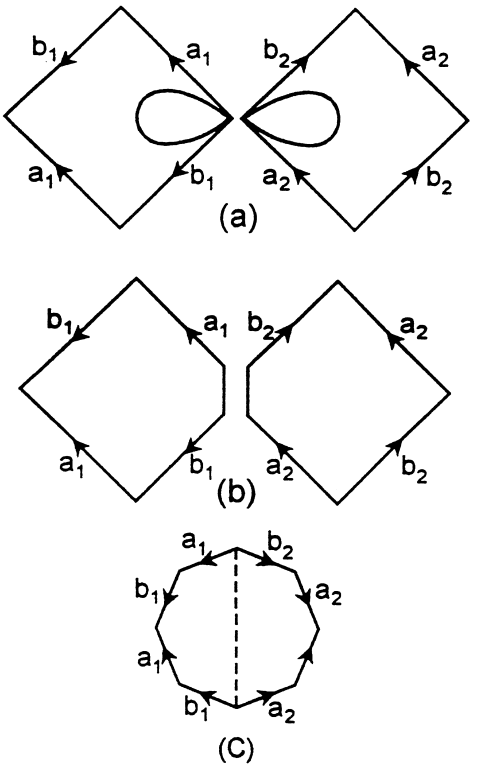

Fig. 14. Two punctured tori in planar representation: (a) can be transformed into (b) and, then, glued together along c_1, and c_2 thus resulting in the octagon (c).

$k = \{0,2,\ldots,2m\}$ if m is even or $k = \{1,3,5,\ldots,2m-1\}$ if m is odd. For $m = 1$ using Eq. (8.46) we obtain $g = 2$ in agreement with (Arnold 1978).

Let, as in Section 8.2, $\hat{\rho} = n_t/A$, then, the logic of the previous discussion suggests us to choose

$$n_t = m^2 + k \tag{8.47}$$

so that the filling fraction v can be defined now as (Kholodenko and Vilgis, 1994),

$$v = \pi a^2 \hat{\rho}\,,$$

i.e. we can think of cross sections of tubes as a planar gas of disk of area πa^2. Suppose that there is some sort of interaction between such disks. Then, by analogy with other models of statistical mechanics, it is natural to expect that the system of such disks can undergo a phase transition (e.g. solid–liquid-like) which is controlled by v so that for some critical value $v = v^*$ we would have

$$v^* = \pi a^2(\rho^*)\hat{\rho}(\rho^*)\,, \tag{8.48}$$

where ρ^* is the critical monomer density (recall, that $\rho \sim N/V$). The explicit dependence of a and $\hat{\rho}$ on ρ is unknown in general (but, since $\hat{\rho} = n_t/A$, it is expected that $\hat{\rho} \sim \rho$) and should be dependent upon the details of the model which is used.

Since the punctures in our plane have finite sizes, and since Eq. (8.37) accounts for the curvature effects only, we need to complicate this equation so that it can account for the finite sizes of cross sections. To this purpose we begin with planar case discussed in Sections 6.4 and 8.2. In particular, using Eq. (6.55) we can formally define the averaged size of our tube cross section as

$$\langle q_2^2 + q_3^2 \rangle = l/w \equiv a^2 \,. \tag{8.49}$$

This definition is in accord with that given in Doi and Edwards (1978) (with $\langle \cdots \rangle$ being the usual polymer average, see, e.g. Eq. (8.89) below). By continuously changing w we obtain continuous changes in a^2. This will no longer be true if the above average is considered in the multiply connected plane which is effectively the Riemann surface.

To demonstrate this, we would like to reobtain Eq. (8.49) in a more systematic way which was outlined in Section 6.4. Using Eq. (6.71) we obtain in the limit of small Δp the following result for $\langle A \rangle$:

$$\langle A \rangle \simeq \tfrac{1}{12} \Delta p (Nl)^2 \,. \tag{8.50}$$

For a circle of circumference N the area is $N^2/4\pi$. It is the *maximal* area which can be enclosed by the walk of length N. Whence, one can rewrite Eq. (8.50) in equivalent form as

$$\frac{\langle A \rangle}{\Delta p l^2} \simeq a^2 \,, \tag{8.51}$$

where on the r.h.s. the area a^2 is identified with that given in Eq. (8.50). Since the smallest area $\langle A \rangle$ of the circle cannot be smaller than $\simeq l^2$, then, evidently, in this extreme case we would have

$$1/\Delta p \simeq a^2 \,. \tag{8.52}$$

Since $[\Delta p] = [A^{-1}]$ while $[w] = [l^{-1}]$ we, indeed, have reobtained Eq. (8.49). Use of the area (or magnetic language) formalism to determine the tube cross section is more advantageous, as compared with Eq. (8.49), since it allows to consider problems related to random walks with the area constraint on the Riemann surfaces.

To this purpose, the following key observation is helpful (Kholodenko, 1996a,b). The probability $P(A, N)$ for a random walk to enclose an area A is given by the ratio

$$P(A, N) = Z(A, N)/Z(0, N) \,, \tag{8.53}$$

where $Z(A, N)$ is given by

$$Z(A, N) = \int \mathrm{d}\boldsymbol{r}\, G(\boldsymbol{r}_1 = \boldsymbol{r}_2 = \boldsymbol{r}, N|A) \tag{8.54}$$

with $G(\boldsymbol{r}_1 = \boldsymbol{r}_2 = \boldsymbol{r}, N|A)$ being given by the r.h.s. of Eq. (6.57) (divided by $\pi N l$) and $Z(0, N)$ is the same but with $A = 0$. The r.h.s. of Eq. (8.54) is just the usual statistical mechanical partition function (Feynman, 1972). Whence, by analogy with Section 7.2, to obtain $Z(A, N)$ we need to know only the eigenvalues (and their degeneracies) of the corresponding Schrödinger-like operators. The spectrum of such operators on the Riemann surfaces can be also obtained where the partition function $Z(A, N)$ is known in mathematical literature as Selberg's trace formula (Buser, 1992).

Let us consider this topic in some detail. Since in the flat case the spectrum of Landau "electron" ε_n is known to be just that for the harmonic oscillator (Kholodenko, 1996b),

$$\varepsilon_n = \Delta pl(n + \tfrac{1}{2}) \tag{8.55}$$

with degeneracy $g_n = \Delta pNl/4$, the partition function is easily obtainable

$$Z(\Delta p, N) = \sum_{n=0}^{\infty} g_n \mathrm{e}^{-N\varepsilon_n} = \frac{x}{\sin x}, \tag{8.56}$$

where $x = \Delta pNl/2$. The function $Z(\Delta p, N)$ is related to $Z(A, N)$ via

$$Z(\Delta p, N) = \int_0^{N^2/4\pi} \mathrm{d}A\, \mathrm{e}^{A\Delta p} Z(A, N) \tag{8.57}$$

and is even more convenient since

$$\langle A \rangle \lim_{\Delta p \to 0} (\partial/\partial \Delta p) \ln Z(\Delta p, N). \tag{8.58}$$

Generalization of the result of Eq. (8.56) to the Riemann surface of genus g can be now accomplished without any problems with the result

$$Z(\Delta p, N) = \frac{g-1}{4R^2} \sum_{0 \le n \le |b| - \frac{1}{2}} (2\Delta pNlR^2 - 2n - 1) \exp\{-\varepsilon_n N\} \tag{8.59}$$

with

$$\varepsilon_n = \frac{1}{4R^2}\left[\frac{1}{4} - b^2 - \left(n + \frac{1}{2} - b\right)^2\right] \tag{8.60}$$

and $b = \Delta pNlR^2$, $R^2 = s^2/l^2$ with s being an average distance between the obstacles in the plane. As it was noticed in Kholodenko (1996b) the parameter R plays the role of a radius of curvature of the manifold: for $R^2 \to \infty$ (flat case) one obtains:

$$Z(\Delta p, N) \approx \frac{\Delta pNl}{\sin(\Delta plN/2)} \tag{8.61}$$

which effectively coincides with Eq. (8.56). But for finite $R's$ one has to require that the partition function $Z(\Delta p, N)$ remains nonnegative and well defined. The nonnegativity of $Z(\Delta p, N)$ requires

$$2\Delta pNlR^2 - 2n - 1 \ge 0 \tag{8.62}$$

while for the sum in Eq. (8.59) to be well defined we have to require as well

$$|b| - \tfrac{1}{2} - n \ge 0. \tag{8.63}$$

Taking into account the definition of b given after Eq. (8.60) we conclude that both inequalities Eqs. (8.62) and (8.63) are equivalent. In particular, the inequality (8.63) implies that the reduced "magnetic field" $|b|$ should exceed a certain threshold, in our case,

$$|b| \ge \tfrac{1}{2} \tag{8.64}$$

in order for the tube to exist. Moreover, the theory which produced the result given by Eq. (8.59) dictates, yet another set of constraints:

$$\frac{a}{lR} = \operatorname{arctanh}\left(\frac{\sqrt{B^2 - 4|c|}}{B}\right), \tag{8.65}$$

$$b - 2R^2\sqrt{c} = n + \tfrac{1}{2}, \tag{8.66}$$

where $B = b/R^2$. The constant $|c|$ can be eliminated from these equations thus producing

$$\tanh\left(\frac{a}{lR}\right) = \sqrt{\frac{n+1/2}{b}}\sqrt{\frac{2b-n-1/2}{b}}. \tag{8.67}$$

If $|c| = 0$ in Eq. (8.65) we obtain

$$\tanh(a/(lR)) = 1 \tag{8.68}$$

which leads to the requirement $a \to \infty$ for fixed R. In this case the tube does not exist. Hence, for the tube to exist one must require $|c| \neq 0$ and $(a/lR) \leq 1$. A crude estimate for b can now be obtained from the following self-consistent equation for b which follows from Eq. (8.67) (for $n = 0$)

$$b \tanh 1 \simeq \sqrt{b - \tfrac{1}{4}}, \tag{8.69}$$

e.g. it is assumed that $a \approx R$ (or the size of the tube is of the order of the distance between the obstacles). Numerical solution of Eq. (8.69) produces $b \simeq 0.86(1 \pm 0.643)$. From the theory of the operators on Riemann surfaces (Kholodenko, 1996b), it is known that

$$b \simeq \frac{f}{2(g-1)}, \tag{8.70}$$

where $f = 0, \pm 1, \pm 2, \ldots$ and $g - 1$ is given by Eqs. (8.46) and (8.47). By combining these equations we obtain

$$b \simeq \frac{f}{n_t} = 0.86(1 \pm 0.643). \tag{8.71}$$

If $A = f\pi a^2$, then $\hat{\rho} = n_t/A$ can be rewritten as

$$\pi\hat{\rho}a^2 \simeq n_t/f. \tag{8.72}$$

By combining this result with Eqs. (8.49) and (8.71) produces

$$v^* \simeq 0.708. \tag{8.73}$$

This result is too high as compared to the estimate $v^* \simeq 0.0286$ which was obtained in Kholodenko and Vilgis (1994) with help of other methods to be discussed below. To improve the above estimate we can, e.g., require, by analogy with the theory of coil–globule transitions (Kholodenko and Freed, 1984a), that in addition to $n = 0$ (i.e. to the ground state) there is at least one more discrete state, e.g. $n = 1$. Using Eq. (8.67) and repeating previous calculations, produces

$$v^* \simeq 0.341. \tag{8.74}$$

This result is considerably in better agreement with the earlier obtained as we shall demonstrate now by direct comparison of this result with the experimental data.

To do so, we need to recall some basic facts from chemistry. Let n be the number of moles, then the total number of "particles" (polymers) $\tilde{N}$ is given by $\tilde{N} = nN_A$ where N_A is Avogadro's number. Let W be the total weight (mass) of polymer(s) of molecular weight M, then $n = W/M$ while the density ρ is defined by $\rho = W/V$ where V, as before, is the total volume. Let $V_0 = \hat{A}\langle R_g^2\rangle^{3/2}$ be the volume occupied by a single polymer chain. Here $\hat{A}$ is some unknown constant, of order unity according to Fetters et al. (1994), and $\langle R_g^2\rangle$ is related to M via

$$\langle R_g^2\rangle = \hat{c}M\,, \tag{8.75}$$

where $\langle R_g^2\rangle = \frac{1}{6}\langle \boldsymbol{R}^2\rangle$ and $\hat{c}$ is some proportionality factor. In writing Eq. (8.75) it is being assumed that the individual chains in the melt are effectively at θ point conditions (Fetters et al., 1994) Consider now a combination $V_0\rho N_A/M \equiv \tilde{N}/(V/V_0) = \tilde{c}$. By construction, this combination is just a fraction $\tilde{c}$ of "lattice sites" (of total number V/V_0) which are occupied by polymers. Evidently, $0 \le \tilde{c} \le 1$. If, following Fetters et al. (1994), we assume $\tilde{c} \approx 1$ (i.e. polymer melt), then we obtain

$$1 \simeq \hat{A}6^{-3/2}M^{1/2}\hat{c}^{3/2}N_A\rho\,. \tag{8.76}$$

If M_e is the molecular weight of the segment of polymer chain between the entanglements, then Eq. (8.76) produces

$$M_e = \rho^{-2}6^3(\hat{A}\hat{c}^{3/2})^{-2}N_A^{-2}\,. \tag{8.77}$$

Using Eq. (8.75) we can eliminate the constant $\hat{c}$ from Eq. (8.77) thus producing

$$M_e \simeq \rho^{-2}\hat{A}^{-2}\left(\left\langle\frac{\boldsymbol{R}^2}{M}\right\rangle\right)^{-3}6^3N_A^{-2}. \tag{8.78}$$

In view of Eq. (8.75), it is reasonable to assume that $a^2 \simeq \hat{c}M_e$, which then produces

$$\frac{a^2}{M_e} = \frac{\langle \boldsymbol{R}^2\rangle}{M} \tag{8.79}$$

in agreement with Fetters et al. (1994). Alternative expression was found by He and Porter (1992), who obtain instead $M_e\langle \boldsymbol{R}^2\rangle = 28\pi a^2 M$. The numerical factor of 28π cannot be further checked using the data from Fetters et al. (1994) and, whence, we shall use the result of Eq. (8.79) in order to produce the final numbers. By combining Eqs. (8.78) and (8.79) we can estimate a as

$$a \simeq \sqrt{\frac{\langle \boldsymbol{R}^2\rangle}{M}M_e} \simeq \frac{6^{2/3}}{\hat{A}\rho N_A}\left(\frac{M}{\langle \boldsymbol{R}^2\rangle}\right). \tag{8.80}$$

The last result is in complete accord with Eq. (3.3) of Fetters et al. (1994). According to this reference, Eqs. (8.78) and (8.80) could be used for the independent measurements of M_e and a provided that ρ and $\langle \boldsymbol{R}^2\rangle/M$ are known.

Let us now have another look at these results in the light of the discussion presented earlier in this section. Using Eqs. (8.79) and (8.80) we obtain

$$a \simeq \frac{6^{2/3}}{\hat{A}\rho N_A}\left(\frac{M_e}{a^2}\right) \tag{8.81}$$

Table 1
Molecular characteristics of polymers at $T = 413$ K

Polymer	ρ (g cm^{-3})	M_e	$a = d_t/2$ (Å)	$\hat{A}$
PE	0.784	828	16.4	5.865
PEO	1.064	1624	18.75	5.672
PEB-11.7	0.793	1815	21.3	5.802 1
PMMA	1.13	10013	33.5	5.77
PEE	0.807	11084	39.3	5.543

Table 2
Molecular characteristics of polymers at $T = 298$ K

Polymer	ρ (g cm^3)	M_e	$a = d_t/2$ (Å)	$\hat{A}$
PEB-14	0.860	1522	18.45	6.903
HHPP	0.878	3347	24.2	6.59
PEE	0.866	9536	35.0	6.29
PMA	1.11	8801	30.35	6.94
65-MYRC	0.891	24874	44.05	8.00

or, equivalently,

$$\frac{N_A a^3 \rho}{6^{3/2} M_e} = \frac{1}{\hat{A}}. \tag{8.82}$$

This result can be compared now against Eq. (8.48) which can now be equivalently rewritten as

$$\pi a^3(\hat{\rho}/a) = v. \tag{8.83}$$

Taking into account the definitions of $\hat{\rho}$ and ρ we can now identify $\rho N_A/6^{3/2}M_e$ with $\hat{\rho}/a$ and, hence, v/π with $\hat{A}^{-1}$. The theoretically obtained v^* given by Eq. (8.74) can be used now to obtain $\hat{A} \simeq 9.21$. This result can be compared against the experimental data of Fetters et al. (1994). Based on the data from Tables 1 and 2 of Fetters et al. the Tables 1 and 2 of Kholodenko (1996c) are reproduced here (in units and notations used by Fetters et al., 1994).

In calculating $\hat{A}$ with help of Eq. (8.82) the conversion factor coming from the combination $N_A\rho/6^{3/2}$ is estimated to be 0.04082, based on $N_A = 6 \times 10^{23}$, $1\,\text{Å} = 10^{-8}$ cm. Also, the tube diameter $d_t = 2a$ since a is the tube radius. The results of Tables 1 and 2 are in good agreement with our theoretical estimate $\hat{A} = 9.21$ based on Eq. (8.74).

In addition, by combining Eqs. (8.75) and (8.80) we can also write

$$a\rho = \text{const.} \tag{8.84}$$

This result is obtained *theoretically* in Kholodenko and Vilgis (1994) using the analogy with quantum Hall effect (QHE) formalism. Independently, the same result was obtained by Kavasalis and Noolandi (1988) based on the packing model of reptation. The result of Eq. (8.84) is supported

by numerical simulations of Wittmer and Binder (1992) and Kremer and Grest (1994). Eq. (8.84) is based on the assumption that the combination $\langle \boldsymbol{R}^2 \rangle / M$ is constant. Theoretical calculations performed by Lachowski et al. (1988) and Hutnik et al. (1991) indicate that this should be the case and provide for the above ratio the result: $\langle \boldsymbol{R}^2 \rangle / M \approx 1.03$–$1.1$. This result is only in *qualitative* agreement with the data from Tables 1 and 2 of Fetters et al. (1994) as is acknowledged by the authors. Accordingly, use of the data given in Tables 1 and 2 of *this* work for computation of the product ρa leads to less satisfactory results for $\hat{A}$: the results for $\hat{A}$ are uniformly smaller (roughly by a factor of 6) than those given in Tables 1 and 2. This is not too surprising since the result given by Eq. (8.82) was obtained without restrictions on the ratio to be fixed and *universal*. Since the independent numerical data of Wittmer and Binder (1992) and Kremer and Grest (1994) and the theory of Kholodenko and Vilgis (1994) strongly support Eq. (8.84), we would like to present these theoretical arguments in favor of Eq. (8.84) in Section 8.4.

8.4. Statistical mechanics of planar rings in an array of obstacles (QHE approach)

In Appendix A.1 we have discussed complications which arise from considering the Brownian motion at the twice punctured plane as compared to the well understood one puncture case discussed in Section 5.1. Here, we would like to develop the results of Appendix A.1 in order to illuminate some additional *physical* aspects of the whole problem.

In physics literature, study of path integrals in multiply connected spaces was initiated to our knowledge by Shulman (1971) and later developed by many authors, see, e.g. Levay et al. (1996) and references therein. In the mathematics literature, the same problem was studied by Pitman and Yor (1986, 1989) who use methods which are noticeably different from that used in physics literature. It would be interesting to make a detailed comparison of these approaches in the future. The most typical (hydrogen atom-like) problem which is well studied is the problem related to the quantum mechanics of the particle on a circle which we had discussed in Section 6.2. The key idea of solving the circular problem lies in realizing the fact that the universal covering space for a circle S^1 is just a straight line $\boldsymbol{R}^1$. Since the path integral for $\boldsymbol{R}^1$ is well known, then the path integral for S^1 can be obtained by some sequence of operations leading from S^1 to $\boldsymbol{R}^1$ and back to S^1 (Tanimura and Tsutsui, 1995) (very much in accord with the results of Appendix A.1). Now, if we have a hole in the plane, the closed paths around a hole are homotopic to S^1 (Fulton, 1995). If we would have some interaction between the Brownian particle and the hole (which could be just a world line of another particle), then this would be equivalent to having fractional statistics (with the strength of interaction δ interpolating between the Bose and the Fermi statistics as it was explained in Section 6.2).

Let us now have two holes instead, then we have to consider instead of S^1 a product $S^1 \times S^1$ as depicted in Fig. 15.

The universal covering space for the "figure eight" is known to be (see, e.g. Dubrovin et al., 1985), a four-valent Bethe lattice as depicted in Fig. 16. This explains why, e.g. Nechaev et al. (1987) and others had used a Bethe lattice to study the reptation. The "figure eight" can be also obtained by considering paths on the once punctured torus (which was discussed earlier in connection with Arnold's billiard) as depicted in Fig. 17. If we make a puncture in a sphere S^2 and glue two copies of S^2 together, the result will be S^2 as depicted in Fig. 12a, but if we glue two punctured tori together, as depicted in Fig. 12b, we shall obtain a surface of genus 2. At the same time, if we think about the torus as a square with sides properly identified, then the punctured torus will look like that in

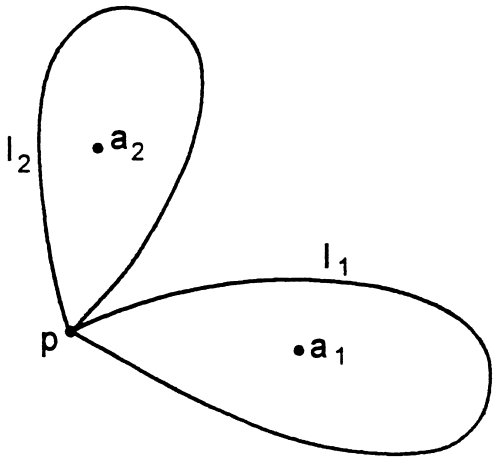

Fig. 15. Homotopy of paths on the twice punctured plane ("figure eight").

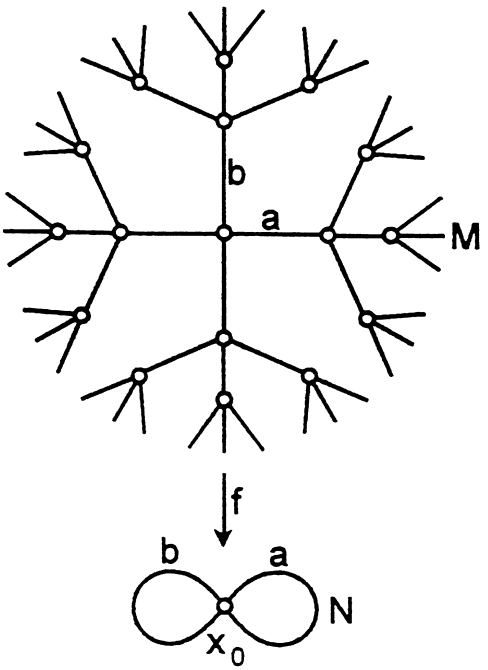

Fig. 16. Universal covering space of the "figure eight".

Fig. 13. If we glue together these polygons as depicted in Fig. 14 we shall obtain a double torus in the planar representation. There are four distinct paths on this torus as depicted in Fig. 18b so that if we make cuts along these paths we re-obtain Fig. 14c.

At the same time, if we would think of homotopy of these paths, we would obtain a bouquet of four circles (instead of two as in Fig. 15). Two out of our four circles had originated from the

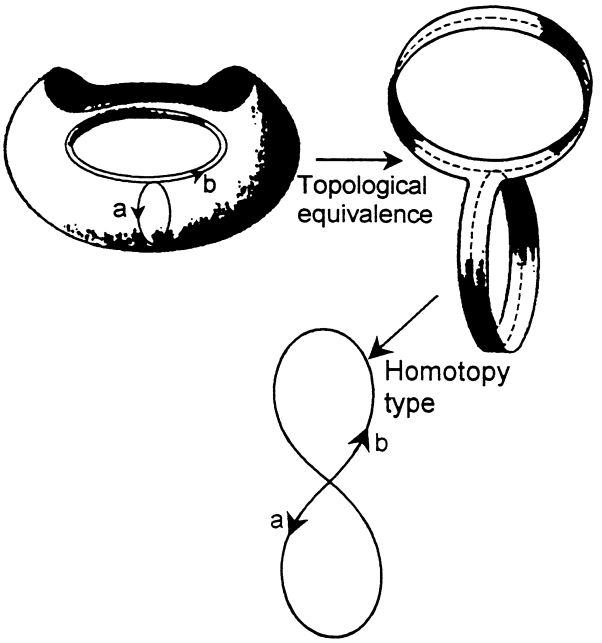

Fig. 17. Topological structure of the once punctured torus.

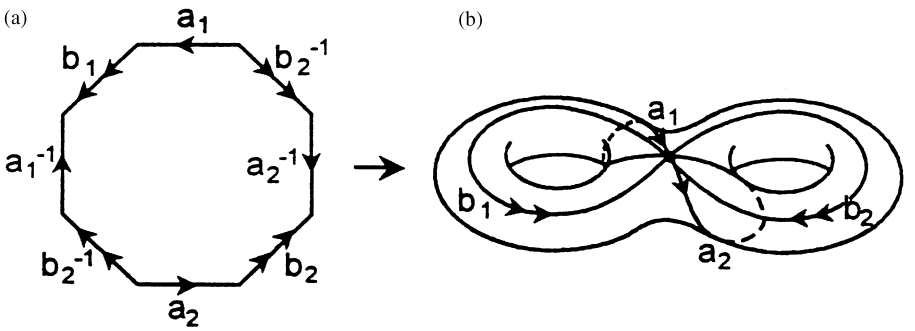

Fig. 18. If the sides of the octagon are glued together in an order shown in (a), then the resulting surface (b) coincides with that depicted in Fig. 12b. Alternatively, if the cuts are made along a_1, a_2 and b_1, b_2 on the double torus, we will obtain again Fig. 14c.

periodic boundary conditions (see, e.g. Fig. 14a) and were left unaccounted in Fig. 15. Evidently, the Bethe lattice structure of Fig. 16 becomes more complicated when the surfaces of higher genus are being considered. But, in any case, the Bethe lattice calculations, e.g. like that discussed in Nechaev (1990), are effectively calculations on the universal covering surface for the Riemann surface of given genus (Stillwell, 1993), so that $S^1 \to \mathbf{R}^1 \to S^1$ calculational procedure for the circle is replaced now by the $H/\Gamma \to T \to H/\Gamma$ where T is the corresponding Bethe lattice. The Bethe lattice calculations are not readily extendable to account for the "magnetic field" effects and, hence, the

Riemann surface approach described in the previous subsection is more advantageous. Moreover, the QHE picture of tube stability developed in Kholodenko and Vilgis (1994) is in complete accord with the Riemann surface approach as we are going to demonstrate shortly.

The QHE model of tube stability is based on the following observations. According to Section 6.4 the Landau Hamiltonian $\hat{H}$ for an "electron" of "mass" m placed in the "magnetic" field $\boldsymbol{H} = \boldsymbol{\nabla} \times \boldsymbol{A}$ is known to be (Sondheimer and Wilson, 1951),

$$\hat{H} = \frac{1}{2m}\nabla_r^2 + \frac{1}{m\mathrm{i}}\boldsymbol{A}\cdot\boldsymbol{\nabla}_r + \frac{\boldsymbol{A}^2}{2m}, \tag{8.85}$$

so that the Bloch equation for the density matrix ρ can be written as

$$-(\partial/\partial\beta)\rho = \hat{H}\rho \tag{8.86}$$

provided that $\rho(\boldsymbol{r}, \boldsymbol{r}'; \beta \to 0) = \delta(\boldsymbol{r} - \boldsymbol{r}')$. Using results of Sections 6.3 and 6.4 the last equation can be equivalently rewritten as

$$\left(\frac{\partial}{\partial\beta} - \frac{1}{2m}\nabla_r^2 - \frac{H}{2m\mathrm{i}}\left(x\frac{\partial}{\partial y} - y\frac{\partial}{\partial x}\right) + \frac{H^2}{8m}(x^2 + y^2)\right)\rho = 0\,. \tag{8.87}$$

The corresponding polymer problem is obtained by the following replacements:

$$\beta \rightleftarrows N\,, \quad \frac{1}{2m} \rightleftarrows \frac{l}{6}, \quad \frac{H^2}{8m} \rightleftarrows \frac{w^2}{6}\,,$$

and, if one considers only the states with the total angular monumentum zero, then the last equation coincides exactly with Eq. (6.55) while the partition function Z, given by

$$Z = \int \mathrm{d}\boldsymbol{r}\,\rho(\boldsymbol{r} = \boldsymbol{r}' = \boldsymbol{r}; \beta) \tag{8.88}$$

coincides with that given by Eq. (8.54) (with obvious redefinitions of w or Δp). If $\Psi_n(\boldsymbol{r})$ is the eigenfunction of the Schrödinger-like operator given by Eq. (8.87), then the size of the tube can be estimated according to Eq. (8.49) as

$$a^2 = \int \mathrm{d}^2 z\,[\Psi_0(z, \bar{z})]^2 |z|^2\,, \tag{8.89}$$

where use was made of the planarity of the magnetic Schrödinger problem which allows us to introduce complex variables $z = x + \mathrm{i}y$ and $\bar{z} = x - \mathrm{i}y$ so that, upon rewriting the whole problem in terms of z and $\bar{z}$, one obtains for the lowest Landau level wave function $\Psi_0(z, \bar{z})$ the following result:

$$\Psi_0(z, \bar{z}) = \tilde{N}\exp\left(-\frac{w}{l}|z|^2\right) \tag{8.90}$$

with $\tilde{N}$ being a normalization constant. The validity of the approximation for a^2 rests on the assumption that for large N's the density matrix ρ can be approximated by

$$\rho(\boldsymbol{r}, \boldsymbol{r}'; N) \simeq \mathrm{e}^{-\varepsilon_0 N}\,\Psi_0^*(\boldsymbol{r})\Psi_0(\boldsymbol{r}')\,. \tag{8.91}$$

The presence of holes (other polymers) in the plane can be accounted for by introducing the mutual winding number θ_{ij} constraint into the corresponding path integrals. In the absence of the "magnetic" field the functional integral for an assembly of topological interacting planar Brownian walks is given by

$$G = \int \prod_{i=1}^{n_t} \mathrm{D}[r(\tau_i)] \exp\left\{ - \int_0^N \mathrm{d}\tau \left[\sum_{i=1}^{n_t} \frac{1}{l} \dot{\boldsymbol{r}}_i^2 + \mathrm{i} \frac{\Phi}{2\pi} \sum_{i<j}^{n_t} \frac{\mathrm{d}}{\mathrm{d}\tau} \theta(\boldsymbol{r}_{ij}(\tau)) \right] \right\}, \tag{8.92}$$

where

$$\theta(\boldsymbol{r}_{ij}(\tau)) = \tan^{-1}\left(\frac{y(\tau)}{x(\tau)} \right), \tag{8.93}$$

n_t was defined e.g. in Eq. (8.47) and Φ is some constant which is related to the filling fraction ν, defined before Eq. (8.48) (for details, please, consult Kholodenko and Vilgis, 1994) as

$$\nu = 4\pi/\Phi \,. \tag{8.94}$$

The result given by Eq. (8.92) should be compared now against earlier discussed Eq. (6.9). The presence of the "magnetic" field which describes the tube(s) cross section(s) can be accounted easily now by analogy with Eq. (6.67). At the same time, although at the classical level the interaction term in the exponent of Eq. (8.92) is the total "time" derivative and, hence, can be discarded, it cannot be ignored at the quantum level as we have explained in Section 6.1. For $\Phi = 0$ the total Hamiltonian $\hat{H}$ is just a collection of single particle Hamiltonians, i.e.

$$\hat{H} = \sum_{i=1}^{n_t} \hat{H}\left(\boldsymbol{r}_i, \frac{1}{\mathrm{i}} \frac{\partial}{\partial \boldsymbol{r}_i} \right) \equiv H\left(\left\{ \boldsymbol{r}_i, \frac{1}{\mathrm{i}} \frac{\partial}{\partial \boldsymbol{r}_i} \right\} \right). \tag{8.95}$$

Topological interactions change $\hat{H}$ into

$$\hat{H}_t = H\left(\left\{ \boldsymbol{r}_i, \frac{\partial}{\partial \boldsymbol{r}_i} - \frac{\Phi}{4\pi} \sum_{i \neq j} \nabla_{r_i} \theta(\boldsymbol{r}_i - \boldsymbol{r}_j) \right\} \right) \tag{8.96}$$

so that the Schrödinger-like equation (with or without magnetic field) can be written now as

$$\frac{\partial}{\partial t} \Psi(\{\boldsymbol{r}_i\}, t) = \hat{H}_t(\{\boldsymbol{r}_i\}, t) \Psi \,. \tag{8.97}$$

Elementary examples of the above procedure were discussed in Section 6.1. Eq. (8.97) *by design* assumes that *all* "particles" are moving in the same "time" t (in case of polymers N). In the theory of Brownian motion there is no need, however, to make such an assumption (McKean, 1969). In case of polymers this was recognized by des Cloizeaux and Jannink (1990). The sychronized "time" is used in the theory of directed polymers (Kardar and Zhang, 1987), without explicitly acknowledging this fact (e.g. see also Blatter et al., 1994). Use of one "time" (instead of many) is equivalent of saying that all polymers are of the *same* length and are indistinguishable. des Cloizeaux and Jannink (1990) had carefully analyzed this issue for polymers and found that this assumption may sometimes lead to wrong results. The indistinguishability is also closely associated with statistics as we have demonstrated in Section 6.2. Extension of the "anionic philosophy" to the case of distinguishable particles was recently made by Liguori and Mintchev (1995) and Isakov et al.

(1995). The Riemann surface approach presented in Section 8.3 *does not* require these assumptions and, hence, is more consistent with the traditional language used in polymer physics, see, e.g. des Cloizeaux and Jannink (1990). Nevertheless, the time peculiarity just described is not a major stumbling block towards obtaining physically meaningful results in the present case.

Indeed, if instead of the correct single valued function Ψ in Eq. (8.97) we would use the multi-valued functions

$$\tilde{\Psi}(\{\boldsymbol{r}_i\},t) = \exp\left\{ -\frac{\Phi}{2\pi}\sum_{i<j}\theta(\boldsymbol{r}_i - \boldsymbol{r}_j)\right\}\Psi(\{\boldsymbol{r}_i\},t) \tag{8.98}$$

then this equation will be replaced by an equivalent single-particle Schrödinger equation for $\tilde{\Psi}$

$$\frac{\partial}{\partial t}\tilde{\Psi} = \hat{H}\tilde{\Psi}\,, \tag{8.99}$$

where $\hat{H}$ is given by Eq. (8.95). The reader is referred again to Section 6.1 for illustrative elementary example of such transformation. Use of complex variables z and $\bar{z}$ and ground state dominance assumption, Eq. (8.91), allow us to write the many-body wave function $\tilde{\Psi}$ for our Landau-like problem in the form

$$\tilde{\Psi}_0(\{z_i\},\{\bar{z}_i\}) = \tilde{N}\prod_{i<j}^{n_t}(z_i - z_j)^{\Phi/2\pi}\exp\left\{ -\frac{w}{l}\sum_i |z_i|^2\right\}. \tag{8.100}$$

For $\Phi = 0$ we obtain back the product of Landau wavefunctions (see, e.g. Eq. (8.90)), while for nonzero Φ we obtain, instead of Eq. (8.89), the following result for a^2:

$$a^2 = \int \mathrm{d}^2 z\,|z|^2\hat{\rho}_{\mathrm{int}}(z,\bar{z}) \tag{8.101}$$

with

$$\hat{\rho}_{\mathrm{int}}(z,\bar{z}) = \int\prod_{i=2}^{n_t}\mathrm{d}^2 z_i|\tilde{\Psi}_0(\{z_i\},\{\bar{z}_i\})|^2\,. \tag{8.102}$$

The combined use of Eqs. (8.100), (8.101) and (8.102) reduces the problem of computation of a^2 to the calculation of the classical statistical mechanical average

$$a^2 = \frac{1}{Z}\int\prod_{i=1}^{n_t}\mathrm{d}^2 z_i|z_1|^2\exp\{-\tilde{H}[z,\bar{z}]\}\,, \tag{8.103}$$

where, in view of Eq. (8.94), we have

$$\tilde{H}[z,\bar{z}] = \frac{-4}{v}\sum_{i<j}\ln|z_i - z_j| + \frac{2w}{l}\sum_i |z_i|^2 \tag{8.104}$$

and Z is a normalization constant (partition function).

The Hamiltonian $\tilde{H}$ is known in the literature as describing the one-component plasma (OCP), (Caillol et al., 1982), while the wave function of Eq. (8.100) is known as Laughlin wave function (Laughlin, 1983), used in the theory of quantum Hall effect (QHE). For $n_t \gg 1$ one can try to

calculate a^2 in Eq. (8.103) by using the saddle point method. By introducing the new variable $x = z/\sqrt{n_t}$ the Hamiltonian $\tilde{H}$ can be rewritten now as

$$\frac{\tilde{H}[x,\bar{x}]}{n_t} = \sum_i |x_i|^2 - \frac{m}{2n_t}\sum_{i<j} \ln|x_i - x_j|^2 , \tag{8.105}$$

where $m = 4/v$. Minimization of Eq. (8.103) produces the following saddle point equations:

$$\bar{x}_i = \frac{m}{n_t}\sum_{\substack{j \\ (i\neq j)}} \frac{1}{x_i - x_j} , \tag{8.106}$$

$$x_i = \frac{m}{n_t}\sum_{\substack{j \\ (i\neq j)}} \frac{1}{\bar{x}_i - \bar{x}_j} . \tag{8.107}$$

To solve these equations, we need to multiply Eq. (8.106) by x_i while Eq. (8.107) by $\bar{x}_i$. By writing

$$x_k = R\exp\left\{\frac{2\pi i k}{n_t}\right\}, \tag{8.108}$$

i.e. by assuming that the "particles" are located on concentric rings of radius R, we obtain,

$$R^2 = \frac{m}{n_t}\sum_j \frac{1}{1-\exp\{2\pi i j/n_t\}} = \frac{m}{n_t}\frac{n_t - 1}{2} \simeq \frac{m}{2} = \frac{2}{v} , \tag{8.109}$$

where in the second line the sum rule was used (Kogan et al., 1992) to arrive at the final result. Using Eq. (8.109) the average distance $\langle r\rangle$ between "particles" can be calculated according to equation

$$\langle r\rangle \simeq \frac{2\pi R}{n_t} = (2\pi/n_t)\sqrt{2/v} . \tag{8.110}$$

Using back z-variable (instead of x) the above result can be written now as

$$\langle r\rangle = 2\pi\sqrt{(2/vn_t)}a . \tag{8.111}$$

Since we can always write $\langle r\rangle = \text{const.}\ a$ (where const. ≥ 2), we obtain using Eq. (8.111) the following result:

$$vn_t = \text{const}' . \tag{8.112}$$

or, in view of Eq. (8.48),

$$\pi a^2 \hat{\rho} n_t = \text{const}' . \tag{8.113}$$

Since $\hat{\rho} \sim n_t$, see, e.g. Eq. (8.48), we obtain

$$a\rho = \text{const}'' . \tag{8.114}$$

and this result *coincides* with Eq. (8.84)!

The equation of state for OCP is known to be (Hague and Hemmer, 1971)

$$P = \rho(k_B T - g^2/4)\,. \tag{8.115}$$

Then, for $T > T_c$, where $T_c = g^2/4k_B$, the system is in a "gas" phase while for $T < T_c$ it is in a liquid phase. For $T < T_c$ the pressure P in the above equation becomes negative and the system undergoes gas–liquid transition. We have shown in Kholodenko and Vilgis (1994), that for our polymer problem $g^2 = \Phi/\pi$ and $v = 4\pi/\Phi$. Caillol et al. (1982) show, by using the Monte Carlo methods, that the OCP can also undergo yet another transition: from "liquid" to "solid" phase. This happens for $v^* \approx 0.0286$ to be compared with our earlier result, Eq. (8.74). Evidently, the difference in these critical values could be understood using the following physical arguments. The result, Eq. (8.74), is related to the onset of tube formation while the result $v^* = 0.0286$ is related to the regime when the tube already exists and is well defined. Comparison between Eq. (8.73) (obtained for $n = 0$ in Eqs. (8.67) and (8.74)) '(obtained for $n = 1$ in Eq. (8.67)) indicates that for large enough n we can expect the result for v^* coming from OCP calculations. The above qualitative arguments can be made mathematically more precise. This is accomplished in Section 8.5.

8.5. Connections with theories of quantum chaos

In this section we want to demonstrate that QHE and Riemann surface approaches to reptation are not only interconnected but also could be viewed from the broader angle provided by theories of quantum chaos and quantum mesoscopic systems. Following Kholodenko (1996b), let us take another look at Eq. (8.37). By using the conformal transformation

$$w = (z - \mathrm{i})/(z + \mathrm{i})\,, \quad z \in H\,, \tag{8.116}$$

where H was defined in Eq. (8.41), the metric, Eq. (8.42), can be transformed into

$$\mathrm{d}s^2 = \frac{4((\mathrm{d}u)^2 + (\mathrm{d}v)^2)}{[1 - (u^2 + v^2)]^2}\,, \tag{8.117}$$

where $w = u + \mathrm{i}v$. The above metric converts the Poincare H-plane model into the Lobachevski unit circle model. Evidently, both descriptions are equivalent (Stillwell, 1992), but use of the unit circle formulation allows us to obtain some additional information a bit easier. To this purpose let now $u = \sinh\theta\cos\varphi$, $v = \sinh\theta\sin\varphi$ and $r = \tanh(\theta/2)$ where $0 \le \theta < \infty$, $0 < \varphi \le 2\pi$. In terms of such parametrization Eq. (8.37) can be rewritten now as

$$\tfrac{1}{4}\nabla^2_{r,\varphi} P(r,\varphi;\tau) = [1/(1 - r^2)]\,(\partial/\partial\tau)P(r,\varphi;\tau) \tag{8.118}$$

where

$$\nabla^2_{r,\varphi} = \frac{\partial^2}{\partial r^2} + \frac{1}{r}\frac{\partial}{\partial r} + \frac{1}{r^2}\frac{\partial^2}{\partial\varphi^2}\,. \tag{8.119}$$

Eq. (8.118) coincides with Eq. (3.6) of Nechaev (1988) (if the last one is rewritten in dimensionless units). Notice that if instead of r we would use the original θ-variable, then Eq. (8.118) would

acquire the following form (which we shall use in subsequent discussion):

$$\left(\frac{1}{\sinh\theta}\frac{\partial}{\partial\theta}\left(\sinh\frac{\partial}{\partial\theta}\right)+\frac{1}{\sinh^2\theta}\frac{\partial^2}{\partial\theta^2}\right)P(\theta,\varphi;\tau)=\frac{\partial}{\partial\tau}P(\theta,\varphi;\tau)\,. \tag{8.120}$$

The resulting equation looks almost familiar: if instead of the sinh function we would use the sin function the above equation would describe the Brownian motion on a sphere. In the present case, however, we are dealing with the case of pseudosphere. As in Section 8.3, we assume that the distribution function P is φ-independent. Then Eq. (8.120) can be converted into

$$\hat{L}P(x-x';\tau)\equiv\left(\frac{\mathrm{d}^2}{\mathrm{d}x^2}+\coth^2 x\frac{\mathrm{d}}{\mathrm{d}x}\right)P(x-x';\tau)=\frac{\partial}{\partial\tau}P(x-x';\tau)\,, \tag{8.121}$$

where $x=\theta$. Evidently the distribution function $P(x,\tau)$ can be found if the eigenvalue problem for the operator $\hat{L}$ is solved. In connection with this eigenvalue problem, let us consider a seemingly unrelated eigenvalue problem related to the particle in a potential $g^2\sinh^{-2}x$ with g being some adjustable constant. This eigenvalue problem can be formulated, as usual, as

$$\hat{H}\varphi_n=\left[-\frac{1}{2}\frac{\mathrm{d}^2}{\mathrm{d}x^2}+g^2\sinh^{-2}x\right]\varphi_n=E\varphi_n\,. \tag{8.122}$$

It can be shown (Olshanetsky and Perelomov, 1985) that the function

$$\varphi_0=(\sinh x)^{\mu} \tag{8.123}$$

is the solution of Eq. (8.122) with the eigenvalue $E_0=-\mu^2/2$ provided that $\mu(\mu-1)=2g^2$. This function is not normalizable however, since it is increasing for $x\to\infty$. Hence, E_0 does not belong to the spectrum of the operator $\hat{H}$. Upon substitution of $\varphi_n=\varphi_0\phi_n$ into Eq. (8.122), it is converted into the equation

$$\hat{L}\phi_n=-(\mu^2+n^2)\phi_n\,, \tag{8.124}$$

where the operator $\hat{L}$ is *the same* as in Eq. (8.121). Hence, Eqs. (8.121) and (8.124) have *the same* eigenfunctions. The one-body Hamiltonian $\hat{H}$ defined by Eq. (8.122) can be easily generalized to the many-body case and is known in the literature as Calogero–Sutherland (CS) Hamiltonian (Felder and Veselov, 1994). It is given by

$$\hat{H}_{\mathrm{CS}}=-\sum_{i=1}^{n}\frac{1}{2}\frac{\mathrm{d}^2}{\mathrm{d}x_i^2}+\alpha\sum_{i<j}^{n}\frac{\omega}{\sinh^2(x_i-x_j)\omega}\,, \tag{8.125}$$

where n is the number of "particles" in the (one-dimensional) system and α and ω are some constants. For $\omega\to 0$, Eq. (8.125) is known as Calogero Hamiltonian. To use the CS Hamiltonian in the reptation problem, several issues need to be resolved. First, Eq. (8.120) describes the transversal part of the "motion" of an individual primitive chain (so far in the absence of the "magnetic field"). For noninteracting chains the total Hamiltonian should be evidently just a sum of one-body Hamiltonians. Therefore, naively, the total Hamiltonian $\hat{H}^{\mathrm{T}}$ should look like

$$\hat{H}_{\mathrm{CS}}=\sum_{i=1}^{n}\left[-\frac{1}{2}\frac{\mathrm{d}^2}{\mathrm{d}x_i^2}+\frac{g^2}{\sinh^2 x_i}\right]+\hat{H}_{\mathrm{int}}\,. \tag{8.126}$$

Eq. (8.92) suggests that the nature of interaction between tubes is topological so that $\hat{H}_{\text{int}}$ *cannot* have a small parameter and *cannot* be considered as just a small perturbation. The eigenvalue problem for CS Hamiltonian can be solved exactly (Cherednik, 1994). As was noticed already by Sutherland (1985), to find the eigenfunctions and eigenvalues of $\hat{H}_{\text{CS}}$ is sufficient to know only the two-body scattering phase shift. Because the two-body problem is always reduceable to the one-body problem, we are essentially coming back to Eq. (8.122) (*and*, *hence*, *to Eq*. (8.121)!).

Mathematicians have demonstrated rigorously that the wave functions of the CS and Knizhnik–Zamolodchikov (KZ) equations are practically *the same*. But in Kholodenko–Vilgis (1994) it was demonstrated that the Laughlin wave function, given by Eq. (8.100), obeys the KZ equation. Hence, we are left with the conclusion that the CS Hamiltonian (perhaps, with an extra quadratic term to account for the "magnetic field", (see, e.g. Azuma and Ito, 1994) can be also used to describe the interacting tube model which was discussed in Section 8.4. *Hence*, *the Riemann surface and the QHE models of reptation are effectively isomorphic to each other*. Since the CS Hamiltonian is widely used in the theory of chaotic/disordered systems, see, e.g. Mucciolo et al. (1994), Beenakker and Rejaei (1994), etc., one can think of reptation as yet another illustration of the *universality of the description of chaotic systems based on CS-type models.*

8.6. Connections with theories of mesoscopic systems

The formalism developed above closely resembles that developed to describe the conductivity in quasi-one-dimensional metallic wires (Datta, 1995). This theory is known to produce an additional effect, e.g. quantization of conductance: when the cross section of a quasi-one-dimensional wire changes continuously the conductivity changes discontinuously (see, e.g. Figs. 1 and 2 of Jascual et al. (1995) and Fig. 46 of Beenaker and van Houten (1991)). In addition, the same discontinuity effect can be achieved by continuously varying the voltage between the ends of the wire (see, e.g. Fig. 44 of Beenakker and van Houten (1991)).

In Kholodenko (1996b) and Kholodenko and Vilgis (1994) it was emphasized that, "although tubes can apparently appear and disappear, at time scales shorter than the terminal relaxation time $\tau_{\text{T}} \sim N^{3.4}$ (see, e.g. Section 2) the melt of flexible polymers could be viewed as porous continuum with tubes (pores) being randomly distributed in it, Teraoka et al. (1992)". The importance of this point of view was recently emphasized by Milchev and Binder (1994) while Krupenkin and Taylor (1995a,b) had considered a "motion" of polymers through pores using ideas similar to that discussed in Section 6.3. The quantization of force–extension relation (just like quantization of conductance) was discussed in Section 6.1 and is in qualitative agreement with the experimental data of Cluzel et al. (1996) as discussed also in Section 6.1.

In the case of polyelectrolytes, the electric field is used in gel electrophoresis to separate molecules of different sizes. It would be very interesting to develop closer links between the theory of gel electrophoresis (Rubinstein, 1987; Duke, 1989; Prahofer and Spohn, 1996; etc.) and the theory of electronic conduction in mesoscopic systems.

The asymmetry of descriptions of the longitudinal and transversal motions of the polymer along the tube leads to a controversy which is also known in the theory of the QHE. Specifically, if we modify Eq. (8.86) by adding some sort of random potential $\hat{V}$ to the Hamiltonian defined by Eq. (8.85), then, even in the presence of weak disorder, all electronic states are localized in two dimensions (i.e. "conductivity" is zero in QHE language). Once the magnetic field is turned on, the

conductivity reappears. Moreover, the value of Hall conductance *is independent* of the degree of disorder. The shape of the conductance curve for the case of QHE is similar to the shape of conductance curve for quasi-one-dimensional conductors discussed above.

Using polymer language, the above situation can be restated as follows: In the absence of an area constraint, i.e. $\Delta p = 0$, in Eq. (6.70) the propagator of Eq. (8.45) produces the following result for the averaged radius of gyration (Nechaev et al., 1987),

$$\langle R_g^2 \rangle \simeq \frac{z}{z-2}\frac{\sqrt{2\pi}}{8} l\sqrt{N} \tag{8.127}$$

which is *in complete accord with our result* in Eq. (8.32). Incidentally, the same result was obtained by de Gennes (1971) (e.g. see Section 4 of this paper) by completely different methods. If time t is associated with N (as de Gennes did), then the diffusion coefficient D can be estimated as $D \sim \mathrm{d}\langle R_g^2 \rangle / \mathrm{d}N \sim 1/\sqrt{N}$. Because the diffusion and conductivity are related via Einstein relation (Kholodenko, 1985), it is obvious that the result given by Eq. (8.127) leads to the localization (i.e. absence of conductivity in QHE language). At the same time, according to the main postulates of reptation theory (Doi and Edwards, 1986), the statistics of the primitive path (chain) for large N should be Gaussian-like, i.e. "conduction" should take place.

In Section 6.3 we have discussed the longitudinal part of primitive chain "motion" and had indicated that resolution of the localization paradox lies in the assumption that the motion is facilitated by the existence of tube domains which are almost linear (rigid-rod-like). Alternatively, if instead of initially fully flexible (Gaussian) chains, the Dirac (semi-flexible) chains are used (Kholodenko, 1990, 1995), then the localization may be prevented. In the context of QHE this was recently demonstrated by Ludwig et al. (1994). If the Dirac chains are used, then the results of Section 8.3 should be reanalyzed since one should study in this case spinors and Dirac-type equations on the Riemann surfaces, see, e.g. Gilkey (1995). These problems are similar so that studied in the theory of superstings, see, e.g. Green et al. (1987).

Finally, we would like to mention that Hess (1988) had provided a very important alternative dynamical treatment of reptation emphasizing the difference between the longitudinal and the transversal parts of motion of the trapped chain. His treatment, however, does not involve topological considerations and these are quite independent of dynamics as we demonstrate in Appendix A.1.

Acknowledgements

The authors had benefitted from discussions with many people. Professors Kurt Binder (Univ. Mainz), Kurt Kremer (MPI, Mainz), Harry Frisch (Univ. Albany, NY) were instrumental in providing many useful references related to experimental and numerical results which involve entanglements. Dr. Jack Douglas (NIST) had attracted our attention to works of McKean and collaborators. Professors Hagen Kleinert (Freie Universität Berlin) and Dale Rolfsen (Univ. of British Columbia) provided helpful comments related to the Jones polynominals, Chern–Simons field theories, etc. Professor Louis Kauffman (UIC) had provided us with historical and technical

references related to applications of knot theory to various physical problems. Generous support of this project by the Max-Planck Gesellschaft and the staff of MPI (Mainz) is also highly appreciated.

Appendix A.

A.1. Planar Brownian motion in the presence of two holes

McKean and Sullivan (1984) and Lyons and McKean (1984) have studied this problem in some detail. For the case of n punctures (holes) the problem was studied by Pitman and Yor (1986, 1989) (please, see also Yor's book, Yor (1992)). Since their presentation is highly mathematical, it may not be readily accessible to most of physics educated readers. Hence, we would like to present here only the intuitive arguments.

As it was noticed in Lyons and McKean (1984) (Section 2 of their paper), the Brownian motion in the presence of two holes in the plane is essentially the same as the Brownian motion on the thrice punctured sphere. This is so because, as is well known, the sphere is isomorphic to $\mathbf{R}^2 \cup \{\infty\}$, where $\{\infty\}$ is the point at infinity. In Section 8.3 it is argued that the thrice punctured sphere is the main building block of any Riemann surface.

The nontrivial case of Brownian motion on the thrice punctured sphere can be readily understood from the point of view of homotopy theory. To this purpose, let us recall the case of just one puncture we have considered in Section 5.1. When we have two (or three) holes (punctures), the single winding number constraint used in Section 5.1 can no longer be used. The above single hole problem can be generalized if we take into account that the winding number constraint can be replaced (via Hubbard–Stratonovich transformation) by an electromagnetic-like field so that effectively, one has to consider the propagator for the nonrelativistic "charged" particle in the presence of the Abelian gauge field. This approach was discussed in Sections 4.2 and 8.2. The fact that the field is Abelian is caused by the group structure of the rotations around the circle which is Abelian. In physics literature the above type of problem is usually associated with the Aharonov–Bohm effect (Kleinert, 1995). This well-developed picture breaks down as soon as we include the second hole. In this case, one has to consider three types of homotopically distinct paths: (a) around the first hole, (b) around the second hole and (c) around both holes (see, e.g. Figs. 15 and 16). Let g_1, g_2 and g_∞ be the generators of the above motions, then, according to McKean and Sullivan (1984), they are not independent since they are subject to the constraint: $g_\infty g_2 g_1 = 1$. This constraint makes the homotopy group non-Abelian. Hence, one has to calculate path integrals for the planar Brownian motion of "charged" particles in the presence of the non-Abelian gauge field (Balachandran et al., 1991). Alternatively, following McKean (1969), one can develop a completely different approach by noticing the following. For the case of three punctures it is possible to find the conformal transformation of the interior of the punctured triangle into the upper Poincare half-plane H which was defined in Eq. (8.41). Normally, the conformal transformation will transform the interior of the punctured triangle into H so that the vertices $\mathrm{A}, \mathrm{B}, \mathrm{C}$ of the original triangle will be transformed into the points $\mathrm{a}, \mathrm{b}, \mathrm{c}$ on the x axis of the H model. Since, however, we are interested not only in the interior of the triangle but in the mapping of the *entire* twice (or thrice) punctured complex plane into H, the standard approach via

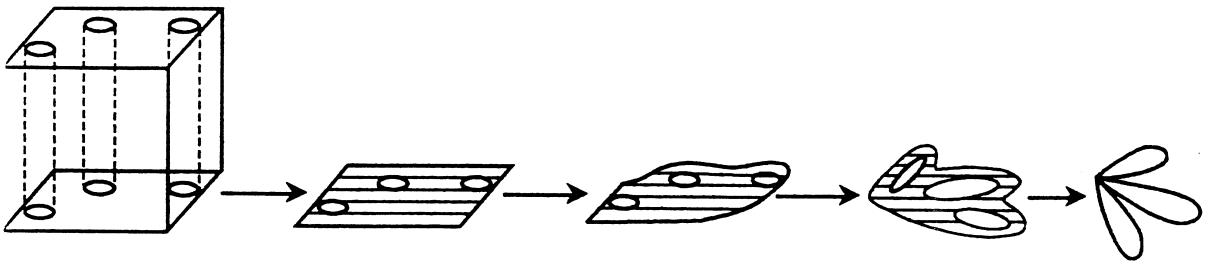

Fig. 19. Sequence of operations leading from $\mathbf{R}^3\backslash\{\text{no. of lines}\}$ to $\mathbf{R}^2\backslash\{a_1,\ldots,a_{n_i}\}$.

Schwarz–Christofel conformal transformation (Nechaev, 1988) cannot be used. Following McKean (1969), let us reconsider the once punctured plane results. McKean argues that, instead of considering the Brownian motion on the punctured plane, i.e. on $\mathbf{R}^2\backslash\{0\}$, one can consider the Brownian motion on the Riemann surface (i.e. universal covering surface for $\mathbf{R}^2\backslash\{0\}$). It happens that if $z\in\mathbf{R}^2\backslash\{0\}$, then $w=\ln z$ defines the desired mapping into the Riemann surface for the logarithm. For the case of the twice punctured plane, the functional mapping analogous to $z=\exp w$ is found to be $z=\lambda(w)$, where

$$\lambda(w)=16q\prod_{n=1}^{\infty}\left(\frac{1+q^{2n}}{1+q^{2n-1}}\right)^8 \tag{A.1}$$

with $q=\exp(\mathrm{i}\pi w)$ and $w=u+\mathrm{i}v$. The above transformation maps the fundamental domain of the H plane ($w=u+\mathrm{i}v, v>0$) so that the entire H plane is covered by translations (tessellations) of this domain as discussed in Section 8.3 into the whole z-plane which contains cuts along the real axis from $-\infty$ to 0 and from 1 to $+\infty$. The inverse function $w=\lambda^{-1}(z)$ is regular in the cut z-plane and maps it conformally to the fundamental domain in the H plane. It can be shown (e.g. Dubrovin et al., 1985) that, homotopically, $\mathbf{R}^3\backslash\{line\}$ is equivalent to $\mathbf{R}^2\backslash\{0\}$. This means that in the case of many lines in $\mathbf{R}^3$, the space $\mathbf{R}^3\backslash\{\text{no. of lines}\}$ is *homotopically equivalent* to $\mathbf{R}^2\backslash\{a_1,\ldots,a_{n_i}\}$ where $a_1,\ldots,a_{n_i}$ are punctures in $\mathbf{R}^2$ plane. This can be intuitively understood with help of Fig. 19.

More details can be found in Stillwell (1993) or Massey (1967). The above results provide the required topological justification for the separation of "motion" of the trapped polymer chain into the transversal and the longitudinal parts as discussed in the main text in Sections 6.3, 8.3 and 8.4. Evidently, these results are valid for both static and dynamic treatments of polymer melts.

We have argued in Section 8.3 that the planar Brownian motion in the presence of many holes can be described by the diffusion on the hyperbolic surface of constant negative curvature. We just had seen that this fact remains unchanged in the presence of a set of lines in $\mathbf{R}^3$. The question arises: Will the motion in $\mathbf{R}^3$ remain hyperbolic if $\mathbf{R}^3$ contains some knot? Below we provide some evidence in favor of the hyperbolicity leaving practical applications of this fact outside the scope of this review.

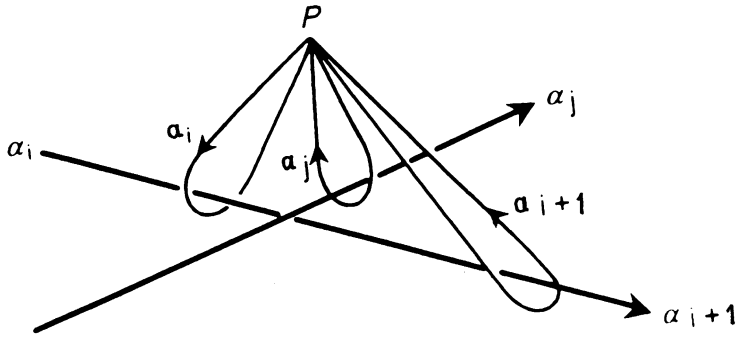

Fig. 20. Geometry of loops a_i around each crossing. Here a_i, a_j and a_{i+1} denote arcs which join different neighboring crossings.

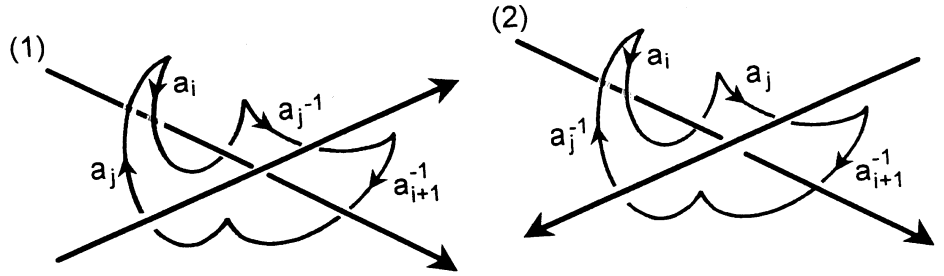

Fig. 21. Disentangled paths around each crossing according to the convention explained in the text.

A.2. Spatial Brownian motion in the presence of knots (*links*)

Three-dimensional description of knots (links) can be made very similar to that we have just encountered in Section A.1. Specifically, in the planar case, we have chosen some reference point $p \in \mathbf{R}^2$ and have encircled each hole with paths which begin and end at p. The same procedure is possible to generalize to $\mathbf{R}^3$. One point compactification of $\mathbf{R}^3$(or $\mathbf{C}$) produces S^3 (as much as one point compactification of $\mathbf{R}^2$ (or C) produces S^2). So, we embed our knot K into S^3 and study homotopy of paths in $S^3 \backslash K$ with respect to some point p inside S^3 which do not belong to K. Let us choose an orientation for K and then encircle each knot crossing by loops a_i as depicted in Fig. 20. More advantageous, however, is to disentangle these loops as depicted in Fig. 21.

To this purpose the convention must be introduced that, e.g., the lower arc a_i *into* the crossing is followed by the arch a_{i+1} *out* of the crossing. This leads to the result that for the crossing of type (1) the curve $a_i a_j^{-1} a_{j+1}^{-1} a_j$ contracts to the point, hence, producing the relation

$$a_i a_j^{-1} a_{j+1}^{-1} a_j = 1 \,, \tag{A.2}$$

or

$$a_j a_i = a_{i+1} a_j \,. \tag{A.3}$$

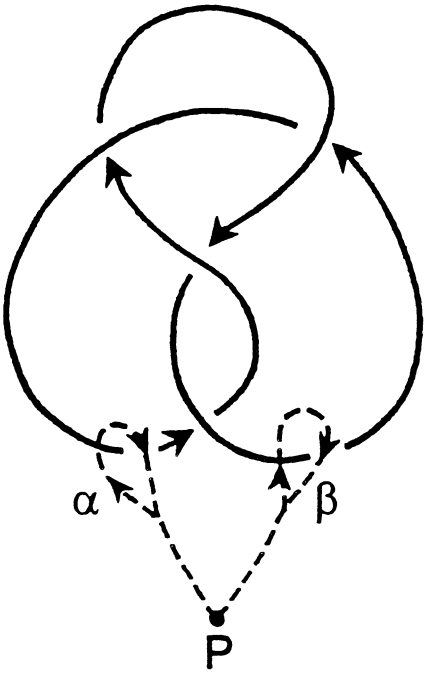

Fig. 22. Figure eight knot together with the basic loop generators α and β.

Alternatively, for the crossing of type (2) we have

$$a_i a_j = a_j a_{i+1}\,. \tag{A.4}$$

Let, in general, $\{a_i\}$ denote a set of loops for K. They are called *generators* of the knot group $G(K)$. Every element of $G(K)$ can be written as

$$G(K) = a_1^{n_1} a_2^{n_2} \cdots a_{n_t}^{n_t}\,, \tag{A.5}$$

where each n_i is a *nonzero* integer. The type of Eq. (A.2) or Eq. (A.4) are called *relations* (in general, they are denoted by r_i). A presentation for $G(K)$ consist of *finite* sets $\{a_i\}$ and $\{r_i\}$ and is usually written as (Gilbert and Porter, 1994)

$$G(K) = (a_1, \ldots, a_{n_t} \,|\, r_i, \ldots, r_m)\,. \tag{A.6}$$

Following Milnor (1982, 1994) and Riley (1975) consider now the figure eight knot as shown in Fig. 22. The generators α and β are subject to a single relation

$$(\alpha\beta^{-1}\alpha^{-1}\beta)\alpha = \beta(\alpha\beta^{-1}\alpha^{-1}\beta)\,. \tag{A.7}$$

The generators α and β will correspond to some matrices A and B which must satisfy a single matrix equation. It is found that these matrices belong to the group $PSL(2,C) = SL(2,C)/\{\pm 1\}$. Recall (Kholodenko, 1996b), that in the case of H-model $PSL(2,R)$ group was used so that if

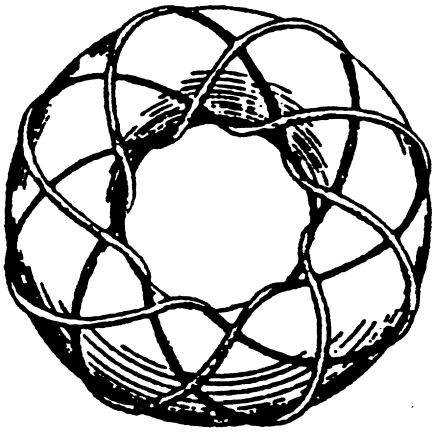

Fig. 23. A representative example of a torus knot.

$\gamma \in SL(2,R)$ and if $z \in H$, then

$$\gamma z = \frac{az + b}{cz + d} \tag{A.8}$$

with a, b, c, d being real and $\{ \pm 1\}$ factor are 2×2 identity matrices responsible for reflections. The planar H-model, Eq. (8.41), can be easily extended to the $\mathbf{R}^3_+$ model defined by

$$\mathbf{R}^3_+ \{(x, y, t) \in \mathbf{R}^3; z = x + \mathrm{i}y = \mathbf{C},\ t > 0\} . \tag{A.9}$$

Then, instead of z used in H, one can use $z + \mathrm{j}t$ in $\mathbf{R}^3_+$ where

$$z + \mathrm{j}t = x + \mathrm{i}y + \mathrm{j}t + k0 \tag{A.10}$$

is a quaternion. The transformation γ now becomes a transformation $\hat{\Gamma}$ which has the same form as Eq. (A.8) but with *complex coefficients*. The quotient $\mathbf{R}^3_+/\hat{\Gamma}$ which is an hyperbolic 3-manifold is very much like the H/Γ which is a hyperbolic 2-manifold discussed in Section 8.3. For an introduction to the theory of 3-manifolds we recommend Meyerhoff (1992). Thurston (1979, 1982) had shown that $S^3 \backslash K$ has a hyperbolic structure if K is not a torus knot and does not contain satellites. An example of a torus knot is given in Fig. 23 while Fig. 24 illustrates the concept of a satellite knot.

From the previous discussion it follows that

(a) one can think about knots in terms of their $S^3 \backslash K$ complements (Gordon and Luecke, 1989);

(b) if in the planar case the Aharonov–Bohm effect is a "hydrogen atom" model for all fractional, QHE, etc. features, in the three-dimensional case, the Brownian motion in the presence of a knot K should play the same role.

Classical dynamics of such a motion was considered by Goodman (1983) while the study of the Brownian motion in the presence of a knot was initiated in the work of Varopoulos (1985) (please,

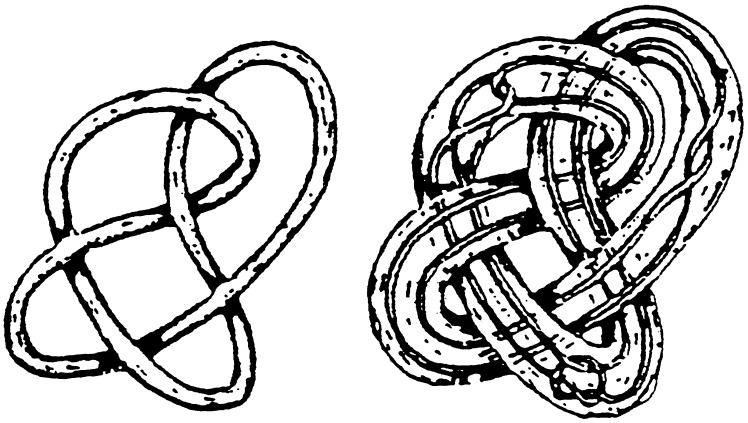

Fig. 24. Some knot and its satellite.

see also Varopoulos et al. (1992) and references therein). It remains to apply these results to physical and biological problems.

References

Adams, C., 1994. The Knot Book. Freeman, New York **.
Aharonov, Y., Bohm, D., 1959. Phys. Rev. 115, 485 *.
Aitchinson, I., 1987. Acta Phys. Pol. B 18, 207 *.
Akao, J., 1996. Phys. Rev. E 53, 6048.
Aldaya, V., Calixto, M., Guerrero, J., 1996. Comm. Math. Phys. 178, 399.
Aldinger, J., Klapper, I., Tabor, M., 1995. J. Knot Theory and Ramifications 4, 343.
Alekseev, A., Shatashvili, S., 1988. Mod. Phys. Lett. A 3, 1551.
Ambjorn, J., Durhuus, B., Jossen, T., 1997. Quantum Geometry: A Statistical Field Theory Approach. Cambridge University Press, Cambridge.
Ao, P., Thouless, D., 1994. Phys. Rev. Lett. 72, 132.
Armand-Ugon, D., Gambini, R., Obregon, O., Pullin, J., 1996. Nucl. Phys. B 460, 615.
Arnold, V., 1986. Sel. Math. Sov. 5, 327 *.
Arnold, V., 1978. Mathematical Methods of Classical Mechanics. Springer, Berlin.
Arteca, G., 1994. Phys. Rev. E 49, 2417.
Arteca, G., 1995. Phys. Rev. E 51, 2600.
Ashtekar, A., 1996. Polymer geometry at Planck scale and quantum Einstein equations. Preprint, Center for Gravitational Physics and Geometry, Univ. Park, PA.
Azuma, H., Ito, S., 1994. Phys. Lett. B 331, 107.
Balachandran, A., Marmo, G., Sagerstam, B., Stern, A., 1991. Classical Topology and Quantum States. World Scientific, Singapore.
Bar-Natan, D., 1995. J. Knot Theory Ramifications 4, 503.
Bar-Natan, D., 1996. In: Proc. Symp. Appl. Math. American Mathematical Society, Providence, RI.
Baxter, R., 1982. Exactly Solved Models in Statistical Mechanics. Academic Press, New York *.
Bear, J., 1972. Dynamics of Fluids in Porous Media. Dover, New York.
Beenakker, C., Rejaei, B., 1994. Phys. Rev. B 49, 7499.
Beenakker, C., van Houten, H., 1991. Quantum Transport in Semiconductor Nanostructures. Academic Press, New York.
Bennequin, D., 1983. Asterisque 107–108, 87 *.

Bing, R., Klee, V., 1964. J. London Math. Soc. 39, 86 *.
Blatter, G., Feigelman, M., Geshkenbein, V., Larkin, A., Vinokur, V., 1994. Rev. Mod. Phys. 66, 1125.
Brereton, M., Shah, S., 1980. J. Phys. A 13, 2751 **.
Brereton, M., Vilgis, T., 1995. J. Phys. A 28, 1149 **.
Brinke ten, Haziioannou, G., 1987. Macromolecules 20, 480, 493 **.
Brochard, F., de Gennes, P.G., 1977. Macromolecules 10, 115 ***.
Brulet, A., Cotton, J., Lapp, A., Jannik, G., 1996. J. Phys. II France 6, 331.
Bryant, R., Griffiths, P., 1986. Am. J. Math. 108, 525.
Burgess, M., Jensen, B., 1993. Phys. Rev. A 48, 1861.
Burkchard, W., Michel, E., Trappe, V., 1996. Macromolecules 29, 5934.
Buser, P., 1992. Geometry and Spectra on Compact Riemann Surfaces. Birkhauser, Boston *.
Caillol, J., Levesgue, D., Weis, J., Hansen, J., 1982. J. Stat. Phys. 28, 325.
Calugareanu, G., 1961. Czech. Math. J. 11, 588 *.
Cardy, J., 1994. Phys. Rev. Lett. 72, 1580.
Casassa, E., 1965. J. Polymer Sci., Part A 3, 605.
Chari, V., Pressley, A., 1995. A Guide to Quantum Groups, Cambridge University Press, Cambridge, UK *.
Chen, Y., 1981. J. Chem. Phys. 75, 2447.
Cherednik, I., 1994. Adv. Math. 106, 65.
Chu, B., Ying, Q., Grosberg, A., 1995. Macromolecules 28, 180.
Chu, B., Ying, Q., 1996. Macromolecules 29, 1824.
Clark, I., Bracken, A., 1996. J. Phys. A 29, 339.
Cluzel, P., Leburn, A., Heller, C., Lavery, R., Viovy, J.-L., Chatenay, D., Caron, F., 1996. Science 271, 792.
Cotta-Ramusino, P., Gudagnini, E., Martellini, M., Mintchev, M., 1990. Nucl. Phys. B 330, 557 *.
da Costa, R., 1981. Phys. Rev. A 23, 1982 *.
Datta, S., 1995. Elecronic Transport in Mesoscopic Systems. Cambridge University Press, Cambridge.
de Gennes, P.G., 1971. J. Chem. Phys. 55, 572 ***.
de Gennes, P.G., 1979. Scaling Concepts in Polymer Physics. Cornell University Press, Ithaca ***.
de Gennes, P.G., 1982. In: Ciferi, A., Krigbaum, W., Meyer, R. (Eds.), Polymer Liquid Crystals, Academic Press, New York *.
de Gennes, 1984. Macromolecules 17, 703 *.
de Gennes, P.G., 1985. J. Phys. Lett. 46, L-639 **.
de Gennes, P.G., 1990a. Introduction to Polymer Dynamics. Cambridge University Press, Cambridge **.
de Gennes, P.G., 1990b. C.R. Acad. Sci. Paris, Ser. II, 310, 1327 *.
Deam, R., Edwards, 1976. Roy. Soc. London Phil. Trans. A 280, 27 ***.
Deguchi, T., Tsurusaki, K., 1994. In: Millet, K., Sumners, D. (Eds.), Random Knotting and Linking, World Scientific, Singapore.
Delbrück, M., 1962. Knotting Problems in Biology, Proc. Symp. Pure Appl. Math., vol. 14. American Mathematical Society, Providence, RI **.
des Cloizeaux, J., Jannik, G., 1990. Polymers in Solution: Their Modelling and Structure. Clarendon Press, Oxford **.
Diao, Y., 1993. J. Knot Theory Ramifications 2, 413 *.
Diao, Y., 1994. J. Stat. Phys. 14, 1247.
Dirac, P., 1931. Proc. R. Soc. London Ser. A 133, 60.
Doi, M., Edwards, S., 1986. The Theory of Polymer Dynamics. Clarendon, Oxford ***.
Doi, M., Edwards, S., 1978. Faraday Trans. II 74, 1789, 1802, 1818 ***.
Dotsenko, V., Fateev, V., 1984. Nucl. Phys. B 240, 312.
Dubrovin, B., Fomenko, A., Novikov, S., 1985. Modern Geometry – Methods and Applications, vol. 2. Springer, Berlin ***.
Duering, E., Grest, G., Kremer, K., 1994. J. Chem., Phys. 101, 8169 **.
Duke, T., 1989. Phys. Rev. Lett. 62, 2877.
Dunne, G., 1992. Ann. Phys. (NY) 215, 233 *.
Duplantier, B., 1989. J. Phys. A 22, 3033 *.
Edwards, S., 1967a. Proc. Phys. Soc. 91, 513.

Edwards, S., 1967b. Proc. Phys. Soc. 92, 9 ***.
Edwards, S., 1968. J. Phys. A 1, 15 ***.
Edwards, S., Vilgis, T., 1988. Rep. Progr. Phys. 51, 243 ***.
Eisenziegler, E., 1993. Polymers Near Surfaces. World Scientific, Singapore *.
Everaers, R., Kremer, K., 1996. Phys. Rev. E 53, R37 ***.
Felder, G., Veselov, A., 1994. Comm. Math. Phys. 160, 269.
Fetters, L., Lohse, D., Richter, D., Witten, T., Zirkel, A., 1994. Macromolecules 27, 4639 **.
Feynman, R., 1972. Statistical Mechanics. A Set of Lectures. Benjamin, Reading, MA **.
Finkelstein, D., Rubinstein, J., 1968. J. Math. Phys. 9, 1762.
Freedman, M., He Z-Hu, 1991. Ann. Math. 134, 189 **.
Freedman, M., He Z-Hu, Wang, Z., 1994. Ann. Math. 139, 1–50 **.
Frenchel, W., 1951. Bull. Am. Math. Soc. 57, 44 **.
Frisch, H., Wasserman, E., 1961. J. Am. Chem. Soc. 83, 3789 **.
Frölich, J., King, C., 1989. Comm. Math. Phys. 126, 167 *.
Fulton, W., 1995. Algebraic Topology: First Course. Springer, Berlin *.
Gambini, R., Pullin, J., 1996. Loops, Knots, Gauge Theories and Quantum Gravity. Cambridge University Press, Cambridge *.
Gaveau, B., Schulman, L., 1986. J. Phys. A 19, 1833 *.
Gilbert, N., Porter, T., 1994. Knots and Surfaces. Oxford University Press, Oxford ***.
Gilkey, P., 1995. Invariance Theory, the Heat Equation and the Atiah–Singer Index Theorem. CRC Press, London *.
Goodman, S., 1983. In: Lecture Notes in Mathematics, vol. 1007. Springer, Berlin, p. 300.
Gordon, C., Luecke, J., 1989. J. Am. Math. Soc. 2, 371 *.
Graessley, W., Pearson, D., 1977. J. Chem. Phys. 66, 3363 **.
Green, M., Schwarz, J., Witten, E., 1987. Superstring Theory, vol. 2. Cambridge University Press, Cambridge.
Griffiths, P., 1983. Exterior Differential Systems and the Calculus of Variations. Birhauser, Boston.
Grosberg, Y., Khokhlov, A., 1989. Statistical Physics of Macromolecules. Nauka, Moscow **.
Grosberg, Y., Nechaev, S., Shakhnovich, E., 1988. J. Chem. Phys. (France) 49, 2095 *.
Grosche, C., 1996. Path Integrals, Hyperbolic Spaces and Selberg Trace Formulae. World Scientific, Singapore *.
Guadagnini, E., 1993. The Link Invariants of the Chern–Simons Field Theory. Walter de Gruyter, Berlin **.
Guadagnini, E., Martellini, M., Mintchev, M., 1989. Phys. Lett. B 228, 489 *.
Guadagnini, E., Martellini, M., Mintchev, M., 1990. Nucl. Phys. B 330, 575 ***.
Guillemin, V., Pollack, A., 1974. Differential Topology. Prentice-Hall, Englewood Cliffs, NJ **.
Hague, E., Hemmer, P., 1971. Phys. Norvegica 5, 209.
Harpe, P., Kervaire, M., Weber, C., 1986. L'Enseignement Mathematique 32, 271 ***.
He, T., Porter, R., 1992. Macromol. Chem. Theory Simul. 1, 119.
Helfand, E., Pearson, D., 1983. J. Chem. Phys. 79, 2054 *.
Hess, W., 1988. Macromolecules 21, 2620 *.
Hickl, P., Ballauff, M., Scherf, U., Mullen, K., Linder, P., 1997. Macromolecules 30, 273.
Hill, T., 1956. Statistical Mechanics. McGraw-Hill, New York.
Hutnik, M., Argon, A., Suter, U., 1991. Macromolecules 24, 5956.
Isakov, S., Mashkevich, S., Ouvry, S., 1995. Nucl. Phys. B 448, 457.
Iwata, K., 1989. Macromolecules 22, 3702.
Iwata, K., Edwards, S., 1988. Macromolecules 21, 2901.
Iwata, K., Edwards, S., 1989. J. Chem. Phys., 90, 4567 *.
Iwata, K., Kimura, T., 1981. J. Chem. Phys. 74, 2039.
Jähnig, F., 1979. J. Chem. Phys. 70, 3279.
Jascual, J., Mendez, J., Gomez-Herrero, J., Baro, A., Garcia, N., Landman, U., 1995. Science 267, 1793.
Jones, V., 1985. Bull. Am. Math. Soc. 12, 103 ***.
Kardar, M., Zang, Y., 1987. Phys. Rev. Lett. 58, 2087.
Karowski, M., 1988. Nucl. Phys. B 300, 473.
Katrich, V., Bednar, J., Michoud, D., Scharein, R., Dubochet, J., Stasiak, A., 1996. Nature 384, 142.

Kauffman, L., 1987a. On Knots. Princeton University Press, Princeton, NJ ***.
Kauffman, L., 1987b. Topology 26, 395 *.
Kauffman, L., 1988. Am. Math. Monthly 95, 195.
Kauffman, L., 1990. Trans. Am. Math. Soc. 318, 417 ***.
Kauffman, L., 1993. Knots and Physics. World Scientific, Singapore *.
Kauffman, L. (Ed.) 1995. Knots and Applications. World Scientific, Singapore.
Kauffman, L., 1996. Proc. Symp. in Appl. Math. 51, 1.
Kauffman, L., Saleur, H., 1993. Comm. Math. Phys. 152, 565 **.
Kavasalis, J., Noolandi, J., 1988. Macromolecules 21, 1629 *.
Khandekar, D., Wiegel, F., 1988. J. Phys. A 21, L563.
Kholodenko, A., 1985. J. Phys. A 18, 3227.
Kholodenko, A., 1990. Ann. Phys. N.Y. 202, 186 *.
Kholodenko, A., 1991. Phys. Lett. A 159, 437.
Kholodenko, A., 1992. J. Chem. Phys. 96, 700.
Kholodenko, A., 1993. Macromolecules 42, 4179.
Kholodenko, A., 1994. Trends in Chem. Physics, vol. 3, pp. 63–94. Research Trends, Inc., Trivandrum, India ***.
Kholodenko, A., 1995. Faraday Trans. 91, 2473 *.
Kholodenko, A., 1996a. J. Math. Phys. 37, 1287 ***.
Kholodenko, A., 1996b. J. Math. Phys. 37, 1314 ***.
Kholodenko, A., 1996c. Macromol. Chem. Theory and Simulations 5, 1031 ***.
Kholodenko, A., Bearden, D., Douglas, J., 1994. Phys. Rev. E 49, 2206 *.
Kholodenko, A., Borsali, R., 1995. Physica A 221, 389.
Kholodenko, A., Freed, K., 1983. J. Chem. Phys. 78, 7390.
Kholodenko, A., Freed, K., 1984a. J. Phys. A 17, 2703.
Kholodenko, A., Freed, K., 1984b. J. Chem. Phys. 80, 900.
Kholodenko, A., Nesterenko, V., 1995. J. Geom. Phys. 16, 15.
Kholodenko, A., Quian, C., 1988. J. Chem. Phys. 89, 2301.
Kholodenko, A., Rolfsen, D., 1996. J. Phys. A. 29, 6577 ***.
Kholodenko, A., Vilgis, T., 1994. J. Phys. (Paris) 4, 843 ***.
Kholodenko, A., Vilgis, T., 1995. Phys. Rev. E 52, 3973 *.
Kholodenko, A., Vilgis, T., 1996. J. Phys. A 29, 939 ***.
Kholodenko, A., Vilgis, T., 1997. Europhys. Lett., submitted.
Kleinert, H., 1995. Path Integrals in Quantum Mechanics, Statistics and Polymer Physics. World Scientific, Singapore **.
Knott, C.G., 1911. Life and Scientific Work of P.G. Tait. Cambridge University Press, Cambridge.
Kogan, I., Perelomov, A., Semenoff, G., 1992. Phys. Rev. B 45, 12 084 *.
Kramer, O., Ferry, J., 1975. Macromolecules 8, 87.
Kremer, K., Binder, K., 1988. Comp. Phys. Rep. 7, 259.
Kremer, K., Grest, G., 1994. Entanglement Effects in Polymer Melts and Networks. Inst. für Festkörperforschung, Jülich ***.
Krupenkin, K., Taylor, P., 1995a. Phys. Rev. B 52, 6400.
Krupenkin, K., Taylor, P., 1995b. Macromolecules 28, 5819.
Kugler, M., Shtrikman, N., 1988. Phys. Rev. D 37, 934.
Kuiper, N., Meeks, W., 1984. Invent. Math. 77, 25.
Lachowski, B., Yeon, D., Mclean, D., 1988. Macromolecules 21, 1629.
Landau, L., 1930. Z. Phys. 64, 629.
Langer, J., Singer, D., 1984a. J. Diff. Geom. 20, 1.
Langer, J., Singer, D., 1984b. J. London Math. Soc. 30, 512.
Langevin, R., Rosenberg, H., 1976. Topology 15, 405 *.
Laughlin, R., 1983. Phys. Rev. Lett. 50, 1395 *.
Le Bret, M., 1980. Biopolymers 19, 619.

Levay, P., Mullan, D., Tsutsui, I., 1996. J. Math. Phys. 37, 625.
Levene, S., Donahue, C., Boles, C., Cozzarelli, N., 1995. Biophys. J. 69, 1036.
Levi, P., 1965. Processes Stochastiques et Movement Brownien. Deuxieme Edition Revue et Augmentee, Paris *.
Li, M., Brulet, A., Cotton, J., Davidson, P., Strazielle, C., Keller, P., 1994. J. Phys. (Paris) II 4, 1843.
Lickorish, W.B.R., Millet, K., 1987. Topology 26, 107 ***.
Liguori, A., Mintchev, M., 1995. Comm. Math. Phys. 169, 635.
Ludwig, A., Fischer, M., Shankar, R., Grinstein, G., 1994. Phys. Rev. B 50, 2615.
Lyons, T., McKean, H., 1984. Adv. Math. 51, 212 *.
Ma, J., Straub, J., Shakhnovich, E., 1995. J. Chem. Phys. 103, 2615.
Magnus, W., Winkler, S., 1966. Hill Equation. Interscience, New York.
Maraner, P., 1995. J. Phys. A 28, 2939.
Martin, S., 1989. Nucl. Phys. B 327, 178.
Massey, W., 1967. Algebraic Topology: An Introduction. Springer, Berlin **.
Matsutani, S., 1992. J. Phys. Soc. Japan 61, 55 *.
Meyerhoff, 1992. Math. Intelligencer 14, 37 ***.
McKean, H., 1969. Stochastic Integrals. Academic Press, New York *.
McKean, H., Sullivan, D., 1984. Adv. Math. 51, 203 *.
McKena, G., Hostetter, B., Hadjichristidis, N., Fetters, L., Plazek, D., 1989. Macromolecules 22, 1834 *.
Mehta, A., Needs, R., Thouless, D., 1991. Europhys. Lett. 14, 113 *.
Menasco, W., 1994. Comptes Rendus (Ser. I) 318, 831.
Mezard, M., Parisi, G., Virarsoro, M., 1988. Spin Glasses Theory and Beyond. World Scientific, Singapore *.
Milchev, A., Binder, K., 1994. Europhys. Lett. 26, 671 *.
Milnor, J., 1950. Ann. Math. 52, 248 ***.
Milnor, J., 1982. Bull. Am. Math. Soc. 6, 9 **.
Milnor, J., 1994. Collected Papers, vol. 1. Publish or Perish, Houston, TX *.
Monastyrsky, M., 1993. Topology of Gauge Fields and Condensed Matter. Plenum Press, New York *.
Morton, H., 1986. Math. Proc. Camb. Phil. Soc. 99, 107 **.
Mucciolo, E., Shastry, B., Simmons, B., Altshuler, B., 1994. Phys. Rev. B 49, 197.
Mumford, D., 1983. Tata Lectures on Theta. Birkhauser, Basel *.
Müller, M., Wittmer, J., Cates, M., 1996. Phys. Rev. E 53, 5063 *.
Murasugi, K., Przytycki, J., 1993. Mem. Am. Math. Soc. 508.
Murasugi, K., 1987. Topology 26, 187 **.
Murasugi, K., 1996. Knot Theory and its Applications. Birkhauser, Boston *.
Nechaev, S., 1990. Int. J. Mod. Phys. B 4, 1809 **.
Nechaev, S., 1996. Statistics of Knots and Entangled Random Walks. World Scientific, Singapore *.
Nechaev, S., Rostiashvili, V., 1993. J. Phys. II 3, 91 *.
Nechaev, S., Semenov, A., Koleva, M., 1987. Physica A 160, 506 **.
Nechaev, S., 1988. J. Phys. A 21, 3659 ***.
Obukov, S., Rubinstein, M., Duke, T., 1994. Phys. Rev. Lett. 75, 1263 *.
Olshanetsky, A., Perelomov, A., 1985. Phys. Rep. 94, 313 *.
Ono, T., 1994. In: Proc. Symp. in Appl. Math. American Mathematical Society, Providence, RI.
Oono, Y., Kohmoto, M., 1982. Phys. Rev. Lett. 49, 1397.
Orlandini, E., Tesi, M., van Rensburg, E., Wittington, S., 1996. J. Phys. A 29, L-299 *.
Otto, M., Vilgis, T., 1996. J. Phys. A 29, 3893 *.
Panykov, S., Rabin, Y., 1996. Phys. Rep. 269, 1 *.
Pastor, R., Zwanzig, R., Szabo, A., 1996. J. Chem. Phys. 105, 3878.
Perico, A., Selifano, A., 1995. Macromolecules 28, 1709.
Pippenger, N., 1989. J. Discrete Appl. Math. 25, 273 **.
Pitman, J., Yor, M., 1986. Ann. Probab. 14, 733 *.
Pitman, J., Yor, M., 1989. Ann. Probab. 17, 965 *.
Pohl, W., 1968. J. Math. Mech. 17, 975 *.

Poincare, H., 1882. Acta Math. 1, 1 **.
Polyakov, A., 1988. Mod. Phys. Lett. A 3, 325 *.
Polyakov, A., 1990. In: E. Brezin, J. Zinn-Justin (Eds.), Fields, Strings and Critical Phenomena. North-Holland, Amsterdam ***.
Prager, S., Frisch, H., 1967. J. Chem. Phys. 46, 1474 *.
Prahofer, M., Spohn, H., 1996. Physica A 233, 191.
Quake, S., 1994. Phys. Rev. Lett. 73, 3317 **.
Rabin, Y., Grosberg, A., Tanaka, T., 1995. Europhys. Lett. 32, L-505 *.
Randell, R., 1994. J. Knot Theory Ramifications 3, 279.
Ricca, R., Berger, M., 1996. Phys. Today 49, 28.
Riley, R., 1975. Math. Proc. Cambridge Phil. Soc. 77, 281 *.
Rolfsen, D., 1976. Knots, Links. Publish or Perish, Houston, TX *.
Roovers, J., 1985. J. Polym. Sci. Phys. Ed. 23, 1117.
Roovers, J., Toporowski, P., 1983. Macromolecules 16, 843 *.
Rostiachvili, V., Nechaev, S., Vilgis, T., 1993. Phys. Rev. E 48, 3314 **.
Rubinstein, M., 1987. Phys. Rev. Lett. 59, 1946 *.
Rubinstein, M., Helfand, E., 1985. J. Chem. Phys. 82, 2477 **.
Rusakov, V., Shliomis, M., 1985. J. Phys. (Paris) Lett. 46, L935.
Rybenkov, V., Cozzarelli, N., Vologodskii, A., 1993. Proc. Nat. Acad. Sci. 90, 5307.
Saito, N., Chen, Y., 1973. J. Chem. Phys. 59, 3701 *.
Sakharov, A.D., 1972. In: Problems in Theoretical Physics, Memorial Volume Dedicated to I.E. Tamm. Nauka, Moscow.
Saleur, H., 1990. Comm. Math. Phys. 132, 657 *.
Shaw, S., Wang, J., 1993. Science 260, 533.
Shifman, M., 1991. Nucl. Phys. B 352, 87.
Shulman, L., 1971. J. Math. Phys. 12, 304 **.
Solf, M., Vilgis, T., 1996. J. Phys. I (France) 6, 1541 ***.
Solf, M., Vilgis, T., 1997. Phys. Rev. E 55, 3037 **.
Solf, M., Vilgis, T., 1995. J. Phys. A 28, 6655 ***.
Sondheimer, E., Wilson, A., 1951. Proc. Roy. Soc. London. Ser. A 210, 173 *.
Soteros, C., Sumners, D., Whittington, S., 1992. Math. Proc. Camb. Phil. Soc. 111, 75 ***.
Starting, P., Wiegel, F., 1994. J. Phys. A 27, 3731.
Stasiak, A., Katritch, V., Bednar, J., Michaud, D., Dubochet, J. 1996. Nature 384, 122 *.
Stillwell, J., 1992. Geometry of Surfaces. Springer, Berlin **.
Stillwell, J., 1993. Classical Topology and Combinatorial Group Theory. Springer, Berlin ***.
Straube, E., Urban, V., Pyckhout-Hintzen, W., Richter, D., Glinke, C., 1995. Phys. Rev. Lett. 74, 4464.
Sumners, D., Whittington, S., 1988. J. Phys. A 21, 1689 ***.
Sutherland, B., 1985. In: Exactly Solvable Problems in Condensed Matter and Relativistic Field Theory. Springer, Berlin.
Symanzik, K., 1969. In: Jost, R. (Ed.), Local Quantum Field Theory. Academic Press, New York.
Szabo, A., Schulten, K., Schulten, Z., 1980. J. Chem. Phys. 72, 4350.
Tanaka, F., 1982. Progr. Theor. Phys. (Japan) 68, 164.
Tanaka, F., 1984. J. Phys. Soc. Japan 53, 2205.
Tanimura, S., Tsutsui, I., 1995. Mod. Phys. Lett. A 10, 2607.
Teraoka, I., Langley, K., Karasz, F., 1992. Macromolecules 25, 6106 *.
Thistlethwaite, M., 1987. Topology 26, 297 *.
Thurston, W., 1979. Lectures on Hyperbolic 3-Manifolds. Princeton University Press, Princeton *.
Thurston, W., 1982. Bull. Am. Math. Soc. 6, 357 *.
Tinland, B., Maret, G., Rinaudo, M., 1990. Macromolecules 23, 526 *.
Treloar, L., 1975. The Physics of Rubber Elasticity. Clarendon, Oxford.
Turaev, V., 1987. L'Enseignement Mathematique 33, 203.

Turaev, V., 1989. In: Yang, C., Ge, M. (Eds.), Braid Group, Knot Theory and Statistical Mechanics. World Scientific, Singapore, pp. 59–95∗.
Tutte, W., 1963. Can. J. Math. 15, 249.
Ueda, M., Yoshikawa, K., 1996. Phys. Rev. Lett. 77, 2133.
Urwin, K., Arscott, F., 1970. Proc. R. Soc. Edinburgh 69, 28.
Varopoulos, N., 1985. Math. Proc. Cambridge Phil. Soc. 97, 299 ∗.
Varopoulos, N., Saloff-Caste, L., Coulhon, T., 1992. Analysis and Geometry on Groups. Cambridge University Press, Cambridge.
Vilenkin, N., 1968. Special Functions and the Theory of Group Representations. American Mathematical Society, Providence, RI ∗.
Vilgis, T., Otto, M., 1997. Phys. Rev. E 56, R1314 ∗.
Vologodskii, A., Lukashin, A., Frank-Kamenetski, M., 1975. Sov. Phys. JETP 40, 932 ∗∗.
Vologodskii, A., Anshelevich, V., Lukashin, A., Frank-Kamenetski, M., 1979. Nature 280, 294 ∗.
Vologodskii, A., Cozzarelli, N., 1993. J. Mol. Biol. 232, 1130.
von Rensburg, J., Wittington, S., 1990. J. Phys. A 23, 3573 ∗.
von Rensburg, E., Wittington, S., 1991. J. Phys. A 24, 3935 ∗.
Wadati, M., Deguchi, T., Akutsu, Y., 1989. Phys. Rep. 180, 247.
Wang, Z-G., 1995. Macromolecules 28, 570.
Warner, M., Gunn, J., Baumgartner, A., 1985. J. Phys. A 18, 3007 ∗.
Wasserman, S., Cozzarelli, N., 1986. Science 232, 951 ∗.
Welsh, D., 1993. Complexity: Knots, Colourings and Counting. Cambridge University Press, Cambridge ∗∗∗.
Whittington, S., van Rensburg, J., Orlandini, E., Sumners, D., Tesi, M., 1993. J. Phys. A 26, L981 ∗.
Whittington, S., van Rensburg, J., Orlandini, E., Sumners, D., Tesi, M., 1994a. J. Phys. A 27, L333 ∗.
Whittington, S., van Rensburg, J., Orlandini, E., Sumners, D., Tesi, M., 1994b. Phys. Rev. E 50, R4279 ∗.
Wiegel, F., 1980. Fluid Flow Through Porous Macromolecular Systems. Springer, Berlin ∗.
Wilczek, F., 1990. Fractional Statistics and Anion Superconductivity. World Scientific, Singapore ∗.
Wilemski, G., Fixman, M., 1974. J. Chem. Phys. 60, 866 ∗.
William, P., 1991. Phys. Lett. A 152, 83.
Willmore, T., 1982. Total Curvature in Riemannian Geometry. Halsted Press, New York ∗∗.
Windwer, S., 1990. J. Chem. Phys. 93, 765 ∗∗.
Witten, E., 1981. Nucl. Phys. B 188, 513.
Witten, E., 1989a. Comm. Math. Phys. 121, 351 ∗∗∗.
Witten, E., 1989b. Nucl. Phys. B 322, 629 ∗∗∗.
Wittmer, J., Binder, K., 1992. Macromolecules 25, 7211.
Wu, F., 1992. Rev. Mod. Phys. 64, 1099 ∗∗.
Wu, F., 1982. Rev. Mod. Phys. 54, 235 ∗.
Yor, M., 1992. Some Aspects of Brownian Motion. Birkhauser, Basel ∗.
Zinn-Justin, J., 1993. Quantum Field Theory and Critical Phenomena. Clarendon Press, Oxford ∗.
Zurer, P., 1996. Chem. Eng. News 74 (50), 43.